



CONTAMINATION STUDY OF A MICRO PULSED PLASMA THRUSTER

THESIS

Ceylan Kesenek, 1ST Lt, TUAF

AFIT/GA/ENY/08-M03

**DEPARTMENT OF THE AIR FORCE
AIR UNIVERSITY**

AIR FORCE INSTITUTE OF TECHNOLOGY

Wright-Patterson Air Force Base, Ohio

APPROVED FOR PUBLIC RELEASE; DISTRIBUTION UNLIMITED

The views expressed in this thesis are those of the author and do not reflect the official policy or position of the United States Air Force, Department of Defense, or the U.S. Government.

AFIT/GA/ENY/08-M03

CONTAMINATION STUDY OF A MICRO PULSED PLASMA THRUSTER

THESIS

Presented to the Faculty

Department of Aeronautics and Astronautics

Graduate School of Engineering and Management

Air Force Institute of Technology

Air University

Air Education and Training Command

In Partial Fulfillment of the Requirements for the
Degree of Master of Science in Astronautical Engineering

Ceylan Kesenek, BS

1ST Lt, TUAF

March 2008


APPROVED FOR PUBLIC RELEASE; DISTRIBUTION UNLIMITED

CONTAMINATION STUDY OF A MICRO PULSED PLASMA THRUSTER

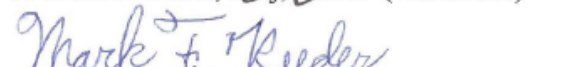
Ceylan Kesenek, BS

1ST Lt, TUAF

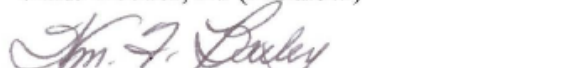
Approved:


Richard Branam, Maj, USAF (Chairman)


7 Mar 08
Date


Mark Reeder, Dr (Member)

11 Mar 08
Date


William Bailey, Dr. (Member)

7 Mar '08
Date


William A. Hargus, Dr. (Member)

6 Mar 08
Date

Acknowledgments

I would like to express my sincere appreciation to my faculty advisor, Maj Richard Branam, for his guidance and support throughout the course of this research project. The insight and experience was certainly appreciated. I would, also, like to thank AFIT laboratory staff Sean Miller, Barry Page, Chris Zickefoose and Jay Anderson for their effort and their help on this research project.

Ceylan Kesenek

Table of Contents

	Page
Acknowledgments.....	vii
Table of Contents.....	ii
List of Figures.....	iv
List of Tables	viii
List of Symbols.....	ix
Abstract.....	x
I. Introduction	1
Background.....	1
Problem Statement.....	3
Research Objectives	4
Methodology.....	5
Assumptions/Limitations.....	5
Preview	6
II. Literature Review.....	7
Chapter Overview.....	7
Pulsed Plasma Thrusters (PPT)	7
Micro Pulsed Plasma Thrusters (μ PPT)	10
Mass Expulsion/Deposition.....	15
Operational Limits.....	20
Plume Models.....	22
Summary.....	24
III. Methodology	25

Chapter Overview.....	25
Vacuum Facility	25
Control Configuration	28
Contamination Test Setup	30
Summary.....	39
IV. Analysis and Results.....	40
Chapter Overview.....	40
μ PPT Operational Tests:	40
μ PPT Contamination Study.....	45
Particle Size Distribution.....	46
Mass Deposition Profile	48
Propellant Distribution	50
Comparisons to the Previous Research	53
V. Conclusions and Recommendations	57
Conclusions of Research	57
Recommendations for Future Research.....	59
Summary.....	60
Appendix.....	61
Test-1 Results	61
Test-2 Results:	68
Test-3 Results:	80
Vita.....	96
Bibliography	97

List of Figures

	Page
Figure 1. Schematic of a PPT	8
Figure 2. EO-1 Pulsed Plasma Thruster.....	10
Figure 3. Schematic of a μ PPT	11
Figure 4. Tip of propellant module of an unused μ PPT	14
Figure 5. Experimental Pulsed Plasma Thruster No 1	15
Figure 6. SEM image of particulate deposits on an aluminum witness plate	16
Figure 7. μ PPT exhaust plume taken by G.G.Spanjers et al. AFRL Electric Propulsion Laboratory	17
Figure 8. Net mass deposition on quartz sensors	18
Figure 9. Solar transmittance of quartz sensors for far field measurements.....	19
Figure 10. NASA Lewis/PRIMEX breadboard PPT	20
Figure 11. “Charred area on the propellant surface of the 3.6-mm μ PPT”	21
Figure 12. Cross section of pressure probe	22
Figure 13. Schematic of Plasma-surface interaction in a μ PPT	23
Figure 14. Schematic of near surface layers	24
Figure 15. AFIT’s Micro propulsion vacuum facility	26
Figure 16. Oil Diffusion pump of the vacuum facility	27
Figure 17. μ PPT with pulse initiator.....	29
Figure 18. “Xenon Model-437B Nanopulse System” used for pulse initiator for μ PPT..	30
Figure 19. AutoCAD design of Thruster holder	31

Figure 20. Bowl-shaped witness plate holder (Test-1 Configuration).....	32
Figure 21. Bowl-shaped witness plate holder (Test-2, 3 Configuration).....	33
Figure 22. Angular locations that the pictures were taken.....	34
Figure 23. Test Setup	35
Figure 24. Test Setup	36
Figure 25. Single particles at higher magnification levels.....	37
Figure 26. Particles on witness plate at angle of 22.5°	39
Figure 27. μ PPT with Pulse initiator	42
Figure 28. Carbonization μ PPT tip after 3 hours of operation	44
Figure 29. Particle size vs. particle count TEST-3 (960 pulses).....	47
Figure 30. Mass contribution of each particle size TEST-3 (960 pulses).....	47
Figure 31. Mass Deposition Profile TEST-3 (960 pulses).....	49
Figure 32. Deposition Rates per Pulse per Steradian.....	50
Figure 33. μ PPT on scale.....	51
Figure 34. Angular location 90° TEST-3.....	52
Figure 35. Angular location 0° TEST-3.....	53
Figure 36. Mass deposition profile found at previous study.....	54
Figure 37. Comparison of mass deposition of AFRL's PPT and μ PPT in this research ..	55
Figure 38. Comparison of mass deposition normalized by their energy.	56
Figure 39. Particle size vs. Particle count TEST-1 (3960 pulses)	61
Figure 40. Mass Deposition profile TEST-1 (3960 pulses).....	62
Figure 41. Deposition rates TEST-1 (3960 pulses)	62

Figure 42. Angular Location 90° Test-1	63
Figure 43. Angular Location 67.5° Test-1	64
Figure 44. Angular Location 45° Test-1	65
Figure 45. Angular Location 22.5° Test-1	66
Figure 46. Angular Location 0° Test-1	67
Figure 47. Particle size vs. Particle count TEST-2 (744 pulses)	68
Figure 48. Mass Deposition Profile TEST-2 (744 pulses).....	69
Figure 49. Deposition rates TEST-2 (744 pulses)	70
Figure 50. Angular location 90° TEST-2.....	71
Figure 51. Angular location 78.5° TEST-2.....	72
Figure 52. Angular location 67.5° TEST-2.....	73
Figure 53. Angular location 56.25° TEST-2.....	74
Figure 54. Angular location 45° TEST-2.....	75
Figure 55. Angular location 33.75° TEST-2.....	76
Figure 56. Angular location 22.5° TEST-2.....	77
Figure 57. Angular location 11.25° TEST-2.....	78
Figure 58. Angular location 0° TEST-2.....	79
Figure 59. Angular location 90° TEST-3.....	80
Figure 60. Angular location 78.75° TEST-3.....	81
Figure 61. Angular location 67.5° TEST-3.....	82
Figure 62. Angular location 56.25° TEST-3.....	83
Figure 63. Angular location 45° TEST-3.....	84

Figure 64. Angular location 33.75° TEST-3.....	85
Figure 65. Angular location 28° TEST-3.....	86
Figure 66. Angular location 22.25° TEST-3.....	87
Figure 67. Angular location 20° TEST-3.....	88
Figure 68. Angular location 17° TEST-3.....	89
Figure 69. Angular location 14° TEST-3.....	90
Figure 70. Angular location 8° TEST-3.....	91
Figure 71. Angular location 5° TEST-3.....	92
Figure 72. Angular location 4° TEST-3.....	93
Figure 73. Angular location 2° TEST-3.....	94
Figure 74. Angular location 0° TEST-3.....	95

List of Tables

	Page
Table 1. Examples of Electric Thrusters.....	2
Table 2. μ PPT Reliability Study	40
Table 3: μ PPT Test using Pulse initiator	42

List of Symbols

- F = Lorentz force (N)
 q = Charge of moving particle (C)
 E' = Effective electric field (V/m)
 E = Applied electric field (V/m)
 v = Velocity of particle (m/s)
 B = Magnetic field (T)
 C = Electric capacitance (f)
 W_0 = Energy stored in capacitor (j)
 V = Electric potential (V)

Abstract

The trend in satellite design is progressing towards building smaller satellites. Small satellites require micro propulsion devices for accurate control by the propulsion system. Micro-Pulsed Plasma Thrusters (μ PPTs) are highly reliable and simple micro propulsion systems offering attitude control, station keeping, constellation flying, and drag compensation for such satellites. Miniaturized propulsion system μ PPTs are expected to be used for a wide range of propulsion tasks on future space missions ranging from nano-satellites to large spacecrafts requiring precision placement¹.

As an unfortunate side effect, the exhaust plume induces contamination on spacecraft surfaces and may lead to significant problems with sensors and power generation. Solid particulates in the exhaust plume may deposit on spacecraft instrument and the solar array surfaces limiting or reducing the mission capability as well as the lifetime of a satellite. To better understand these contamination issues, a detailed characterization of the exhaust plume is necessary. Several studies have characterized various kinds of pulsed plasma thrusters² but μ PPTs are unique in the level of contamination issue.

This research employs μ PPTs, and is being operated in a simulated space environment at the AFIT's micro-propulsion vacuum facilities. The experimental setup includes a target array consisting of aluminum witness plates placed directly in the exhaust plume in order to capture mass deposition over a wide angle. The mass deposition on the witness plates is analyzed using a scanning electron microscope.

Results show mass deposition along the centerline of the thruster is much more significant and higher when compared to wider angular positions. Angular positions 0° - 30° captured majority of the mass. This region alone captured 93.6% of total mass ejected from the thruster.

CONTAMINATION STUDY OF A MICRO PULSED PLASMA THRUSTER

I. Introduction

Background

For many planetary missions, highly efficient propulsion systems are required in order to reduce total mass of the spacecraft. Electric thrusters are very effective propulsion devices because of their highly efficient mass utilization. Having a high efficient utilization of mass, electric propulsion devices can obtain exhaust velocities above 10,000 m/sec. Electric propulsion concepts can be divided into three categories³:

- Electrothermal propulsion
- Electrostatic propulsion
- Electromagnetic propulsion

Table 1 gives some examples of electric propulsion systems and their performance values^{3,4}: Arcjets and resistojets are good examples for Electro thermal Propulsion technique in which propellant gas is heated by means of electric energy and expanded through the nozzle to convert its thermal energy into thrust. Ion thrusters are electrostatic propulsion devices accelerating the ion propellant by an electrostatic field. Magneto Plasma Dynamic (MPD) thrusters use electromagnetic forces to accelerate the propellant and create the thrust. Pulsed plasma thrusters (PPT) use both electromagnetic and electrostatic force to create the thrust. They are very attractive devices as a propulsion option especially for power and mass limited satellites because of their simplicity, reliability and low dry weight.

Table 1. Examples of Electric Thrusters

Type	Specific Impulse(s)	Thrust(N)	Efficiency (%)
Resistojet	250-800	$5 \cdot 10^{-4}$ -6	50-88
Arcjet	1100-2100	0.05-6.8	35-44
Magneto Plasma Dynamic (MPD) thruster	2500-6000	0.88-2.2	13-35
Ion Thruster	2000-10,000	0.1-1.0	70-90
Pulsed Plasma Thruster (PPT)	1000-1500	10^{-3} - 10^{-5}	10-20

The Zond 2 spacecraft, the first spacecraft using pulsed plasma thrusters, was launched on November 30, 1964 for a Mars fly-by mission. Pulsed plasma thrusters were used for three-axis attitude control for the Zond 2 spacecraft⁵. Thrusters onboard Zond 2 used 50J of energy⁶. PPT development in the U.S. began at Massachusetts Institute of Technology's (MIT) Lincoln Laboratories. The Lincoln Experimental Satellite (LES 6) achieved the first U.S. flight of a PPT in 1968. This thruster was a breech fed design and supplied 312 sec specific impulse with 26 μ N of thrust. The system accomplished its station-keeping mission for five years without a fault.⁷

This research examines the Micro-Pulsed Plasma Thruster (μ PPT). μ PPTs are simplified version of the larger Pulsed Plasma Thrusters (PPT) found on deployed satellites having fewer components and are therefore simpler. μ PPTs are ablative devices using electromagnetic and electrostatic force in order to accelerate the ablated and ionized propellant. μ PPTs fall somewhere between Electromagnetic and Electrostatic Propulsion systems categorically.

The accelerating force in μ PPTs is called the Lorentz Force which can be expressed as:

$$\vec{F} = q\vec{E}' = q(\vec{E} + \vec{v} \times \vec{B}) \quad (1)$$

There is much research in the literature of pulsed plasma thrusters (PPT) and contamination issues of PPTs⁸. The lower power consumption μ PPTs can increase payload size with the mass reduction in the propulsion components. While PPTs have been studied extensively, μ PPTs are very new technology and warrant further examination especially since they are now being used for a propulsion option.

Miniaturization of propulsion system is a very important issue, especially for small satellites. μ PPTs are very reliable and can provide very precise impulse levels. However, the exhaust plume of μ PPTs can be very harmful to satellite surfaces. The exhaust plume consists of ablated solid propellant, Polytetrafluoroethylene (PTFE), which can condense on surfaces of delicate equipment used on satellites. This deposition can cause very significant problems, possibly even limiting mission objectives of the spacecraft. The objective of this research is to better understand contamination effects of μ PPTs and finding the location of contamination from exhaust plume to help satellite designers better employ these potentially beneficial thrusters.

Problem Statement

Size and precision of an impulse bit used to control the attitude of the satellite is very important for a spacecraft especially those with optical sensors and precision instruments. Although μ PPTs provide a very precise impulse bit, there is a negative effect on instrumentation because of contamination from the exhaust plume.

μ PPT exhaust plumes contain hot plasma and ablated particulates from a solid propellant, typically Polytetrafluoroethylene. These particulates can condense and even create a film layer over spacecraft instruments. If this layer happens to be created on the surface of solar arrays, the spacecraft could experience a degradation of power generation. Exhaust plumes can cause contamination on other sensors as well degrading resolution by affecting transmittance and reflectivity.

In order to characterize the contamination effects of μ PPT exhaust plumes, this research focuses on mass deposition, deposition rates and the dependence of these plume characteristics as a function of divergence angle.

Research Objectives

1. Operational Tests of μ PPT

A primary objective in this research was constructing a circuit providing us with a reliable and controllable thruster. A reliable thruster allows us to test a thruster for a typical design life of a μ PPT. The control mechanisms enable the researcher to explore a range of spark generation and sparking frequency.

2. Mass Deposition/Contamination

After developing a reliable circuit allowing consistent spark generation, the next objective was to focus on characterization of mass deposition and deposition rate of plasma particles and particulates from the exhaust plume of a μ PPT. A thruster was fired inside a bell-jar type vacuum chamber to replicate the space environment. Operating conditions were typically pressures as low as 10^{-6} - 10^{-7} torr. To characterize mass deposition, a thruster holder stand was designed and built where witness plates were

placed in a bowl-shaped holder. Witness plates were scanned using AFIT's scanning electron microscope (SEM) to quantifiably measure particulate deposition.

While propellant flow is often assumed to be directed in the primary thruster axis, some particles may actually collide with slower moving particles and reflect in the opposite direction. For this reason, a minor objective of this research is focused on determination of potential back flow of contaminants. In order to detect whether back flow was present, some witness plates were also placed around the tip of μ PPT.

Methodology

A μ PPT was placed in a thrust holder stand directed downward in order to eliminate gravitational effects. Witness plates were placed in 5 arrays inside a bowl shaped holder with the surface of the bowl located 10 cm from the thruster. Tests took place inside a bell jar type vacuum chamber to simulate the space environment. After the tests, witness plates were examined using a scanning electron microscope (SEM) for quantification of the deposition of particles as a function of angular positions. The SEM allows the size and shape of particles on the witness plates to be determined. Ranges of spark generation rates were used in order to see the effects of propellant heating and impulse variation on mass deposition.

Assumptions/Limitations

One of the main objectives in this research was to control the spark generation and also control the spark rate. μ PPTs are designed for small satellites and therefore need to be very simple and reliable. Therefore, the spark generator circuit is required to have

as few components as possible. Tests were made in a bell-jar type vacuum chamber replicating space environment conditions. The space environment conditions give more representative results.

Witness plates were placed at right angles with respect to the plume. Accurate placement of the witness plates directly affects the accuracy of the results. Also, it was assumed the ablated particulates have enough energy to stick and remain on the aluminum surfaces of the witness plates after hitting them. The witness plates were thoroughly cleaned before each test. In addition, the research assumed no other contamination sources of particle inside vacuum chamber leading to overestimates of contamination effects.

The research also assumed axisymmetric discharge of particles for the μ PPT over time. This assumption can be validated by the results of the contamination. Witness plates were placed on a bowl shaped holder to validate this assumption. Mass deposition was not only found in one plane but in several.

Preview

The next section includes an overview of μ PPTs and previous research projects done on PPTs. The third section describes the test setup and experimental methods used to examine contamination effects of μ PPTs. The last two sections provide results of the tests, conclusions and future recommendations on this subject.

II. Literature Review

Chapter Overview

This chapter will provide a discussion about the basic operation of a pulsed plasma thruster and survey previous research with a focus on contamination and performance studies. Previous research projects on μ PPTs focused primarily on performance and operation.

Pulsed Plasma Thrusters (PPT)

Pulsed Plasma thrusters are very attractive propulsion systems especially for small satellites with low mass and power consumption limitations. Because of features like simplicity, robustness and low cost, PPTs were one of the earliest employed electric propulsion systems for space missions⁵. Figure 1 is a schematic of a basic PPT in a breech-fed rectangular form. Conventional PPTs have two electrodes connected to a capacitor and a solid propellant bar (typically Polytetrafluoroethylene) placed between the electrodes⁹. The electrodes have often been arranged coaxially. The system consists of electrodes, capacitors as energy storage units, a spark igniter plug and a propellant feed system. The propellant feed system, the only moving part of the system, consists of a spring pushing the solid propellant through the electrodes.

The PPT operation begins with charging the capacitor using a high voltage potential (as high as 6000 Volts). The spark igniter plug is then activated to form a small amount of initial plasma to complete the circuit causing the energy storage capacitor to discharge across the face of the solid propellant fluorocarbon. This arc discharge causes a

very hot environment permitting the ablation of solid propellant. Heat transfer from the discharge arc produces hot plasma by ionizing ablated propellant.

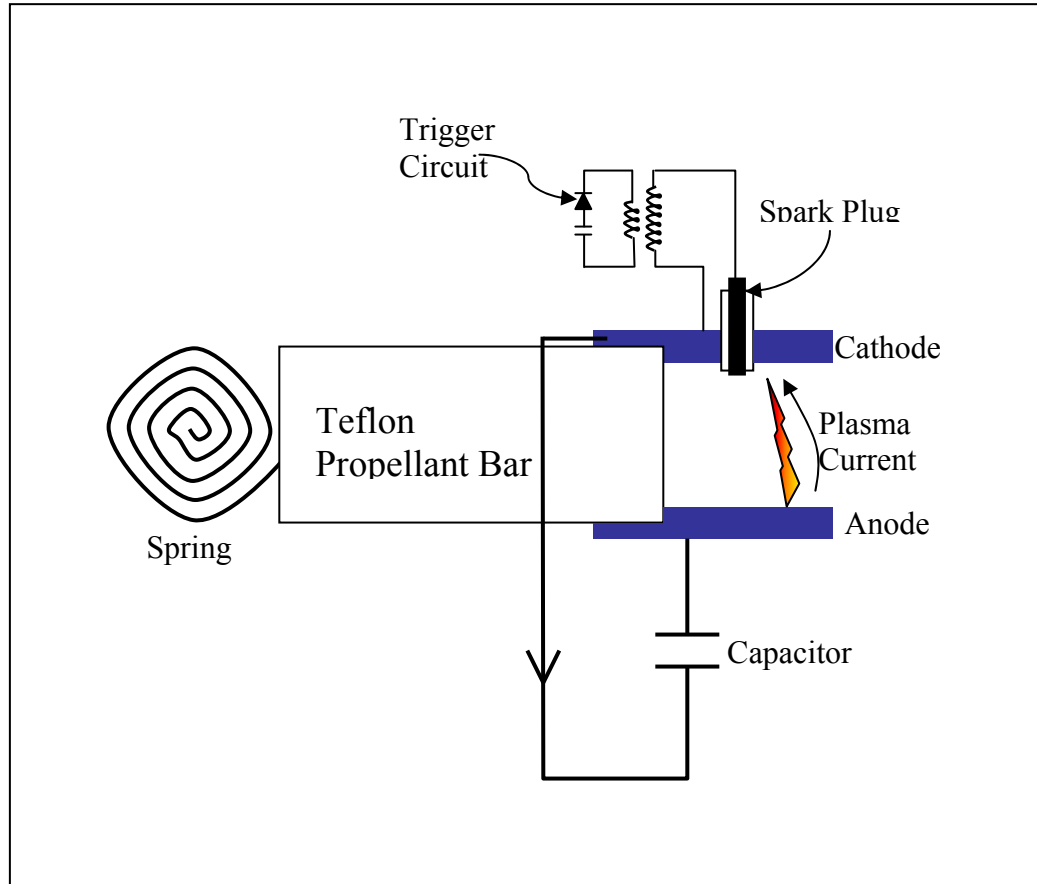


Figure 1. Schematic of a PPT ¹⁰

Peak arc current levels between electrodes during discharge are generally between 2 and 15kA¹¹. A self-generated electromagnetic force known as the Lorentz force then accelerates the ablated material formed by the high current arc. Arc durations are about 5-15 μ sec.

PPT plasma consists of electrons and gasified fluorocarbon particles with various charge levels forming a quasi-neutral gas of charged particles. However, ablated material does not fully gasify or ionize completely. Simple evaporation and rapid expansion of the

solid during and following the discharge arc often causes large solid particles to ablate causing mass loss and therefore total impulse loss. The loss of mass from the solid propellant without being accelerated by the Lorentz force reduces the overall possible total impulse of PPTs and the efficiency of the system. Inelastic processes and radiative heat transfer limit electron temperature to just a few eV. The heavy particulates only get energy from the electrons through heat transfer. The Lorentz force provides a high specific impulse component to the total impulse of PPTs. For this reason, heavy non-ionized particulates are referred to as a mass loss in PPTs. Many experiments suggest almost 40% of the mass loss from a PPT is low-speed non-ionized macro particles that do not contribute to impulse and thrust as much as the ionized gas⁵.

The pulsed plasma thruster (PPT) used on the Earth Observing-1 (EO-1) spacecraft was first operated successfully in 2002. The thruster was used to counter disturbances in the pitch axis. A two-axis thruster system as seen in figure 2 was used for this mission. The EO-1 PPT system demonstrated a very good mass reduction for an attitude control system. The EO-1 two-thruster unit was just less than 5 kg⁶. The EO-1 PPT was tested extensively especially for radiative emissions for each arc level. Flight operation has begun on January 4, 2002 and within one year, 168,000 pulses have been logged with 46.7 hours of operation. EO-1 was carrying optical sensors and precision control of pitch axis of spacecraft was achieved without any kind of damage and any interference during or after PPT firing. As a result, a significant experience with PPT integration flown and operated with a very high degree of compatibility was achieved in this mission⁶.

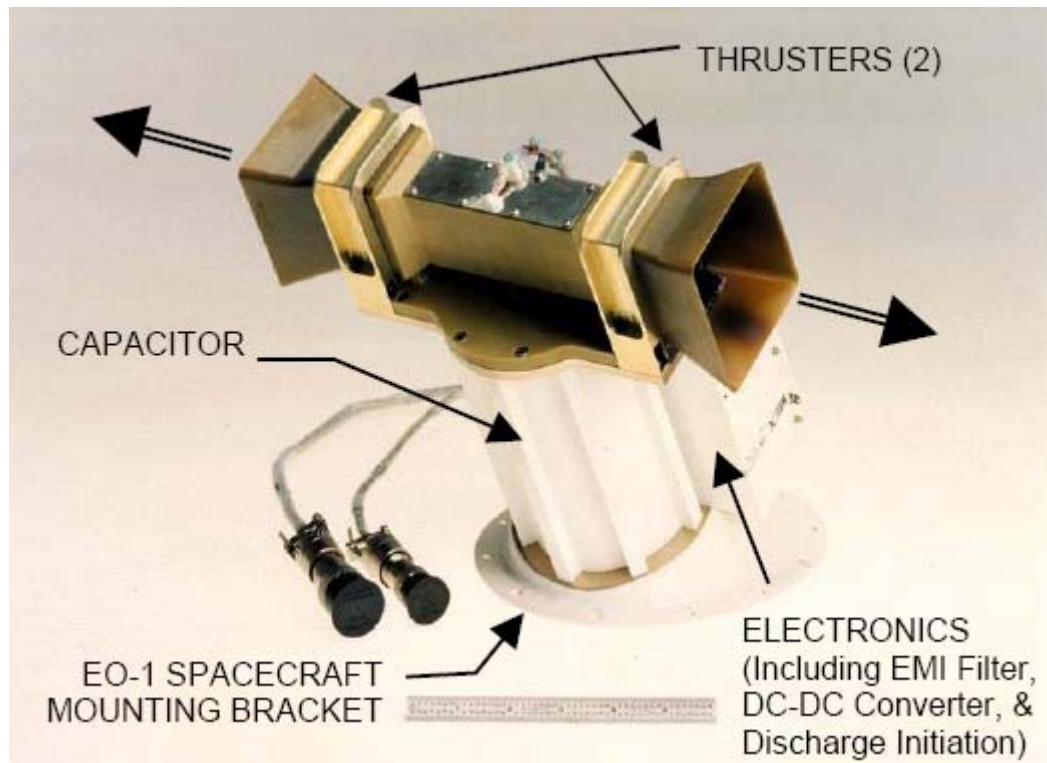


Figure 2. EO-1 Pulsed Plasma Thruster⁶

Micro Pulsed Plasma Thrusters (μ PPT)

There is increasing interest in the so-called micro- and nano-satellites, which are highly maneuverable and have lower cost. These small satellites are aimed to perform various missions like surveillance, space environment research, imaging etc. From a propulsion point of view, these missions require high specific impulse in order to get high impulse levels with lower mass. A μ PPT is another option designed by the Air Force Research Laboratory (AFRL) to create very small impulse bits for small satellites. For 100 kg class micro-satellites, μ PPTs provide attitude control and supplement station keeping. For 25 kg or smaller satellites, μ PPTs can be deployed as the primary propulsion system and can perform both attitude control and station keeping¹².

The μ PPT design is very similar to traditional PPTs. μ PPTs are simplified and miniaturized version of PPTs with μ Newton thrust levels. In some critical areas, μ PPTs are fundamentally different from traditional PPTs enabling an order of magnitude in mass reduction. The most important difference between a standard PPT and μ PPT is circuitry.

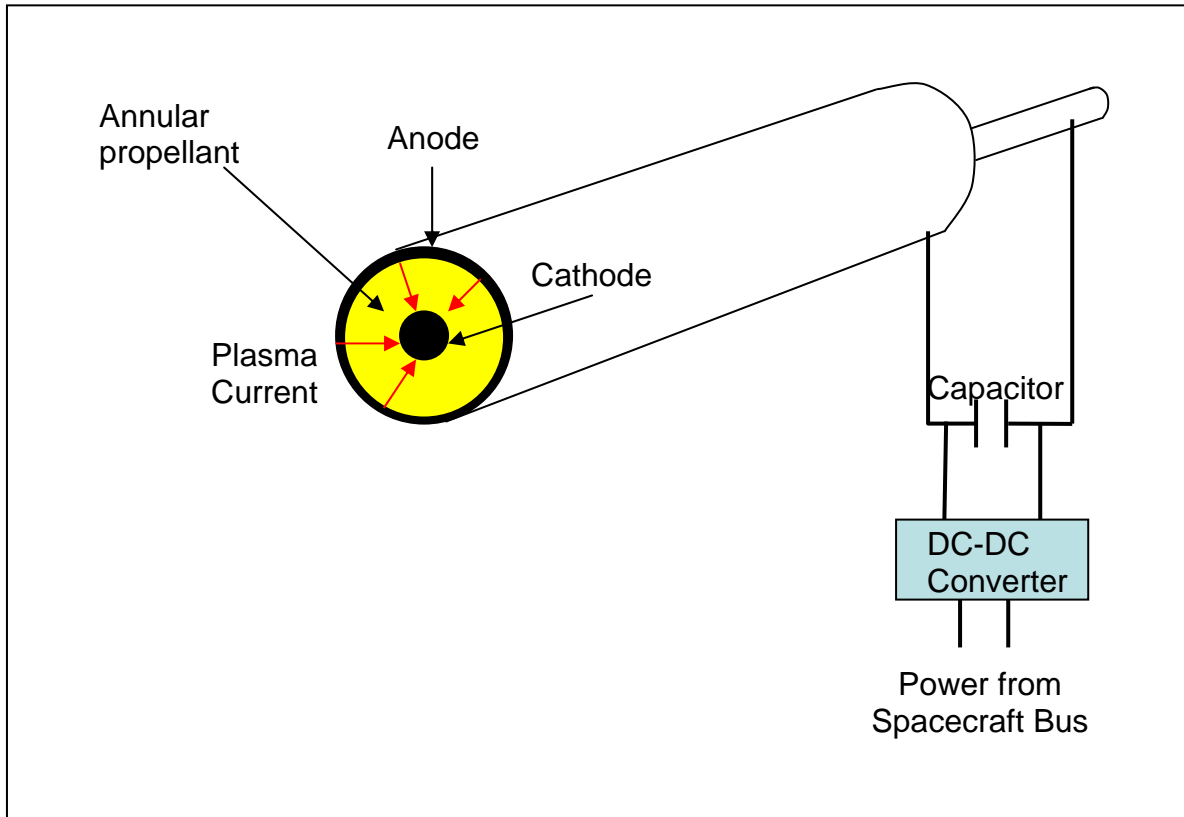


Figure 3. Schematic of a μ PPT

μ PPTs can be designed to use only one circuit as seen in Figure 3, requiring one capacitor, one high voltage converter and a coaxial type electrode arrangement with annular polytetrafluoroethylene propellant for a complete propulsion system. Micro PPTs can be designed without a spark plug. This self triggering spark generation enables a great amount of mass reduction with one less capacitor and therefore one less circuit. A self-triggering μ PPT applies a high voltage potential across the electrodes. When the

potential difference between electrodes exceeds the surface breakdown voltage, the μ PPT creates discharge across propellant between electrodes. The discharge ablates a small amount of solid propellant and ionizes it then accelerates the plasma by means of the Lorentz force.

A spark plug can be used to reduce the amount of potential difference required to create the main discharge between the electrodes as it was done in this research. Lower voltage levels may provide a great deal of mass reduction since the capacitor is the heaviest component of this system.

Whether or not a spark plug is used for the system, the appropriate amount of electrical energy must be accumulated to create discharge across the electrode gap. Since we require very large current (as high as 10^5 10^6 amps) to create a discharge across electrode gap, it is a must to use an electrical storage units such as capacitors³.

Required capacitance and initial voltage V_0 is defined by the requirements that it should be large enough to achieve the discharge event. It was empirically found that a certain amount of linear current density must pass through the surface to accelerate ionized particles effectively³. μ PPT electrode gap is 0.002m and using discharge speed of 10^4 m/sec and 10^4 amps current³ : $\tau = l / \dot{x} \approx 2 \times 10^{-7}$ sec So we require an initial charge storage $Q_0 \approx J\tau > 0.002$ coul to sustain the pulse through the discharge. Hence a capacitance level $C = Q_0 / V_0 > 0.002 / V_0$ farad is required. Using $1500 < V < 5000$ volts, capacitance values about $0.4 < C < 1.33 \mu\text{f}$ is required. A typical value of $1 \mu\text{f}$ capacitor and 2000 volts potential was used in most of the tests. This corresponds to energy of:

$$W_0 = \frac{1}{2} CV_0^2 = 2 \text{ joules} \quad (2)$$

The propellant of μ PPTs has a coaxial geometry with an inner cathode and outer shell anode. The solid propellant is typically Polytetrafluoraethylene. This propellant arrangement highlights another difference from the standard PPTs as well. The standard PPT uses a spring to feed solid propellant as it recedes (Figure 1). For the μ PPT where dimensions are limited and simplicity is required, a spring mechanism to feed the propellant is not used. μ PPTs do not have a propellant feed system. Inner and outer electrodes of μ PPTs ablate and recede as the propellant is used through discharge events. Therefore, no mechanism is required to feed the propellant to the tip of the thruster.

μ PPTs offer a wider range of advantages. Simplicity and tanking is one of the most important characteristics since μ PPTs do not have a propellant feed system. The propellant used (PTFE) is non-toxic and easily handled. μ PPTs also offer low average electric power requirements and higher thruster specific impulse values than chemical systems, as high as 1000 sec^{13} . The electromagnetic acceleration of the plasma in these micro propulsion systems provides $\mu\text{N-s}$ impulse levels, eliminating the need for a nozzle for controlling expansion of a plume.

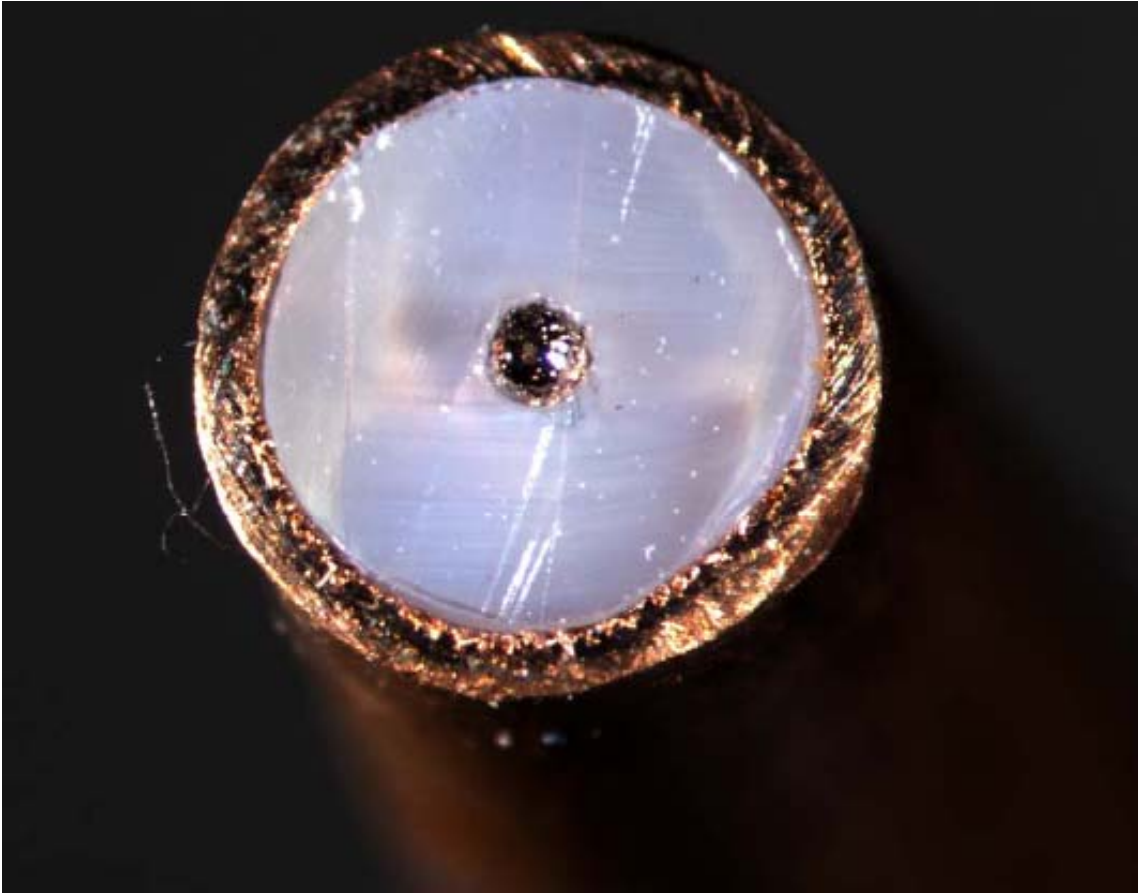


Figure 4. Tip of propellant module of an unused μ PPT

Four μ PPTs are being used by the Air Force's FalconSat-3 satellite for 2-axis attitude control. FalconSat-3, launched in February 2007, is an experimental satellite designed and built by United States Air Force Academy (USAFA)¹⁴. This satellite is a 50 kg satellite and its mission is ionospheric plasma and attitude control propulsion research.¹⁵ Research focuses on the need for precise positioning control of several small satellites for formation flying requiring a propulsion system delivering micro-Newton thrust levels. A μ PPT was developed for FalconSAT-3 with a 0.7 kg weight, using 10W and creating 800 sec specific impulse¹⁶.

Mass Expulsion/Deposition

Contamination effects of micro propulsion devices are very important issues and especially for small satellites. On-board instruments and solar panels can be affected by this contamination. Numerous tests were performed studying contamination effects of PPTs at AFRL Propulsion Directorate at Edwards AFB. In one similar experiment, the XPPT-1 (eXperimental Pulsed Plasma Thruster No. 1) was used. This traditional PPT had 2.5 cm electrode gap which is very large compared with μ PPT used in this research that has 2 mm electrode gap.

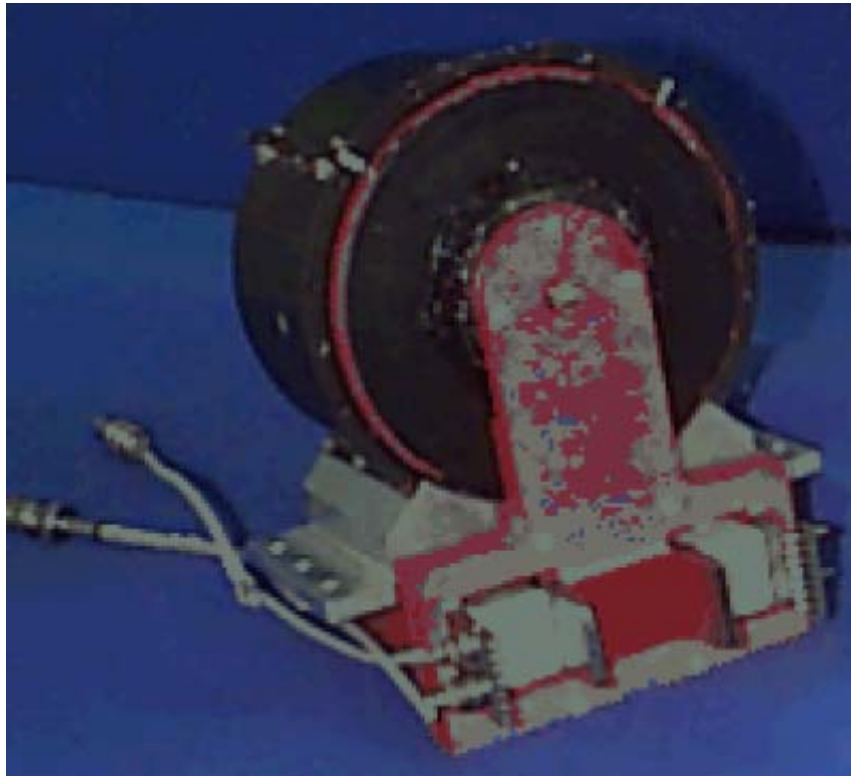


Figure 5. Experimental Pulsed Plasma Thruster No 1 ¹⁷

Particle emissions were characterized by means of an array of aluminum witness plates placed in front of the thruster to collect the exhausted particles. Witness plates

were analyzed by SEM showing a great number of particulate deposits. As seen at Figure 6, images of the witness plates were analyzed at several magnification levels. This analysis showed 30% of the propellant was expelled in the form of particulates. Propellant used in the form of solid particles leads to a large contribution to the inefficiency of this type of device. These are the particulates leading to the contamination on spacecraft surfaces which may reduce transmittance of solar panels or contaminate instrumentation on board the spacecraft¹⁷.

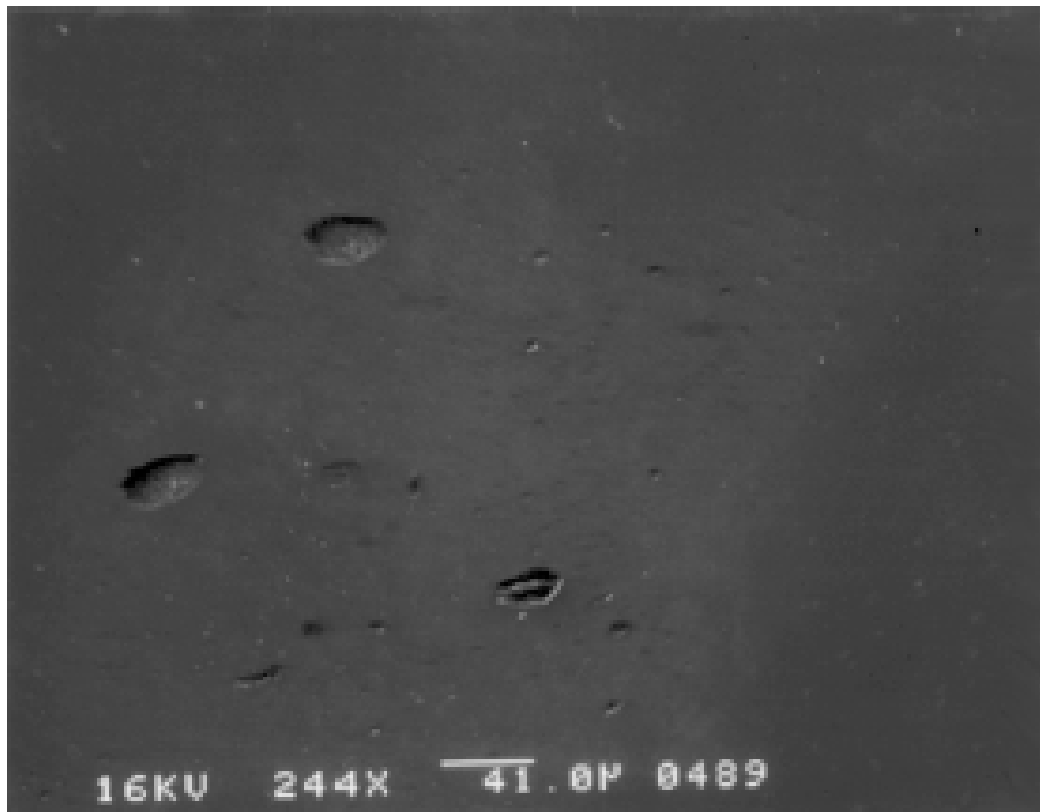


Figure 6. SEM image of particulate deposits on an aluminum witness plate¹⁷

After designing several circuits for μ PPTs with the goal to reduce inert mass, AFRL Propulsion Directorate at Edwards AFB continued plume measurements to further

assess the potential spacecraft contamination induced by μ PPTs. Exhaust plumes of a 5 J μ PPT using 6.35mm diameter propellant modules were imaged using high speed photography to observe the direction of particulates in the exhaust plume. The particulate traces were all directed forward along the primary axis of the thruster. Back flow was not seen in these images. As seen at Figure 7, the coaxial geometry of μ PPT seemed to prevent particulates from back flow trajectories toward the rear part of the thruster¹².

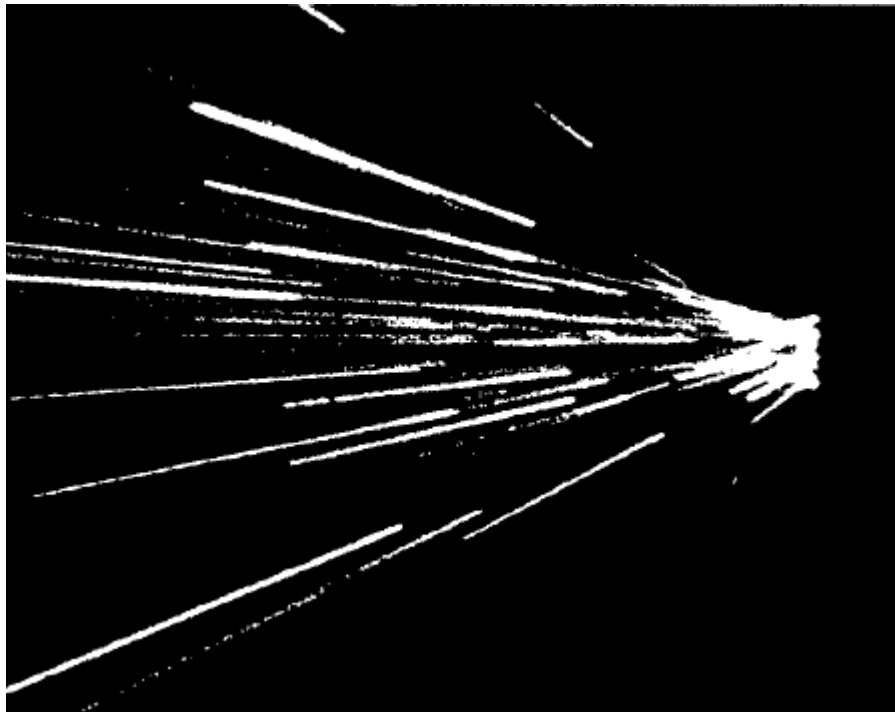


Figure 7. μ PPT exhaust plume taken by G.G.Spanjers et al. AFRL Electric Propulsion Laboratory¹²

Another experiment performed at NASA Lewis Research Center together with Worcester Polytechnic Institute attempted to characterize PPT plumes and assess their contamination characteristics. The Lincoln Experimental Satellite (LES) 8/9 PPT was used. A large number of collimated quartz contamination sensors were used for plume

diagnostics. Potential impact of contamination on solar arrays was evaluated by measuring the transmittance and weight of quartz sensors before and after being exposed to the PPT plume. Contamination measurements were made in both near and far field regions. Results showed no mass deposition at backflow regions. In near field measurements it was also found high-velocity ions caused sensor erosion within -40° and $+5^\circ$ of the thruster centerline. For positive angular locations positive net mass deposition was found. Mass deposition studies also revealed that for angles larger than 50 degrees, no measurable mass deposition was found (Figure 8)¹⁸. Asymmetry was resulted because of enhanced deposition at the cathode side since LES 8/9 thruster was a breech-fed rectangular design.

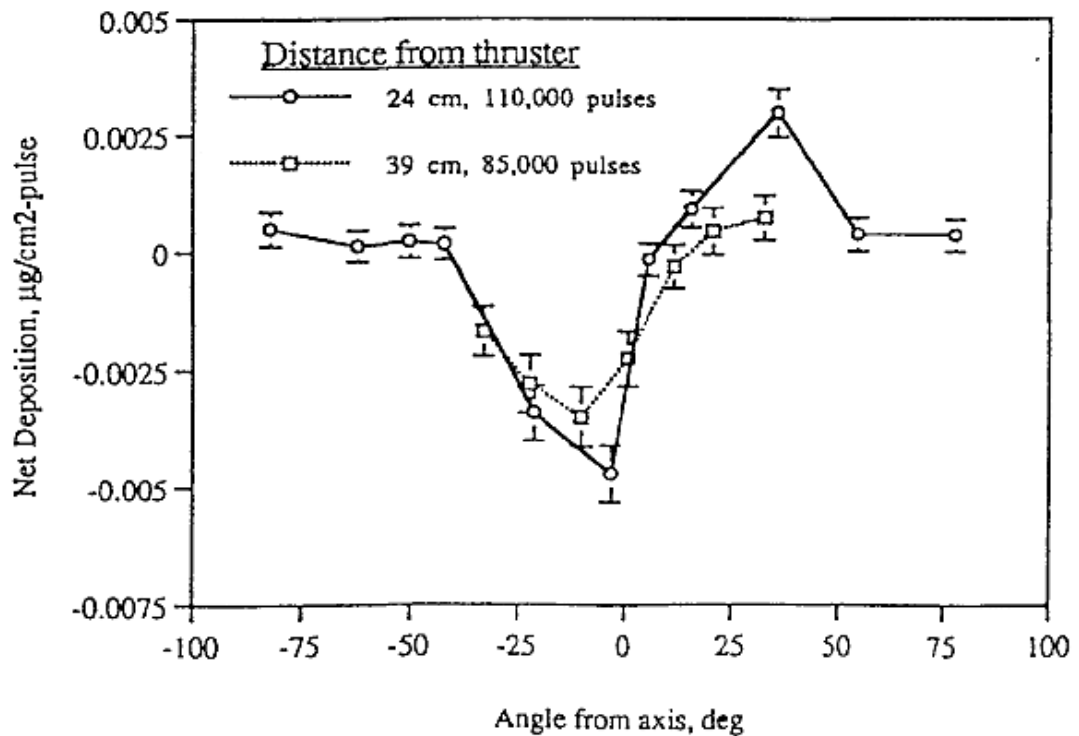


Figure 8. Net mass deposition on quartz sensors¹⁸

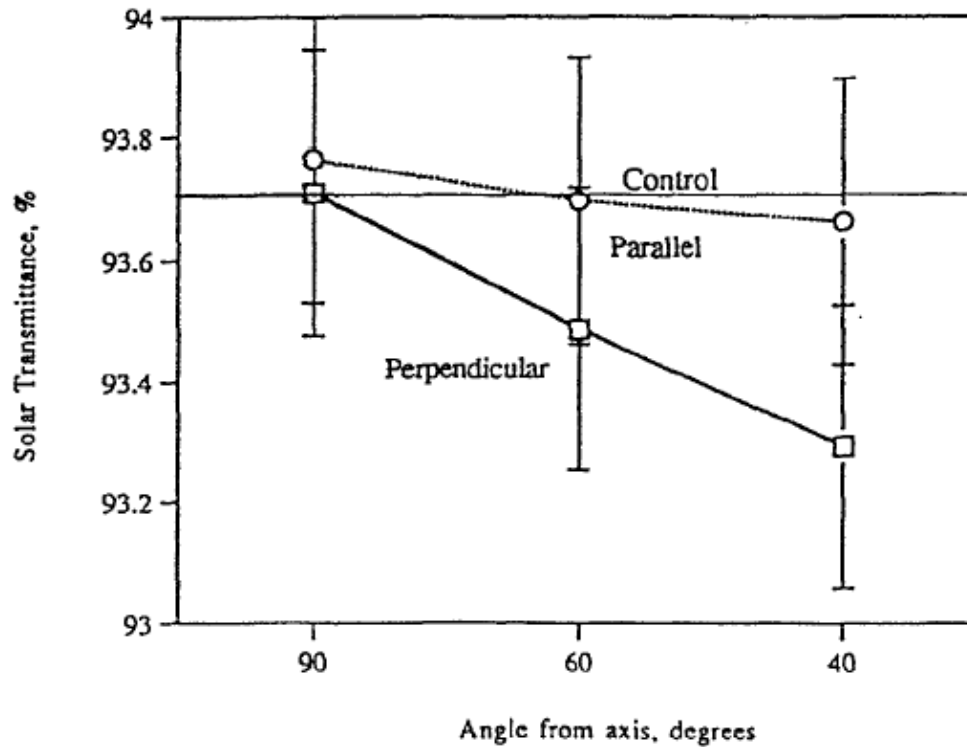


Figure 9. Solar transmittance of quartz sensors for far field measurements¹⁸

Figure 9 above shows solar transmittance decreasing with lower angles where sensors were placed. These measurements were made after 2×10^5 pulses. If the particulates sticking to solar panels cause a decrease of transmittance, then the contamination of solar panels may limit the spacecraft mission and mission duration, highlighting the need to understand the contamination effects of μ PPTs thoroughly.

Pulsed plasma thruster plume symmetry and impact on spacecraft surfaces was also investigated at NASA Glenn Research Center together with California Institute of Technology. Twenty-four witness plates placed perpendicular to the plume were used to collect plume constituents for analysis. A 43 J breadboard PPT was used. Asymmetry of

film deposition on witness plates was analyzed with both mass and optical parameters such as reflectance and transmittance.¹⁹

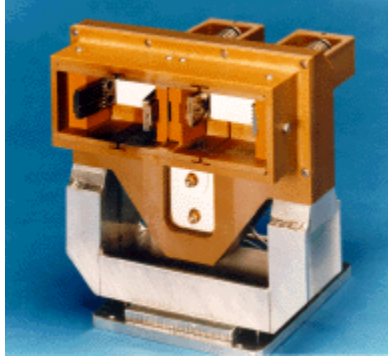


Figure 10. NASA Lewis/PRIMEX breadboard PPT

Changes in masses of witness plates show plates right in front of thruster gained more mass compared to plates at wider angles. Because the thruster was a rectangular arranged PPT rather than a coaxial type, the electromagnetic forces attracted the plume to the cathode resulting in an off-axis thrust component. Cathode side witness plates showed more mass gain. Optical measurements of witness plates were made using a spectrometer. Results showed decreases in transmittance and reflectance.

Operational Limits

Optimization issues of μ PPTs were also investigated focusing on propellant charring. The choice of energy level for a given thruster geometry type is very important²⁰. If a sufficient discharge energy level is not employed, propellant charring is likely to occur limiting the operational life of the thruster. Carbonization on the Polytetrafluoroethylene surface leads to a film growth. Because a carbon layer is more difficult to evaporate, the μ PPT will exhibit discharge problems²⁰.

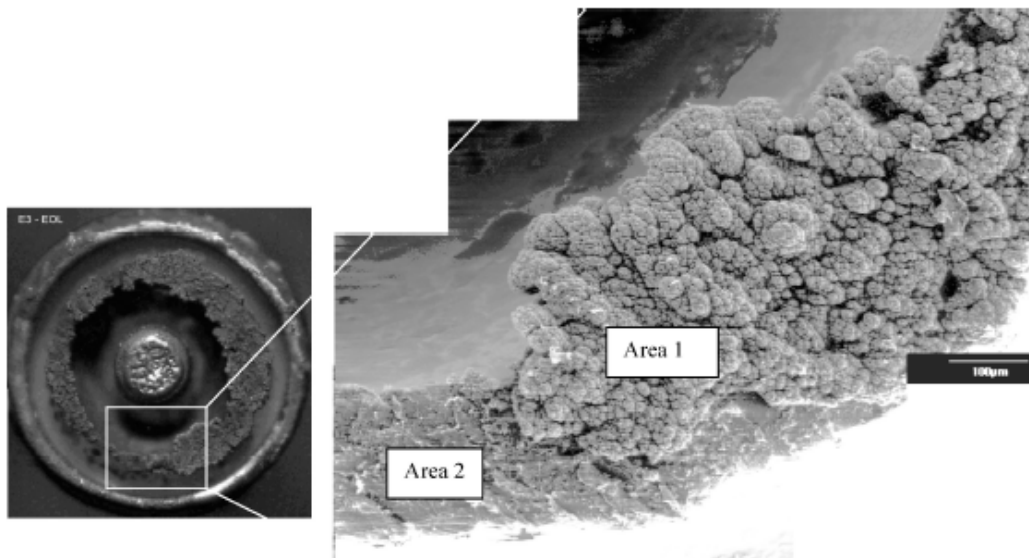


Figure 11. “Charred area on the propellant surface of the 3.6-mm μ PPT²¹”

Current constriction is another issue considered for optimization of μ PPTs. Low discharge energy may cause propellant charring but high energy can also prove to be limited. When the discharge current exceeds some critical value, current constriction might occur causing a higher ablation rate of solid particles and further degradation of the total impulse. Thus, μ PPTs should use a large enough pulse of energy to prevent propellant charring and a yet small enough to prevent current constriction²⁰.

Another research effort with PPT plume diagnostics (C. A. Scharlemann et. al.) analyzed pressure measurements of a PPT plume. Most plasma diagnostic instruments commonly evaluate charged particles only, but piezo ceramic-based pressure probes can capture contributions of heavy neutral particles as well. Time resolved mass distribution data was obtained by utilization of these pressure probes, making it possible to measure the impulse bit and the thrust vector²².

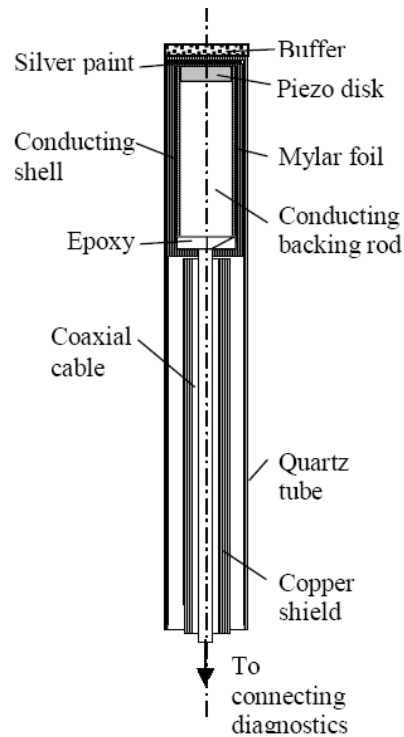


Figure 12. Cross section of pressure probe²²

Using pressure measurements, the mass flux of the exhaust plume was calculated. Evaporated propellant was also found by measuring propellant mass before operating the thruster. Analysis showed 25% of propellant mass contributed to the total impulse and 75% was lost because of thermal evaporation. These pressure probes proved capable of impulse bit and thrust measurements instead of having to use complicated mechanisms like torsional balance thrust measurement stands²².

Plume Models

Numerical methods are also studied in order to investigate the exhaust plume of μ PPTs. For the purpose of investigating plasma acceleration by electromagnetic forces,

plasma plume models were developed combined with plasma generation and Polytetrafluoraethylene ablation models²³.

For the ablation model, two layers are considered; Knudsen layer and a Hydrodynamic layer. The Knudsen layer is only a-few-mean-free-paths thick. Plasma conditions near the Knudsen layer edge strongly affect the ablation process because of the flux of returned particles to the surface of the propellant.

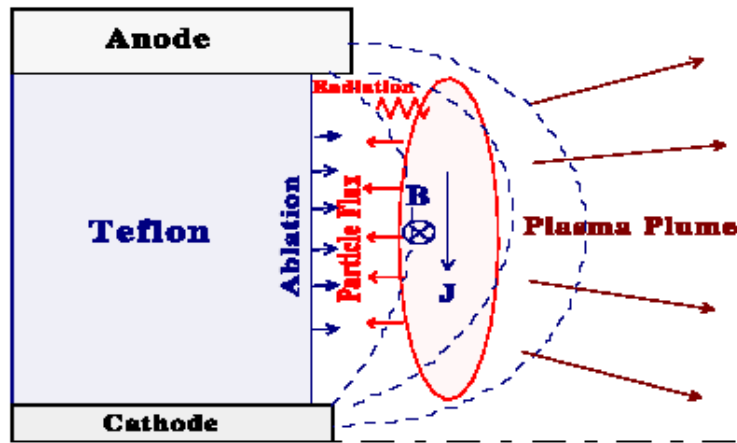


Figure 13. Schematic of Plasma-surface interaction in a μ PPT²³

With the assumption of ionization equilibrium reached at the end of hydrodynamic layer, electron density can be calculated using Saha equilibrium. Mass, momentum, and energy equations can be used with the appropriate boundary conditions. In this research, plasma and neutral density calculations were made and compared to experimental results taken at AFRL. Comparison of experimental data with simulation showed the plasma models agree well for the plasma and neutral density measurements.

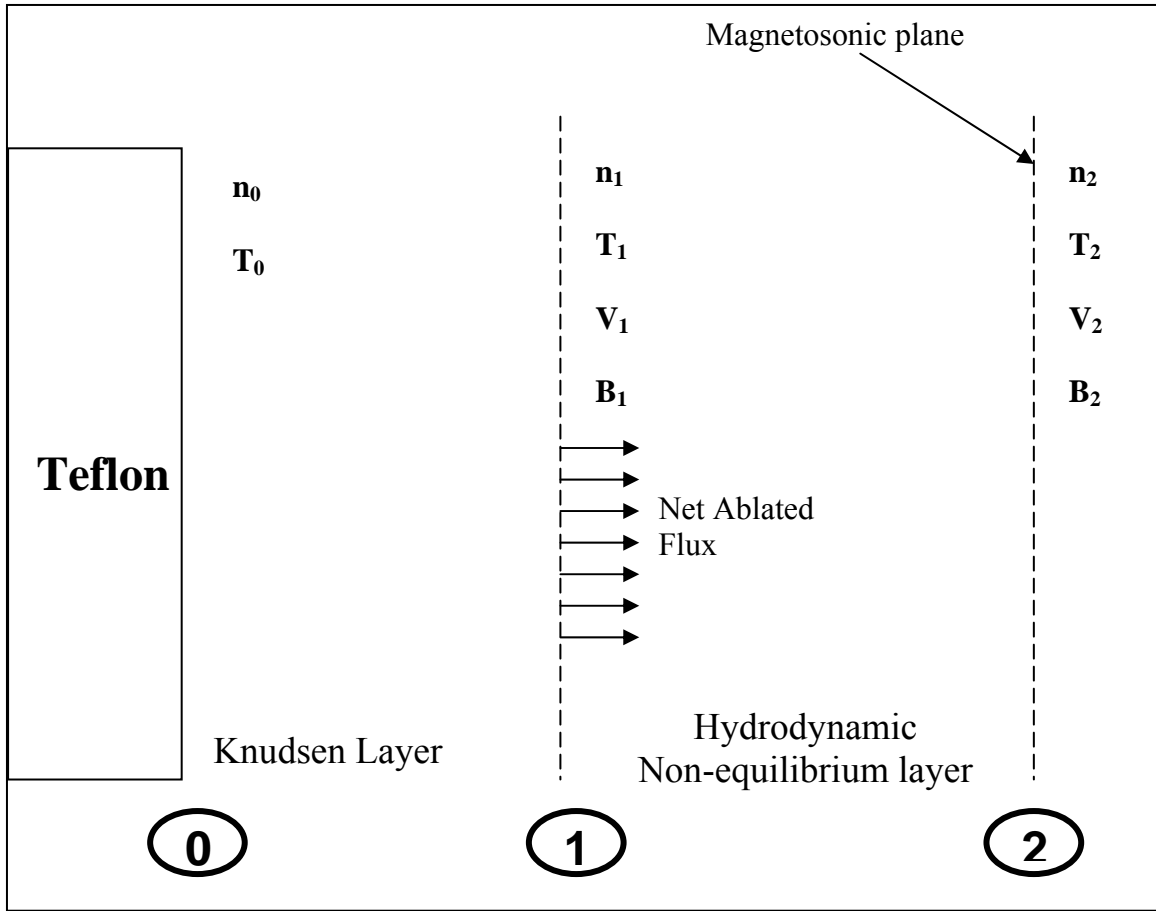


Figure 14. Schematic of near surface layers²³

Summary

PPTs are attractive propulsion systems especially for small satellites with low mass and power consumption limits. A μ PPT is a good option to create very small impulse bits for micro- and nano-satellites. Numerous researchers have studied PPTs but μ PPTs are a new technology and need a thorough analysis in all aspects. Contamination by μ PPTs is a very important issue that will negatively affect spacecraft surfaces and mission life.

III. Methodology

Chapter Overview

This chapter explains the experimental test setup and arrangement of testing tools. This experimental research included development of the μ PPT circuit, assembly of thrusters, construction of the witness plates holder and establishing space conditions in the vacuum chamber is described.

Vacuum Facility

Experiments were conducted in vacuum to simulate a space environment condition. A bell jar vacuum chamber in the AFIT laboratory was used to perform the tests. Dimensions of the chamber are 76.2 cm (30 in) in height and 66.0 cm (26 in) in diameter, large enough to accommodate μ PPTs and the thrust stand components. The vacuum chamber facility uses two types of pumps to achieve high vacuum, 10^{-6} - 10^{-7} torr level. One pump will not take the system to such a low pressure level²⁴. Two pumps are used in this system to reach these pressures.

In this system, a Welch 1374 belt-drive roughing pump is used for the first stage to achieve pressure levels on the order of 10 mtorr (Figure 16). After achieving the crossover pressure, an oil diffusion pump begins operation to continue lowering the pressure. This lab has a Varian VHS-6 oil diffusion pump (Figure 16). A specific crossover pressure level is required before operating the oil diffusion pump.

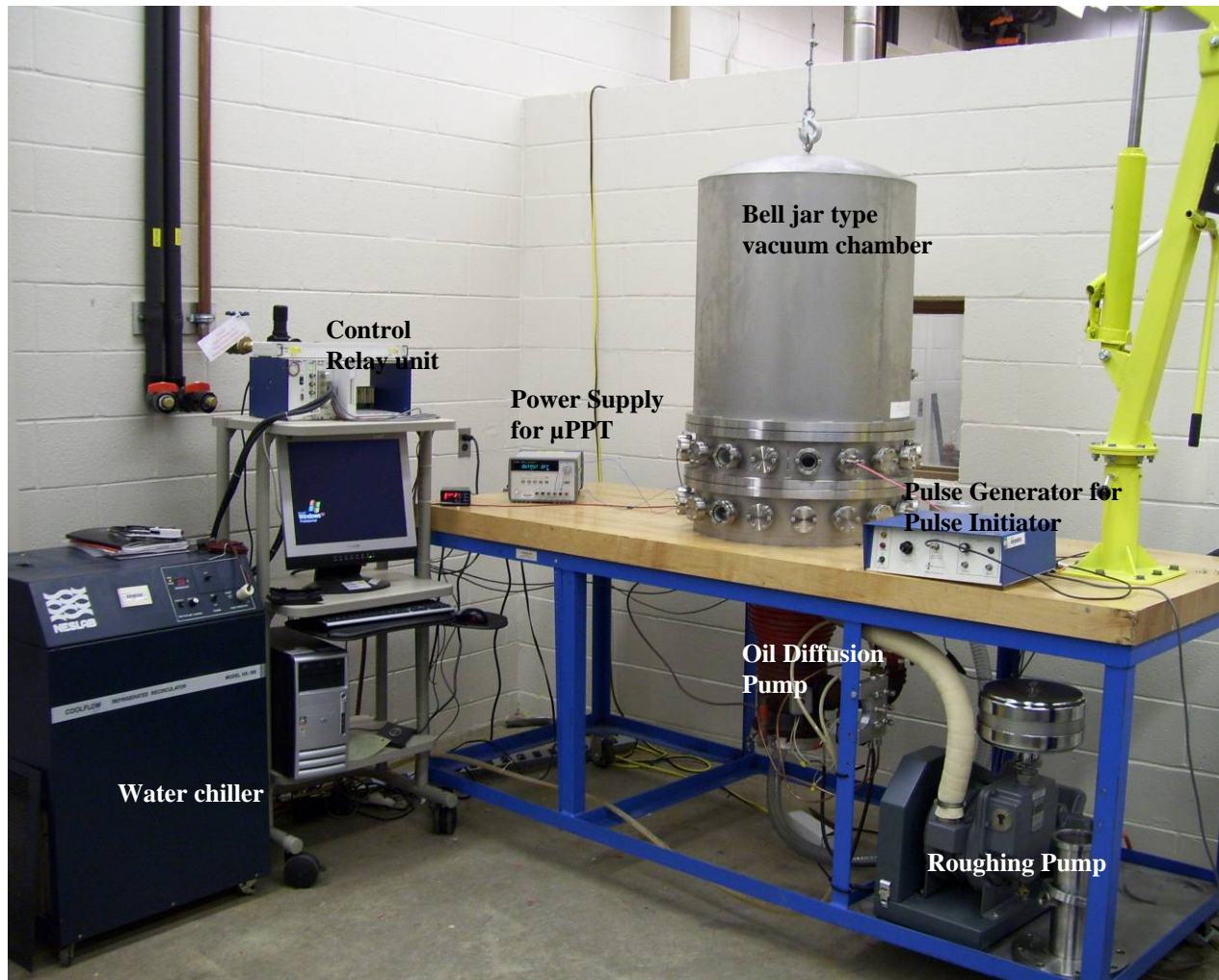


Figure 15. AFIT's Micro propulsion vacuum facility

The operation to bring the vacuum chamber to low pressure requires a special sequence to open and close valves and operate the pumps. Valves used in the system were controlled by the system computer through control relays, making the pumping down process automatic. The control program, written using National Instruments LabVIEW® program interface controls the valves and pumps.

Initially, the roughing pump brings the chamber down to the crossover pressure (Figure 15). During the initial roughing, the oil diffusion pump is heating up the oil; but

the diffusion pump valve is closed. Operating pressure levels for diffusion pump are much lower than atmospheric conditions. So, the chamber must be roughed before operating oil diffusion pump.

Once a 10 mtorr pressure level is reached by the roughing pump, the diffusion pump valve is opened and the roughing pump valve closes. Both pumps run continuously. The roughing pump continues pumping through the diffusion pump. This configuration brings the chamber to vacuum pressure levels as low as 10^{-6} - 10^{-7} torr. All tests were performed under these conditions.

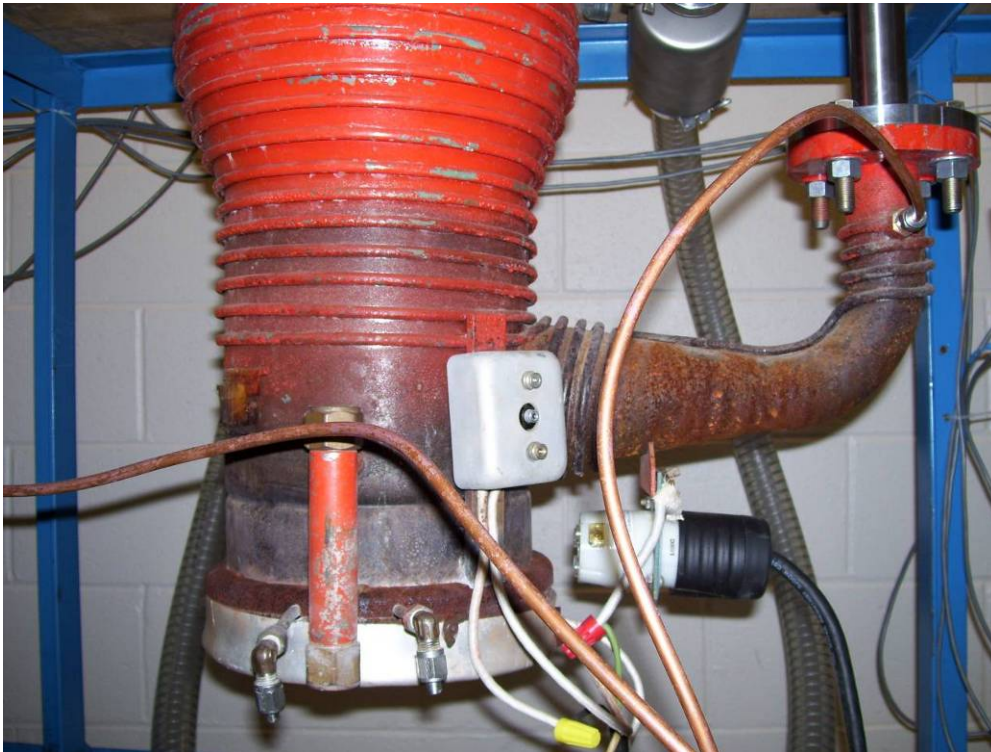


Figure 16. Oil Diffusion pump of the vacuum facility

After the tests are completed, the vacuum chamber is vented. The venting process is also an automated procedure, controlled using the same control relays commanded by

the LabVIEW® interface. Before the venting valve is opened, the oil diffusion pump needs to be turned off and the boiling oil needs to cool. Otherwise, boiling oil might enter the vacuum chamber contaminating the test articles and coating the chamber.

Control Configuration

μPPTs used in this research were first built by AFRL Electric Propulsion Laboratory at Edwards AFB, CA. The control circuit was modified at AFIT. A pulse initiator was added to the system. These thrusters do not have any moving parts and have only three major components. Major parts of thruster are propellant tube with two electrodes, high voltage capacitor, DC-DC high voltage converter and a power supply, simulating a spacecraft power supply unit. Connections between the propellant tube, the capacitor and the DC-DC converter used high voltage cables. The propellant tubes used here have two copper electrodes and annular PTFE propellant separating the anode and cathode (Figure 4). The DC-DC converter operated over the input voltage range of 1 - 15 volts and delivered 0 - 7000 volts. The high voltage capacitor used in this research had a 1μF capacity and had an operating voltage of 5000 volts.

One of the objectives of this study was building a reliable thruster system. The pulse initiator was added as a second circuit to system in order to increase the reliable operation of the thruster. For pulse initiation, the experiment used a separate spark tube with smaller diameter (2mm) (Figure 17).

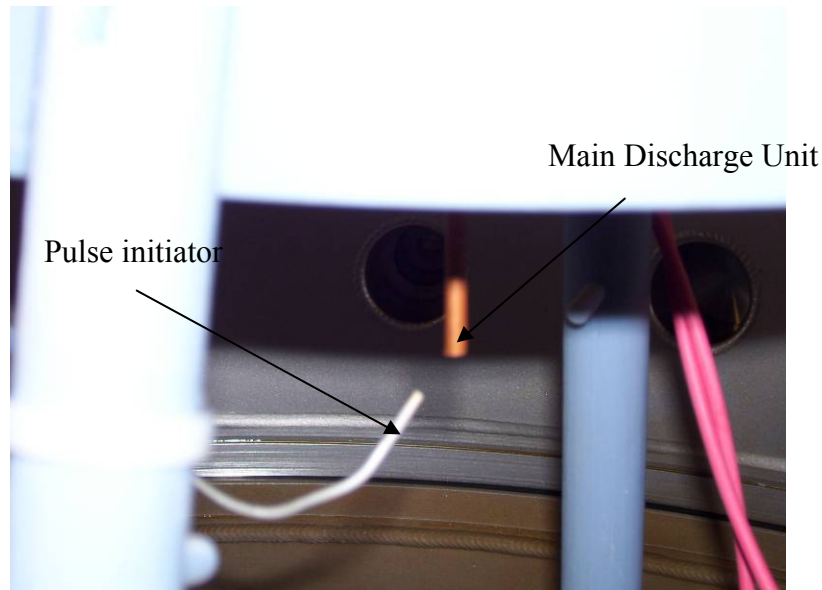


Figure 17. μ PPT with pulse initiator

The pulse initiator was powered by a pulse generation system (Xenon Model-437B Nanopulse System) enabling precise control of the pulse voltage and pulse repetition rate (Figure 18). By controlling the pulse initiation, the main discharge was controlled to generate a single pulse or an automated pulsing at the desired repetition rate. By controlling the pulse initiation, impulse bits and thrust delivery profile can be tailored to the desired test and mission requirements. This pulse generation system also had a remote pulse control mechanism. Remote pulse control mechanism was also used to create individual pulses during reliability tests.

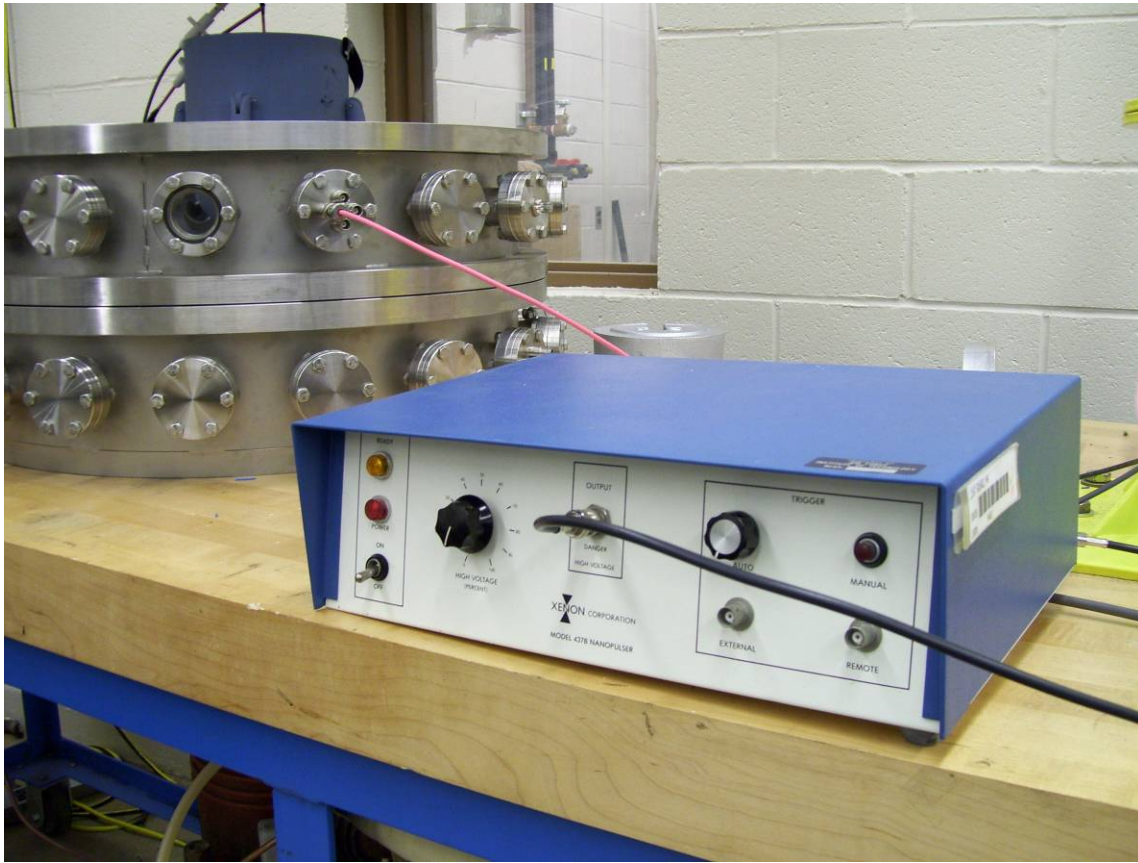


Figure 18. “Xenon Model-437B Nanopulse System” used for pulse initiator for μ PPT

Ensuring the discharge arc occurred only at the propellant tip required some care because high voltage arcs can occur anywhere in the circuit. Insulating the exposed parts solved the problem. For insulation, Corona Dope® liquid insulator tape was used to prevent arcing between circuit components and the vacuum chamber surface.

Contamination Test Setup

The contamination study of μ PPTs was conducted in high vacuum pressure conditions to resemble the space environment. Pressure levels used during these experiments ranged between 10^{-6} - 10^{-8} torr. Before beginning the tests, the thruster and

witness plates had to be secured in order to analyze contamination effects. A thrust holder was designed using AutoCAD® software to secure the thruster. The thrust holder had to be built in such a way to secure a thruster and the witness plates at the same time to investigate mass deposition of the exhaust plume of μ PPTs. The thrust holder was built by AFIT's EDEN 330V 3-D printer.

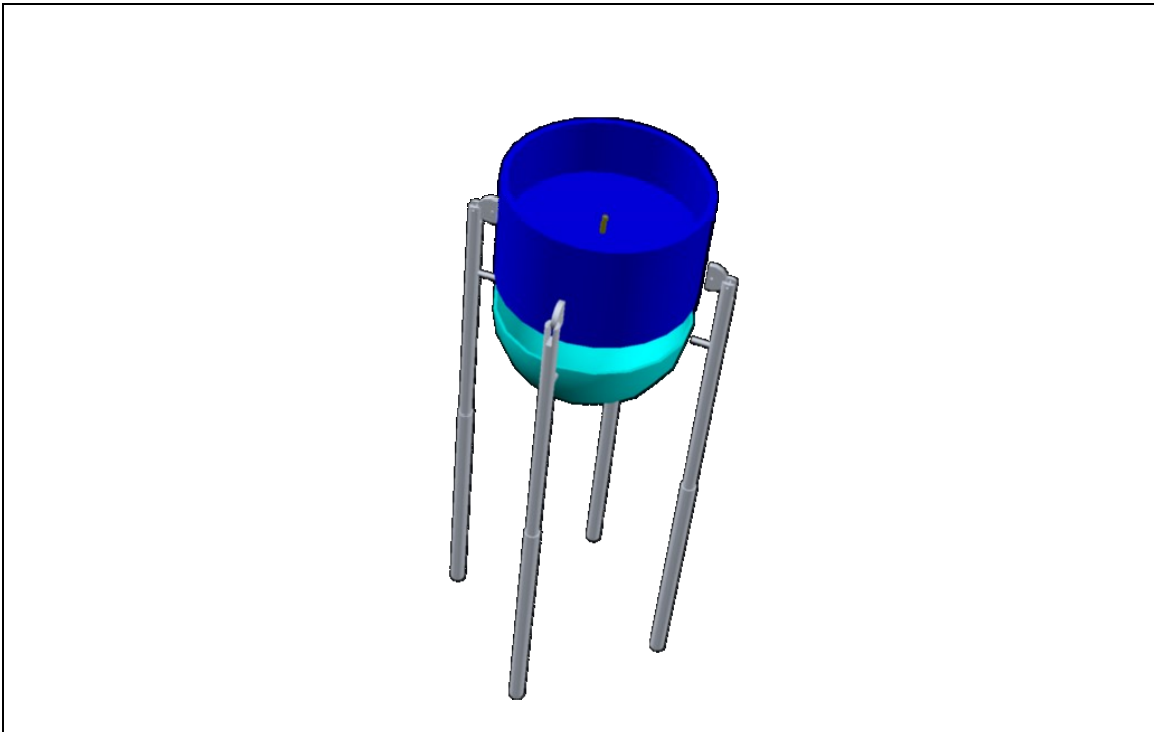


Figure 19. AutoCAD design of Thruster holder

Thrust holder was designed to secure the μ PPT pointing downward so gravitational effects on the particles were minimized. Gravitational effects might have caused error in mass deposition of particles in the μ PPT plume. In order to perform contamination analysis without being effected by gravitation, the μ PPT was secured downward in the thrust holder.

Aluminum witness plates were placed to acquire the mass deposition of solid particles at various angles from the thruster centerline. In order to place the array of witness plates, a bowl shaped witness plate holder was designed and added to the thruster holder. A bowl shape was used to place witness plates at equal distances from the thruster and hence investigate the contamination in all directions to evaluate the contamination effects of the thruster.

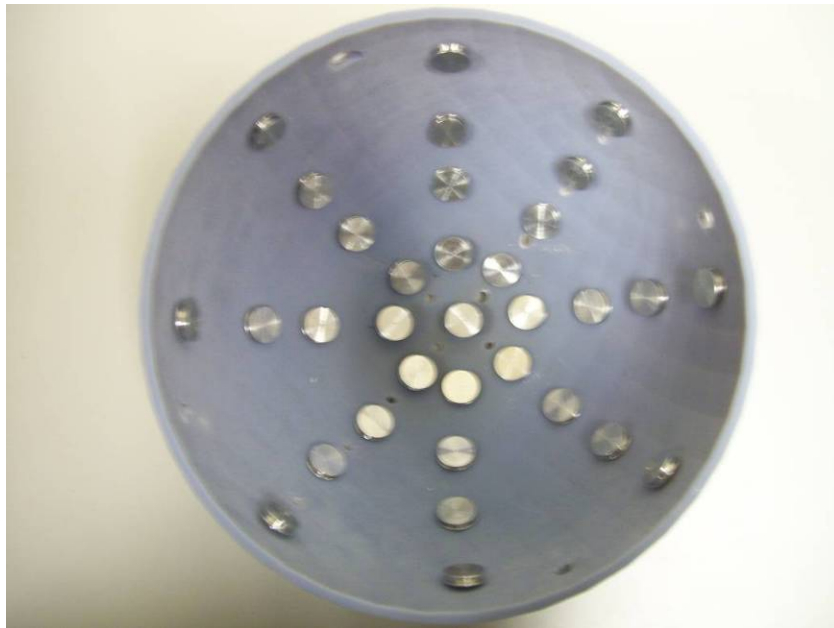


Figure 20. Bowl-shaped witness plate holder (Test-1 Configuration)

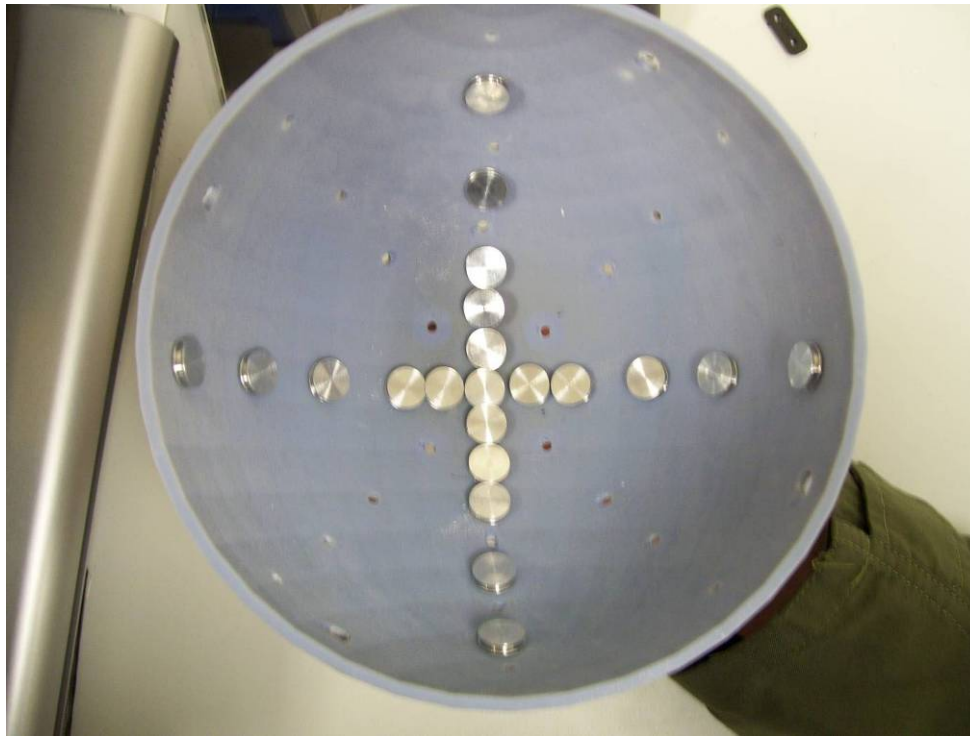


Figure 21. Bowl-shaped witness plate holder (Test-2, 3 Configuration)

To improve resolution and increase the quality of the data collected, several arrays of holes were used to place the witness plates (Figure 20). In each array, eight witness plates were positioned ranging from -90 degrees to +90 degrees with respect to the thruster. A second configuration increased the number of witness plates increasing the number of data points to get a better deposition profile of the particles ejected from the thruster (Figure 21). Because of the expected higher deposition gradients at small angular positions, more witness plates were placed at the central region of the holder. Witness plates were marked to capture the orientation as well, allowing single witness plates to provide several data query points. This technique increased the angular position count and let us to get a smoother curve for mass deposition of the μ PPT exhaust plume.

During the contamination tests, mass deposition gradients were highest along the axis of the thruster. In order to get an efficient statistical data to provide accurate representation of the mass deposition profile, images were taken from many angular locations (Figure 22). As seen in the figure below, a single point measurement included at least five images to allow for better averaging of the results. Each witness plate could provide several single point measurements.

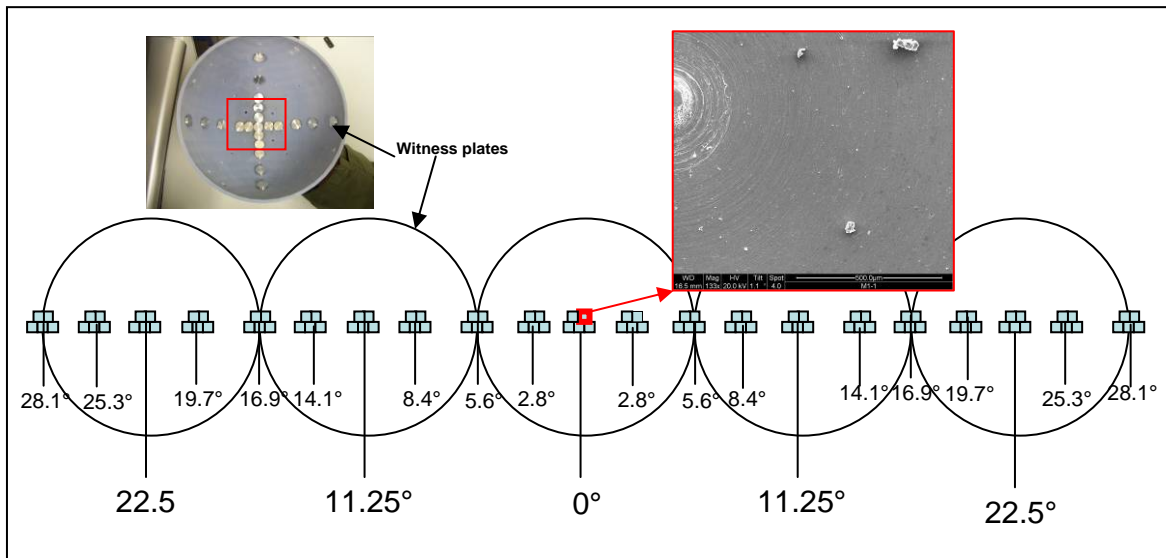


Figure 22. SEM snap-shots were taken from many angular locations

Before the tests, all witness plates were cleaned with alcohol then allowed to dry. After they dried, they were placed in the witness plate holder to collect samples. Cleanliness of witness plates was very important because of the small size of the particles being analyzed, ranging from 5 to 60 micrometers. Witness plates were handled very carefully using gloves and avoiding any contact before being analyzed by SEM.

The test setup can be seen in Figure 23 and Figure 24. The thruster was secured in the thrust holder upside down to minimize gravitational effects. Witness plates were placed in the holder at different angles as seen in the figure. In the first test setup, 33 witness plates were used to analyze mass deposition profile, deposition rates and particle size distribution for contamination study (Figure 20). Witness plates were distributed along four axes with nine witness plates along each. A second configuration employed 21 witness plates in two axes (Figure 21). More plates were used to increase angular position resolution.

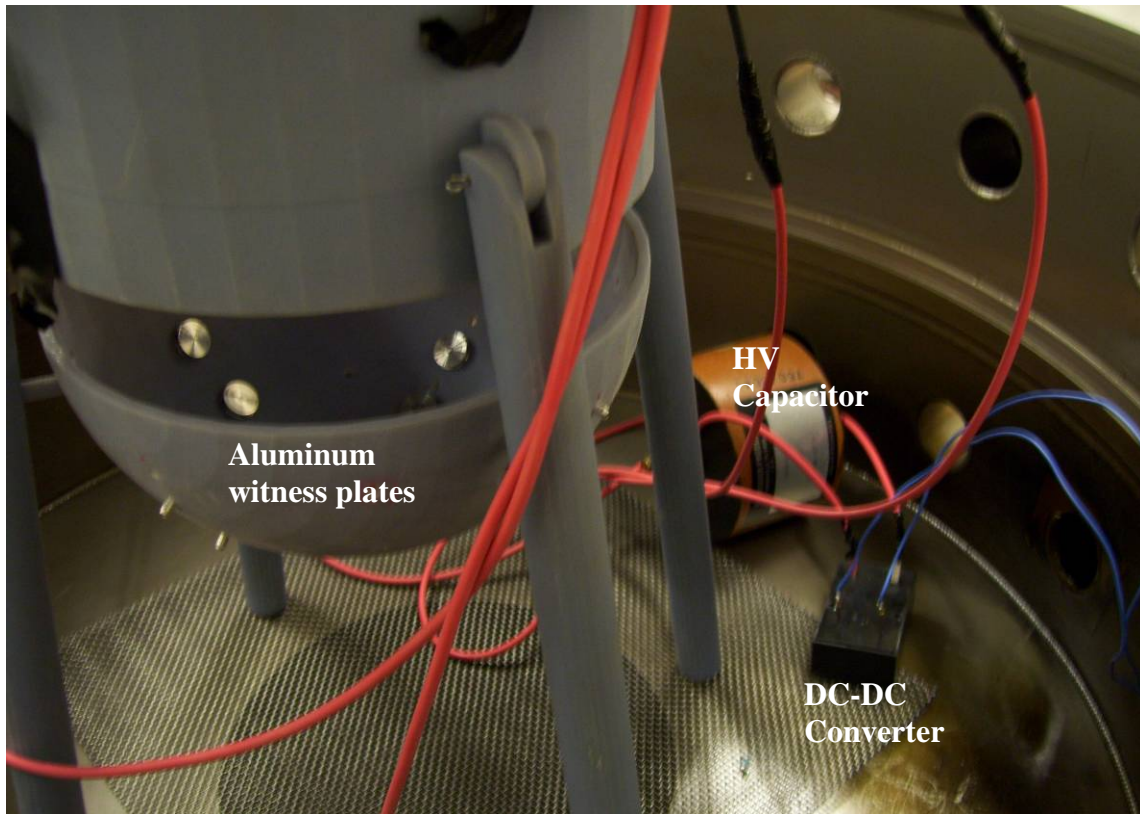


Figure 23. Test Setup

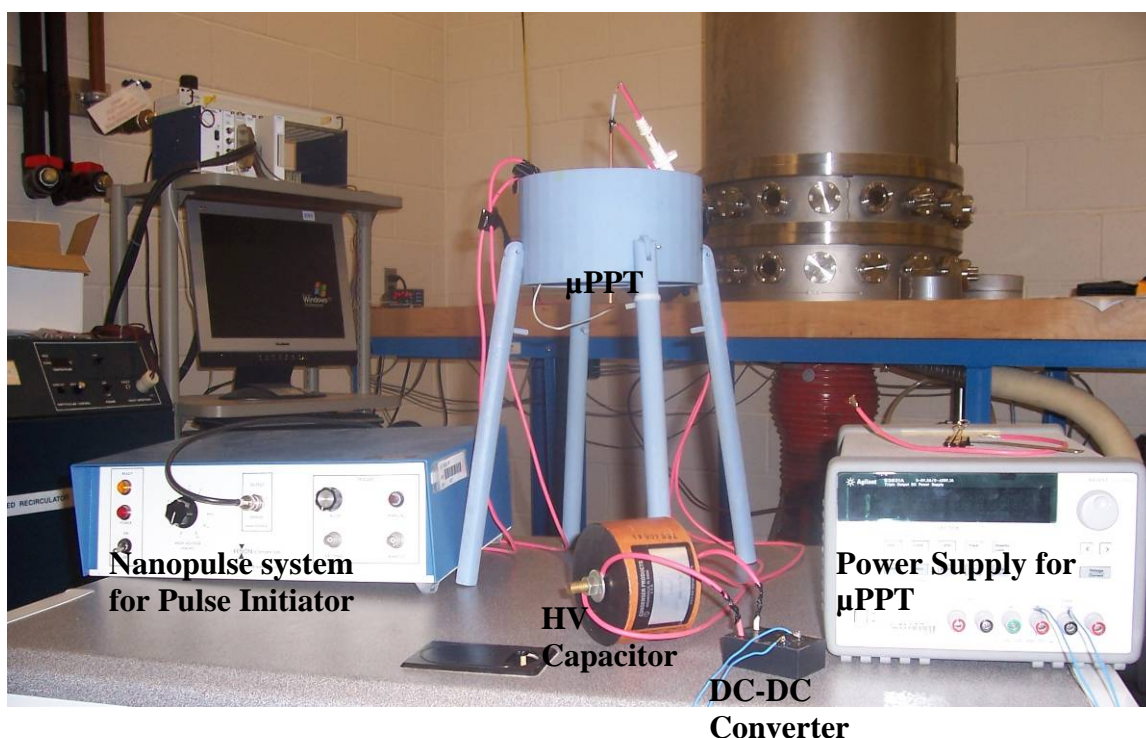


Figure 24. Test Setup

After each test, witness plates were taken out of the plate holder bowl with extreme care. Each witness plate was examined with AFIT's SEM (Scanning Electron Microscope). Pictures of the surface were taken at 133x magnification levels. Different magnification levels were tried to better analyze the mass deposition profile but this magnification level was chosen since it allowed the researcher to distinguish particles as small as 5 μm with sufficient detail. Smaller particles were also detected at higher magnification levels but do not contribute to the overall mass. Particles smaller than 5 μm diameter size were not counted.

Particles were discriminated by their diameters from the SEM snapshot pictures and counted to find mass deposition as a function of angles. For mass calculations, all the particles were assumed half spheres. Several particles were analyzed by SEM at higher

magnification. All particles had a “potato like” shape (Figure 25). Because they stuck to the witness plate, they were all assumed to be half spheres to calculate the volume and mass. Weighting technique for calculating mass deposition was not used because in some of the tests mass deposition values were on the order of nano grams. Therefore it might have been difficult to quantify mass deposition with micro gram level scales. Also, similar study made by Roger Myers et al. showed that high velocity ions caused erosion on quartz collimators and negative mass deposition values was found. This research used calculation of total mass by finding total number and size of particles deposited on the aluminum witness plates in order to analyze mass deposition character of μ PPTs.



Figure 25. Single particles at higher magnification levels

Using SEM snapshot pictures, all the particles were counted (Figure 26) and total number of particles with their diameters was noted down on a spreadsheet. Volume of the particles deposited on a witness plate was calculated with the half-sphere assumption. Volume of the particles was converted to mass using density of PTFE ($2.2 \times 10^6 \text{ g / m}^3$). Hence total mass deposited on a witness plate was calculated. Same procedure was continued for the witness plates at various angular locations with respect to tip of the thruster. Using the spreadsheet all the mass calculations were converted to plots showing mass deposition profile, deposition rates and particle size distribution. Total mass deposition was integrated to quantify total mass that stucked to the witness plates for analyzing propellant utilization efficiency.

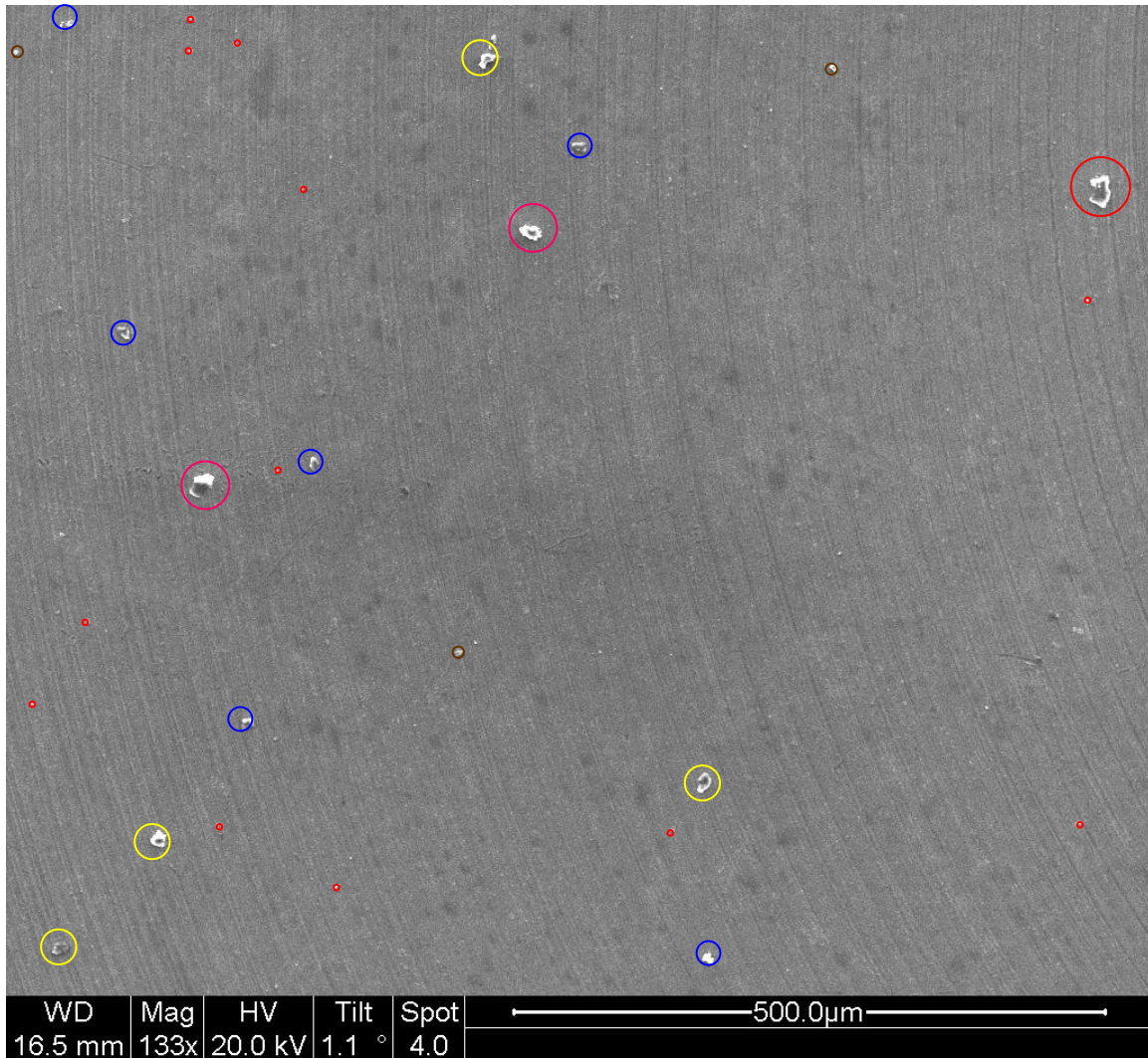
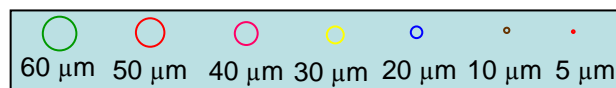


Figure 26. Particles on witness plate at angle of 22.5°



Summary

Mass deposition of exhaust plume of a μ PPT was found by means of aluminum witness plates placed in an array at different angular positions. Tests were made in AFIT's micro propulsion vacuum facility resembling space environment.

IV. Analysis and Results

Chapter Overview

In this study, a μ PPT was tested several times to determine its reliability and then three more tests were conducted using different durations and frequencies to better understand the contamination effects of μ PPTs. Witness plates were analyzed to find the mass deposition profile of particles in the exhaust plume.

μ PPT Operational Tests:

A previous study at AFIT showed pulse generation of μ PPTs was inconsistent during the tests. Therefore, different configurations for a pulse generation circuit (schematic is shown in Figure 3) were tested to achieve pulses in the most reliable way. The first set of tests involved different capacity and voltage levels. A pulse initiator was not used in these tests. The expected result was the circuit would self trigger the pulses at a rate determined by the charging time of the capacitor. After enough time of charging the capacitor the potential difference between electrodes exceeds the surface breakdown voltage and μ PPT discharges at the rate depending on the capacitor charging time.

Table 2. μ PPT Reliability Study

Test Number	Capacitor Capacitance	Input Voltage (Volts)	Vacuum Pressure range (torr)
1	0.5 μ F	3000	10^{-5} - 10^{-6}
2	0.5 μ F	4000	10^{-5} - 10^{-6}
3	0.5 μ F	6000	10^{-5} - 10^{-6}
4	1 μ F	4000	10^{-6} - 10^{-7}
5	1 μ F	5000	10^{-6} - 10^{-7}

In each of these tests, self triggering μ PPT circuit struggled to generate pulses. Theoretically μ PPT should have generated pulses with a frequency determined by the capacitor charging time period. But in these tests, frequency of pulse generation varied significantly. In some cases, it took almost an hour for the circuit to generate a second pulse after the first pulse. Shot to shot variations were visibly high. After each test, input voltage was increased to ensure enough energy to generate a pulse. Capacity of the capacitors was also increased at the same time to increase total energy supplied to generate the pulses. This energy increase continued until the failure of a diode.

For this configuration, the self triggering circuit was not a reliable circuit to be used as a satellite propulsion system. In order to increase reliability and make a more controllable system, a pulse initiator was added. The pulse initiator tube was almost same as μ PPT propellant tube but with a smaller diameter. Therefore lower energy levels were required to generate a discharge. For the pulse initiator, the Xenon Model-437B Nanopulse system was used (Figure 18). This device enabled reasonable control of the pulse rate and voltage input.

The pulse initiator was placed facing the μ PPT main discharge (Figure 27). Because the initiator has a smaller diameter, it did not require as a high voltage. The small pulses generated increased the density of charged particles near the tip of μ PPT, therefore enabling the main discharge to occur easily.

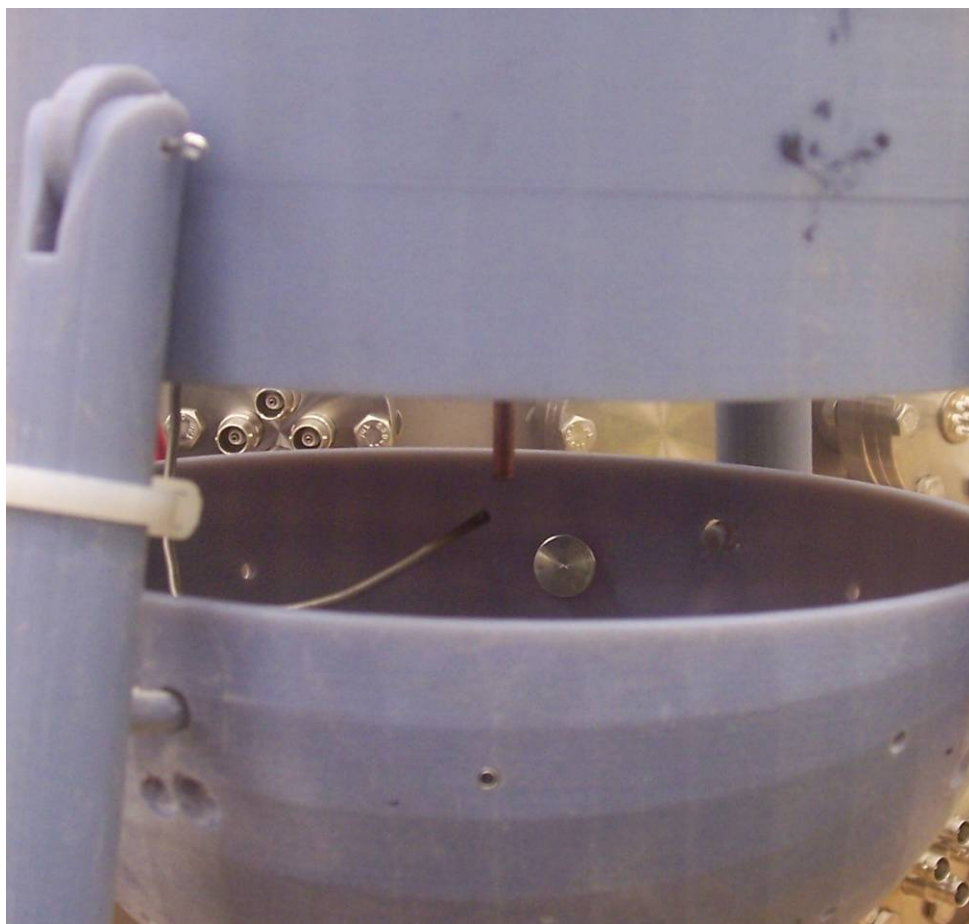


Figure 27. μ PPT with Pulse initiator

The second set of tests was made using the pulse initiator to determine reliability of the system (Figure 27). In these tests, the μ PPT ran without any issues (Table 3).

Table 3: μ PPT Test using Pulse initiator

Test Number	Capacitor Capacitance	Input Voltage (Volts)	Vacuum Pressure (torr)	Duration (Hours)	Frequency (Hz)
1	1 μ F	3000	10^{-6} - 10^{-7}	1	1
2	1 μ F	4000	10^{-6} - 10^{-7}	1	0.5
3	1 μ F	5000	10^{-6} - 10^{-7}	3	0.4

The μ PPTs showed consistent pulsing during the entire test running continuously for as long as three hours without any problem. These tests show μ PPTs with pulse initiators work reliably. By the end of the contamination tests, the μ PPT operated for more than 11 hours generating approximately 40,000 pulses without fault.

But why self triggering circuit did not work? In order to figure out the reason the tip of the μ PPT was analyzed with the SEM after operational tests. A visible carbonization appeared around the tip of the μ PPT (Figure 28). This phenomenon is similar to a previous study by M.Keidar et. al. at the University of Michigan²¹. Carbonization is considered a very serious problem in the operation of μ PPTs. Carbon forming due to the high temperature during discharge changes the composition of propellant on the surface. Evaporation and ionization of a carbonized surface requires much more energy than needed for a pure Polytetrafluoroethylene, therefore making it difficult to generate a discharge event.

The pulse initiator eliminated the high energy requirement problem by increasing the charged particle density around the μ PPT tip and therefore helping the generation of the main discharge between anode and cathode. This process also decreased the required voltage levels required for main discharge reducing the generation of carbon on the surface.

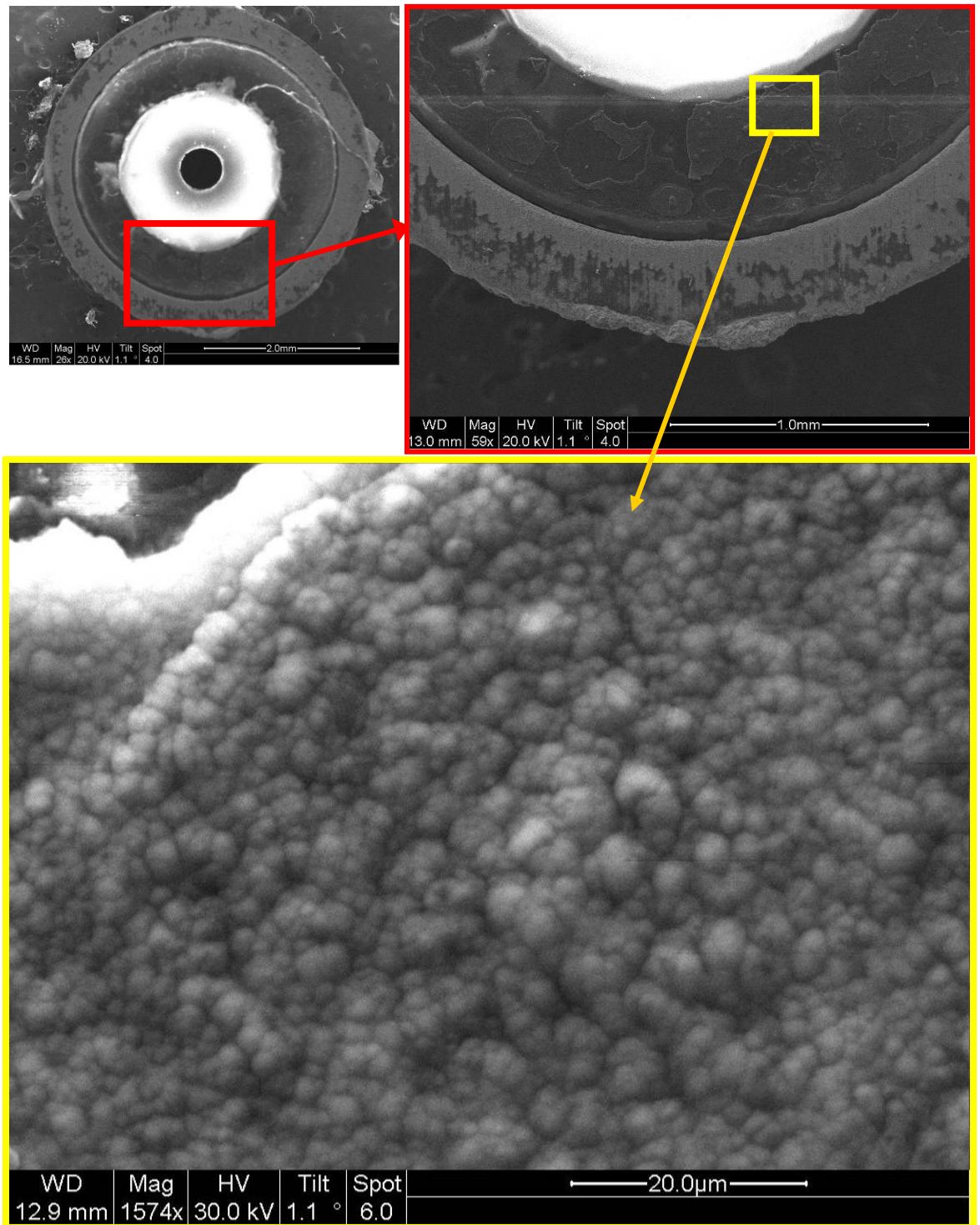


Figure 28. Carbonization μ PPT tip after 3 hours of operation

μPPT Contamination Study

After building a reliable thruster circuit, the focus shifted to the contamination study. Contamination effects of the μPPT exhaust plume were investigated using several arrays of aluminum witness plates placed facing the μPPT tip at different angular positions. The witness plates were placed on a bowl shaped holder (Figure-20, 21). The witness plates were analyzed by using AFIT's SEM. The particles sticking to the witness plates were sorted by their diameter and counted to get mass deposition and deposition rates.

Diameters of the particles ranged from 5-60 μm. For the SEM analysis, 133x magnification was used to take images (Figure 26). In the following images, particle sizes are color coded to distinguish the different sizes. This magnification level was sufficient to distinguish particles with diameter as small as 5 μm. Some smaller particles were evident at higher SEM magnification but did not significantly contribute to the overall mass being deposited.

Counting all the particles on a witness plate would have been cumbersome. At this magnification level, a single witness plate would require approximately 40 images to cover the entire surface. Instead of counting every possible particle present, five images were taken on the witness plates at specific locations and averaged to find the mass deposition as a function of angle. These results were normalized by the distance from the thruster to present them as mass deposition per steradian.

For the contamination study, another three tests were performed with different duration and frequencies. For the first test setup, 33 witness plates were used to analyze mass deposition profile, deposition rates and particle size distribution for contamination

study (Figure 18). In the first test one of the results was axissymmetry of μ PPT plume, therefore in Test -2 instead of using more axes 2 axes were used to capture mass deposition and more witness plates were used to capture a smoother curve. 21 witness plates were used for analysis in two axes (Figure 21). In the first two tests, the mass deposition was highest at angles 0° - 30° . Hence, a third test focused on this high gradient area. The same configuration as test-2 was employed but more images were taken of the witness plates to capture more information. Witness plates were marked before the test to identify orientation. A more statistically significant representation with higher resolution of the mass deposition was the aim. Results agreed in all three contamination tests. Small diameter particles were much more abundant than large diameter particles.

Particle Size Distribution

Particle diameters ranged from 5 - 60 μm . The majority of the mass deposition resulted from particles between 30 and 50 μm diameters. Some smaller particles were evident at higher SEM magnification but did not significantly contribute to the overall mass being deposited. Results showed particles with smaller diameter were much more plentiful than larger particles. A high percentage of particles on each witness plate were small diameter particles (Figure 29). Another significant result showed that size of the particles close to the centerline tended to be larger (Figure 30). Results from all three contamination tests agreed with each other.

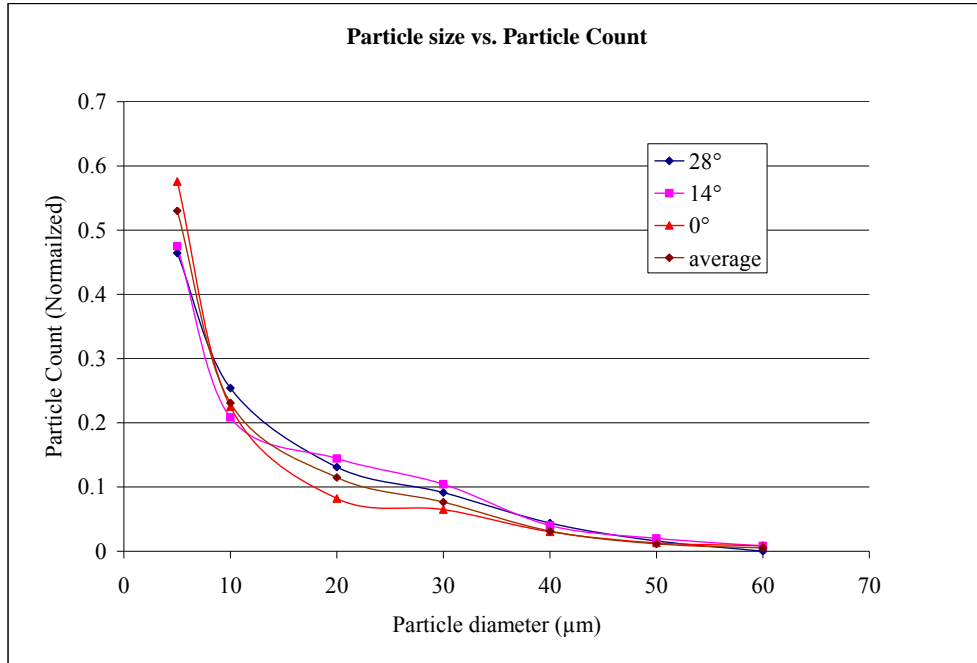


Figure 29. Particle size vs. particle count TEST-3 (960 pulses)

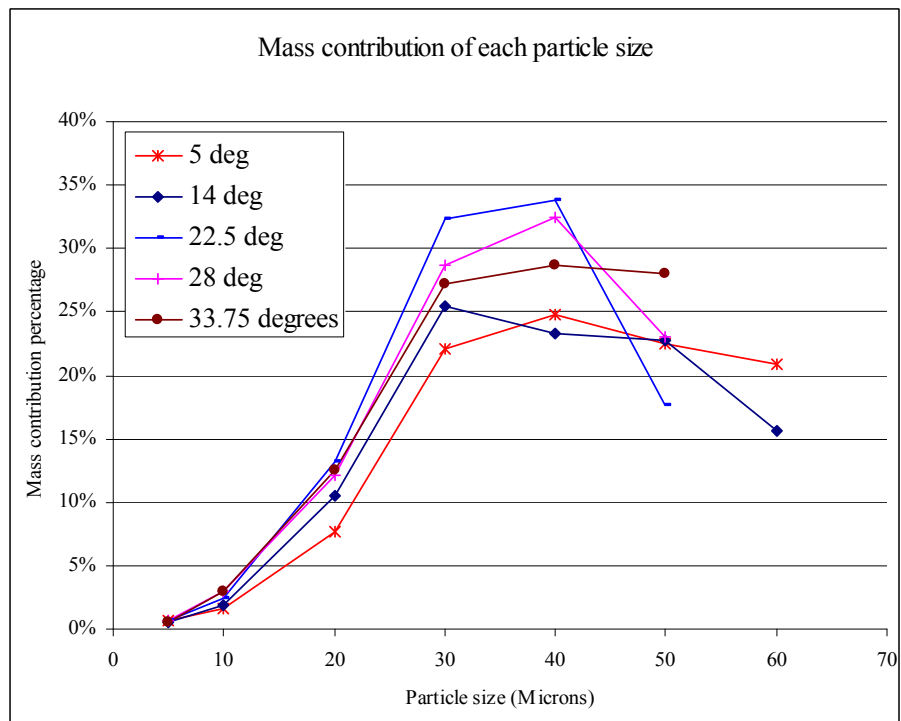


Figure 30. Mass contribution of each particle size TEST-3 (960 pulses)

Mass Deposition Profile

Averaging all the data together, overall trends for the mass deposition are apparent. As expected, mass deposition of the exhaust plume was very high near the axis of the thruster. Figure 31 shows the mass deposition profile that was created after 960 pulses (Test-3). Test duration was 40 minutes with an average pulse frequency of 0.4 Hz. After the test aluminum witness plates were analyzed by SEM and total number of particles and total mass deposited was calculated. The mass deposition between 0° and 30° accounts for the majority of the mass capturing 93.6 %. For angles greater than 60° , mass deposition is very low. This distribution of mass curve is similar to a Gaussian distribution curve (Figure 31). Two distinct regions were found in this mass deposition profile: The first region, between 0° - 27° , exhibits a Gaussian distribution with a standard deviation of 17.5° . The second region between 27° - 90° is a Gaussian distribution with a standard deviation of 32° . The uncertainty of the mass deposition profile has a maximum uncertainty of 14% but is not included in this figure to preserve clarity. As a further contamination analysis, deposition rates were found per steradian per pulse and plotted as a function of angle (Figure 32).

Generating the mass deposition profile was main focus of this research. Mass deposition profile of exhaust plume of μ PPT help determine the spatial distribution of heavy non-ionized solid particles that don't significantly contribute to overall impulse and also cause contamination on spacecraft surface.

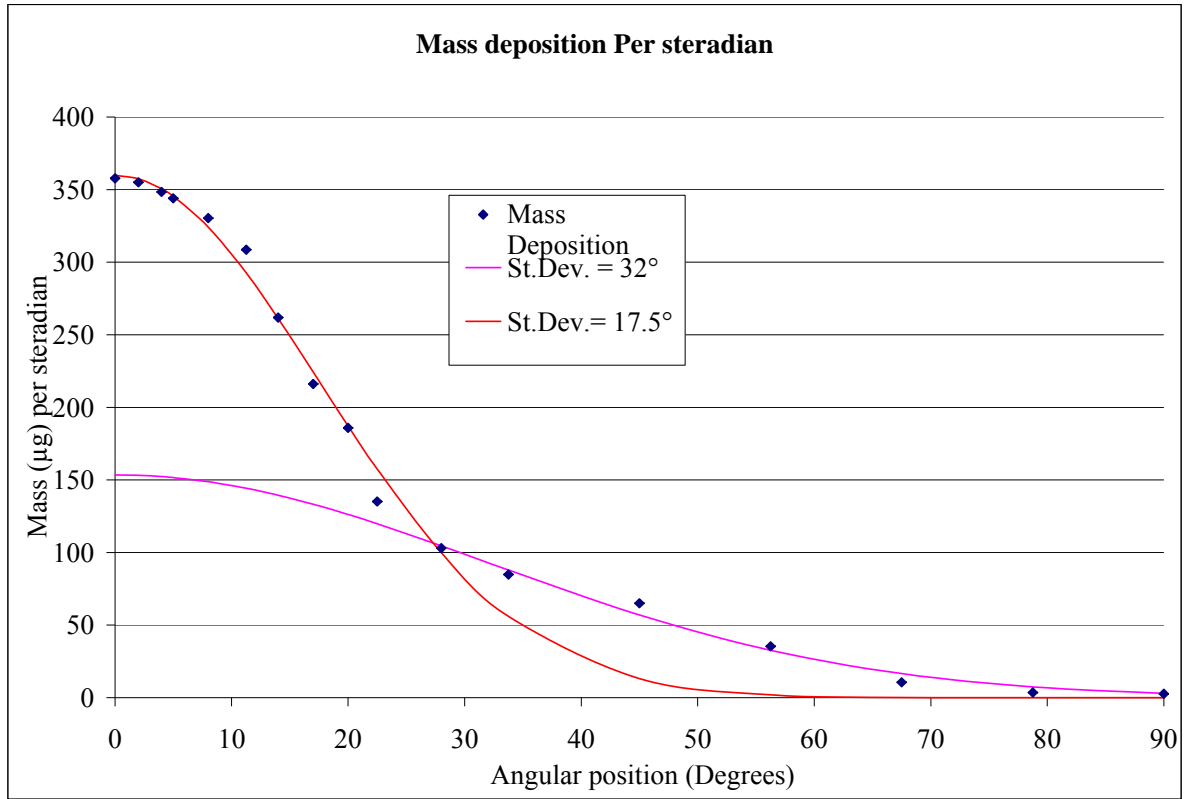


Figure 31. Mass Deposition Profile TEST-3 (960 pulses)

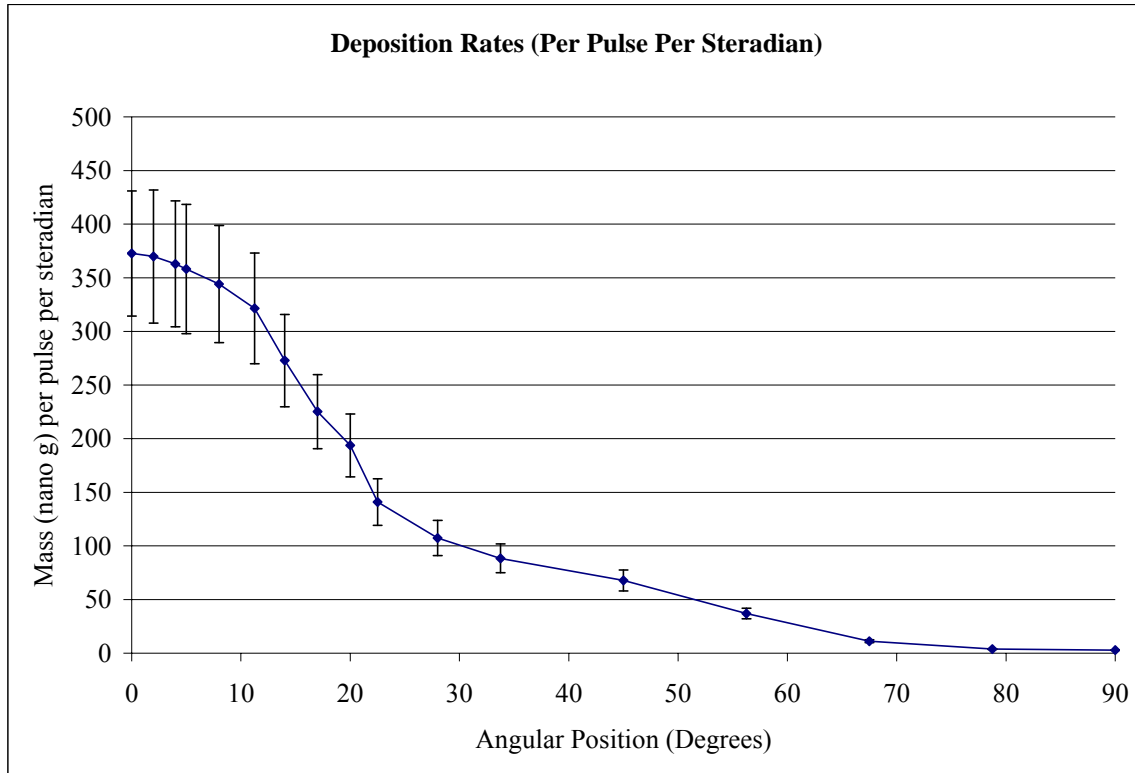


Figure 32. Deposition Rates per Pulse per Steradian

Propellant Distribution

As a way to give an idea of propellant being captured, the μ PPTs were weighed before and after the experiments using a scale with a resolution of 1.0 mg (Figure 33). The results showed the total mass captured by the witness plates represented only a small portion of the propellant being ejected by the μ PPTs. The propellant deposited on a surface is only $4.9 \pm 0.25\%$ of the total mass being ejected from the thrusters. Having this information along with generated thrust, and particle velocities, an actual propellant utilization can be determined.



Figure 33. μ PPT on scale

Pictures below are witness plates at 133x magnification level for third test. Particles in these pictures are circled according to their size to distinguish their diameter size. It is easily seen that for 90° angular location there are very few particles (Figure 34). But for 0° angular location there are much more particles seen on SEM snapshot (Figure 35). Another important consequence is, as angular position gets smaller, particles tend to be larger. Particles are mostly grouped along the centerline of the thruster. Contamination test 1, 2 and 3 results and all pictures taken from various angular positions are in Appendix section.

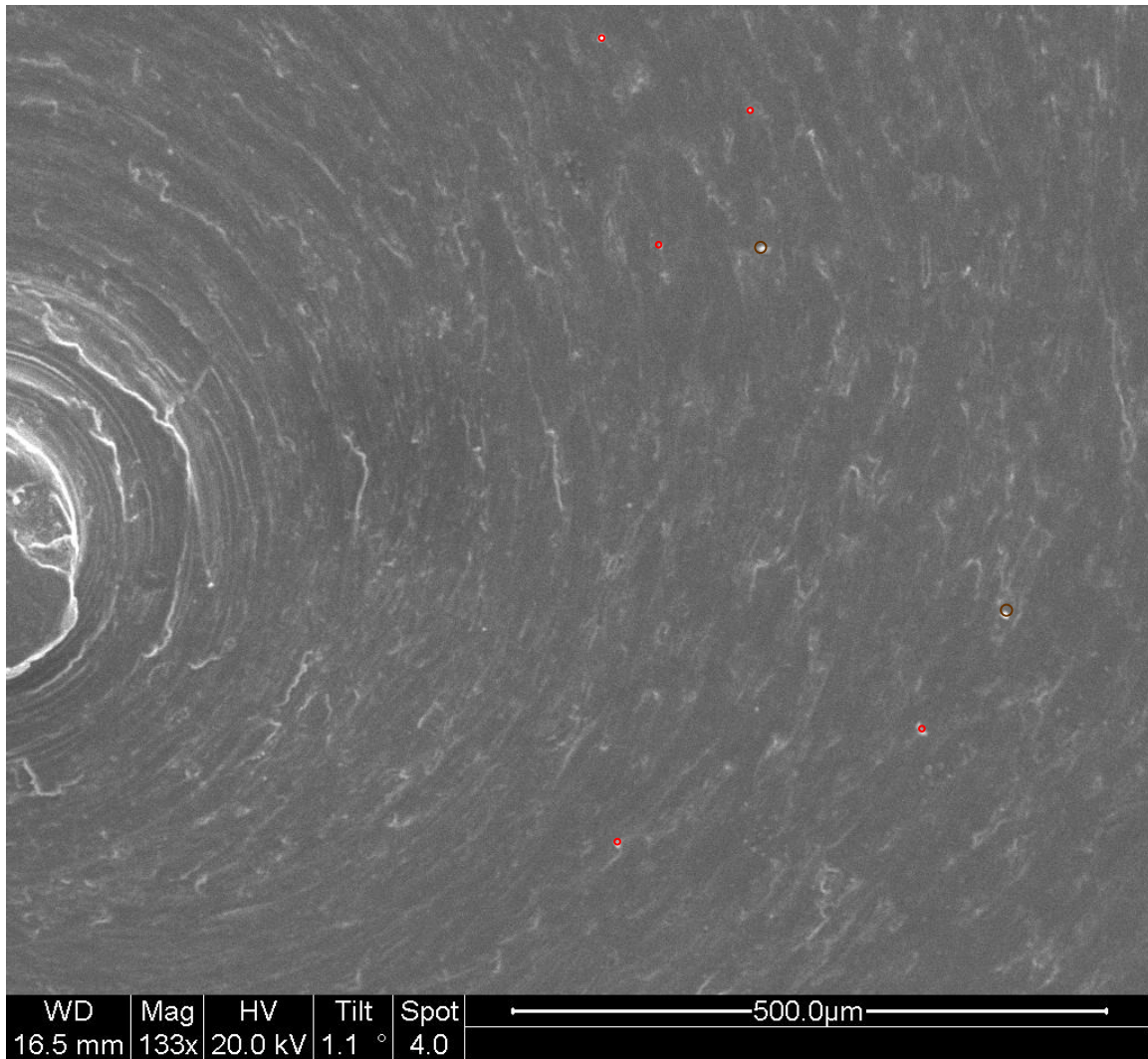
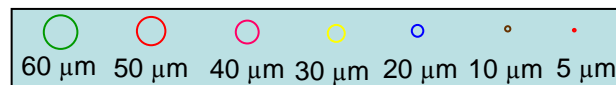


Figure 34. Angular location 90° TEST-3



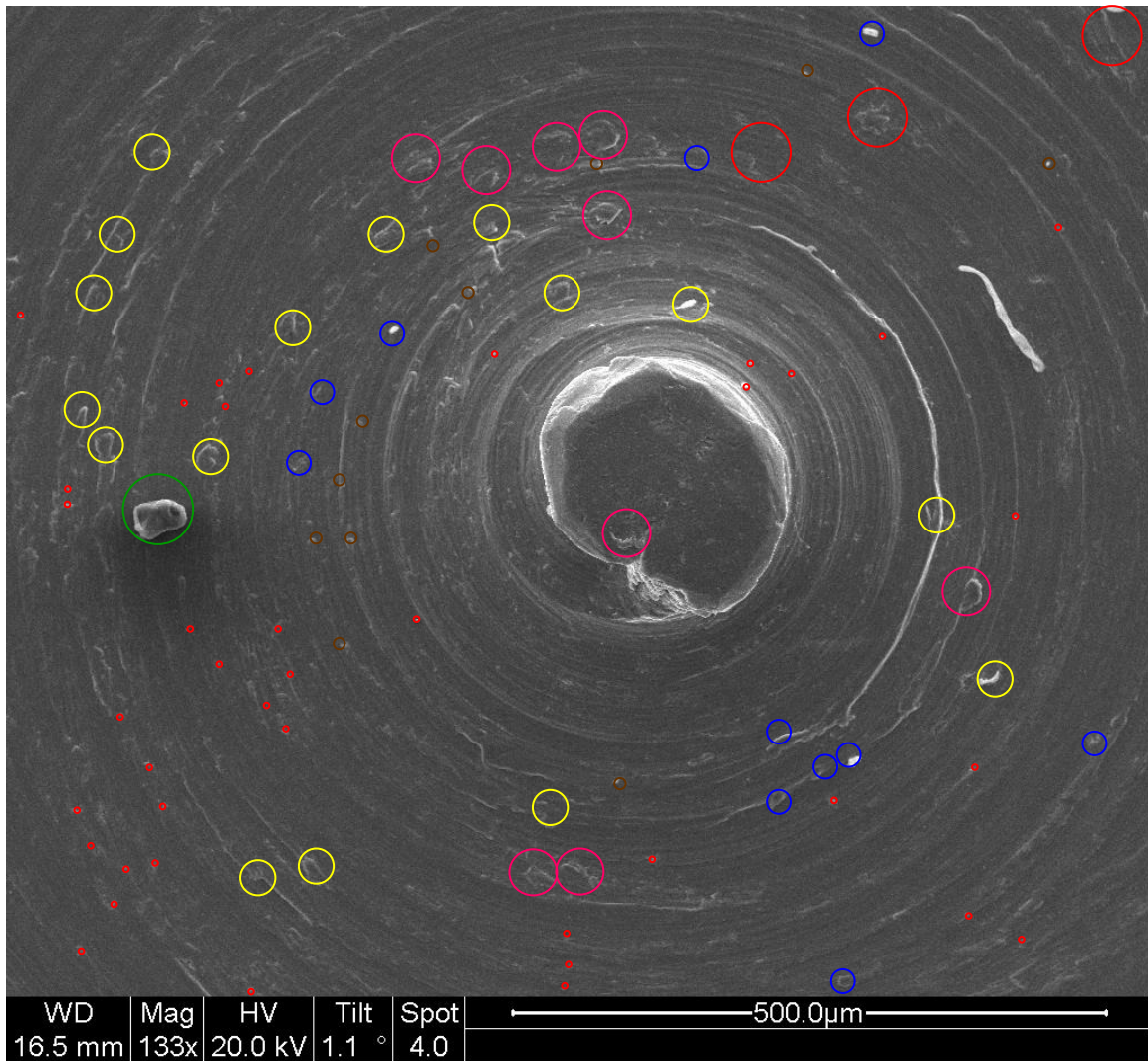
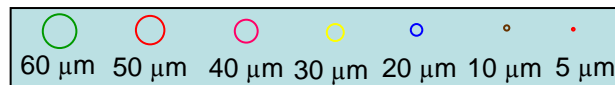


Figure 35. Angular location 0° TEST-3



Comparisons to the Previous Research

When comparing these results with the previous study conducted at AFIT by Debevec, mass deposition profiles and rates agree with these results²⁵. In this study, the

μ PPT results have a higher resolution but the curves for mass deposition profile and deposition rates still compare well.

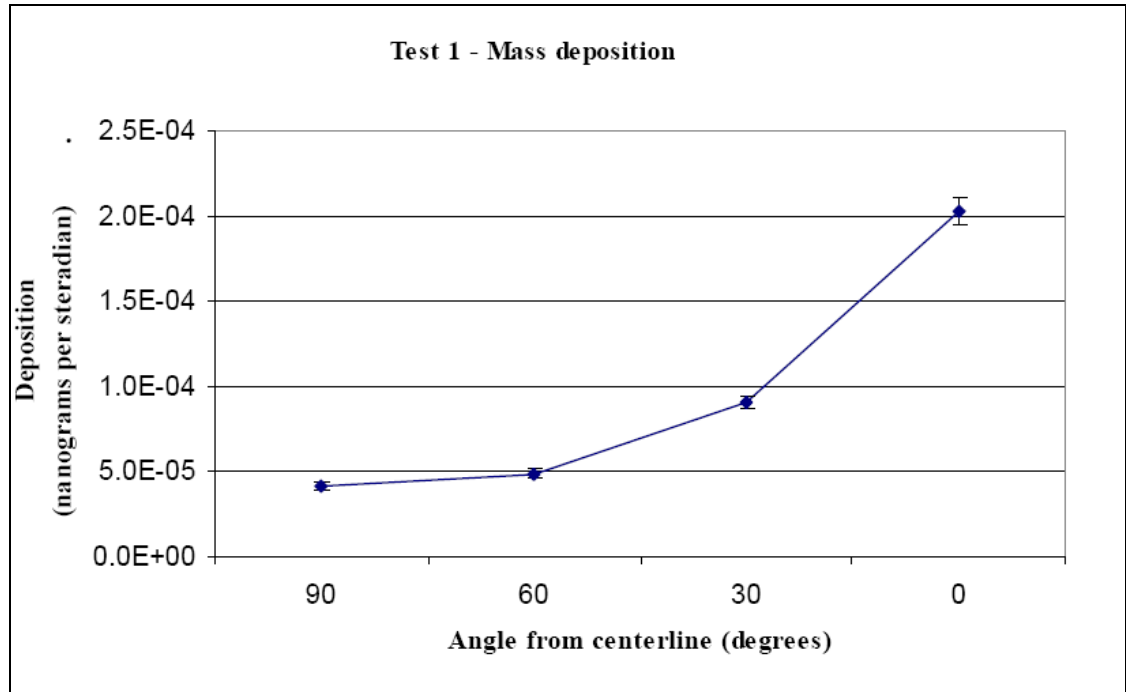


Figure 36. Mass deposition profile found at previous study²⁵

The mass deposition profile seen in Figure 36 is very similar to mass deposition profiles shown in Figure 40, Figure 48, and Figure 32 but the total mass deposited on the plates was much less than for the current research due to the limited ability of the thrusters to self discharge. The most prominent reason for this difference is the more robust control system employed. Also test durations and capacitance and frequency values are different from the previous study. But same trends for mass deposition profile were found.

When comparing the μ PPT results with larger, more traditional pulsed plasma thrusters, we found the mass deposition profile agrees with previous study made by G.

Spanjers, et al, at U.S. Air Force Research Laboratory, Edwards AFB, CA with a 20 J pulsed plasma thruster operating at 1 Hz²⁶. Although the pulsed plasma thruster used in the Spanjers research is larger, the mass deposition profile is similar to what was found in this research.

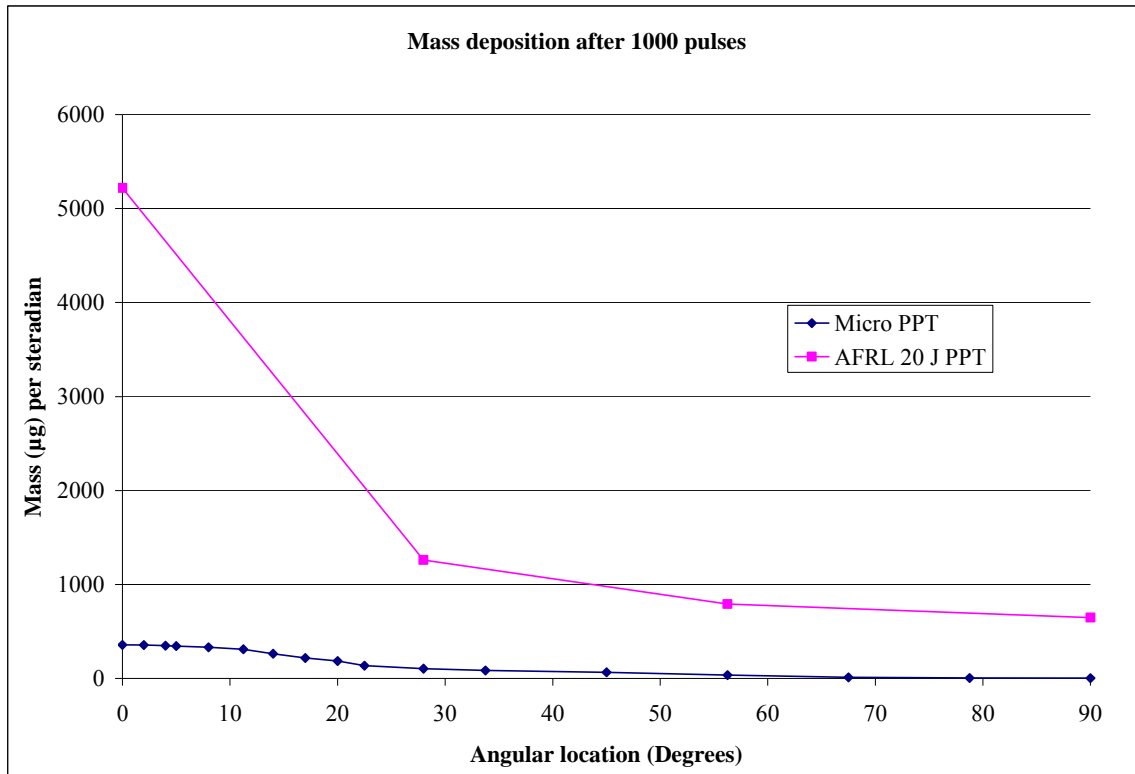


Figure 37. Comparison of mass deposition of AFRL's PPT and μ PPT in this research

If we put two mass deposition profiles on the same graph we see that mass deposition profile agrees for both AFRL 20 J PPT and μ PPT (Figure 37, Figure 38). In the first graph (Figure 37) we see that AFRL 20 J PPT has much more mass deposition. But in the second graph (Figure 38) mass deposition is normalized by their energy and it is seen here that both have same trend of mass deposition.

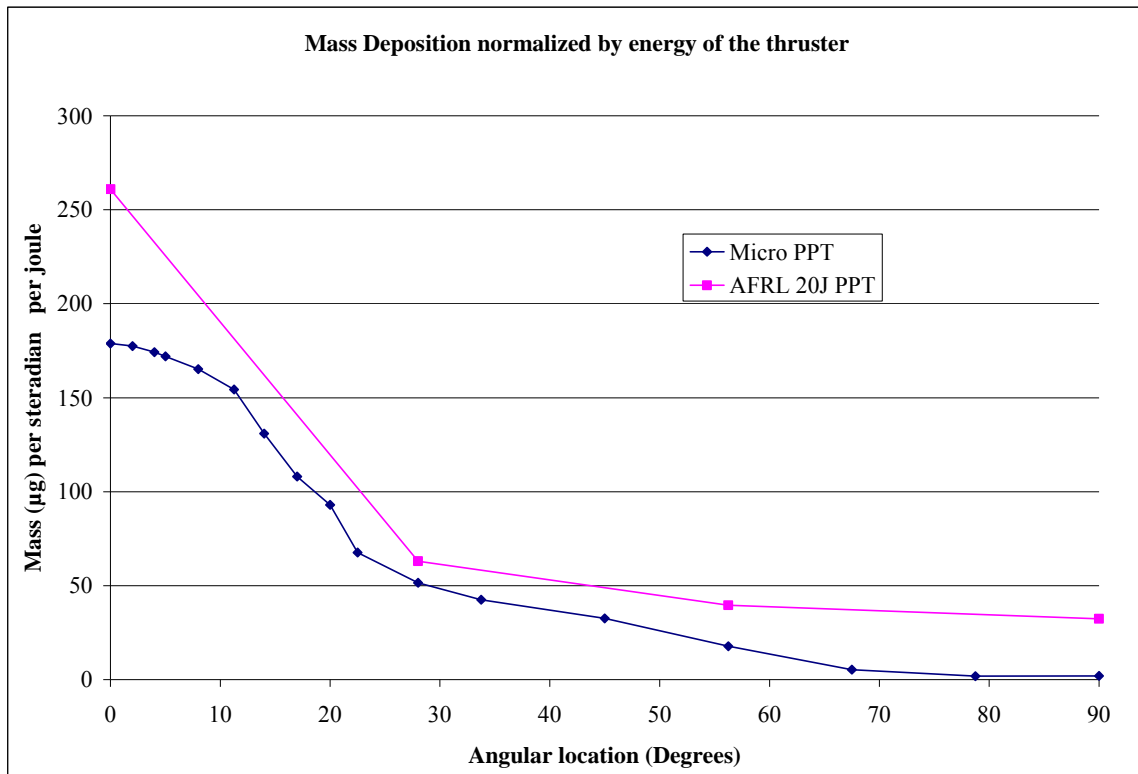


Figure 38. Comparison of mass deposition normalized by their energy.

V. Conclusions and Recommendations

Conclusions of Research

More and more missions are being developed for micro and nano-satellites. These satellites will require miniature propulsion systems for accurate attitude control, station keeping and formation-constellation flying. Thus, a need for reliable, simple propulsion systems with well characterized thrust profiles in the μ PPT capability range is growing.

In this study, a μ PPT was analyzed for reliable operation and contamination effects of the exhaust plume. The plume was characterized by a mass deposition profile and deposition rates. Particle size distribution, mass contributions of each particle diameter size mass deposition and deposition rates were analyzed and plotted as a function of angle over a wide range to get a statistically representative distribution. The contamination data was collected by means of aluminum witness plates placed on a bowl-shaped holder designed to place the plates at a constant distance from the thruster. Each witness plate was placed at a distance of 8.5 cm from the tip of the thruster and analyzed by means of Scanning Electron Microscope.

This research has shown an important way to control μ PPT thrusters reliably. A spark initiator system was added to the self-triggering circuit to control of the main discharge across the polytetrafluoraethylene propellant surface between the anode and cathode. Operational tests of the μ PPT confirm that this miniature thruster with a spark initiator functions reliably. Operational tests showed the system readiness to be used on small space structures and even on large space structures that will need precise impulse bits.

A significant conclusion found in this research was the contamination character of μ PPTs. These miniature thrusters induce contamination on spacecraft surfaces because of the solid polytetrafluoraethylene particles in the exhaust plume and may lead to significant problems reducing mission capability and even the lifetime of the satellite. It is imperative for satellite designers to be aware of this contamination issue when employing this type of thruster.

The majority of the solid particles ejected from the thruster are grouped around the centerline with particles between 30 and 50 μm making up the majority of the mass being ejected in the exhaust plume. When using μ PPTs as a propulsion system on satellite, these thrusters should not be placed directly facing optical instruments, solar arrays, star tracking cameras or other vital instrumentation that might be sensitive to solid particle contamination. Significant deposition rates occurred well past 30° from the centerline. Sensitive instruments should be placed at least greater than 60° away from the centerline of the μ PPTs. The mass deposition was very low for angular positions greater than 60° .

According to the study conducted at NYMA, Inc., NASA, Lewis Research Center, Worcester Polytechnic Inst., (Roger M. Myers et al.) with a 20 J The Lincoln Experimental Satellite (LES) 8/9 thruster, it was found that for 30° angular location after 2×10^5 pulses, transmittance of solar irradiance was calculated and about 0.4% reduction was found¹⁸. Same mass deposition for μ PPT is created after 1.7×10^6 pulses. This translates to after 5×10^6 pulses solar transmittance of the surface will reduce more than 1%. If we assume that these thrusters are used at 1 Hz for a station keeping mission, it will take about 20 days to reduce transmittance about 0.4%. It will take about 5 years for

a solar irradiance reduction of %40 and might cause serious problems for power generation or reduce mission capability of optical systems.

Another important conclusion is inefficiency problem of μ PPT due to propellant utilization as solid particles. In contamination analysis, it was found that the amount of the particles captured by the witness plates is $4.9 \pm 0.25\%$ of the total mass being ejected from the thruster. Majority of the propellant being ejected from the thruster is in ionized plasma form. $4.9 \pm 0.25\%$ was just the solid particles that were captured by the witness plates. It is possible that some of the particles may have bounced from witness plates' surface or didn't stick to the surface because of low velocity. Solid particles in the exhaust plume of μ PPT not only cause contamination on spacecraft instrumentation. Solid particles are not ionized and not able to be accelerated by Lorentz force. They extract the energy of high velocity ions by collisions. Propellant usage in solid particle form not only causes contamination but also causes inefficiency in propellant utilization. Traditionally propellant utilization efficiency of pulsed plasma thrusters has been low. To quantify actual propellant utilization efficiency of μ PPTs a further analysis is required.

Recommendations for Future Research

This study used witness plate to analyze contamination aspect of μ PPTs. Optical diagnostics would also provide valuable information into the impact of contamination effects. It is recommended the optical effects of contamination such as impacts to transmissivity or reflectivity be further researched.

Performance studies also need to be performed to get a more complete picture of propellant utilization. A torsional balance thrust stand can be used to measure μ N-sec level impulse bits directly. Shot to shot variations in thrust and impulse values can be

examined and optimum configuration for capacitance and input voltage values may be analyzed to improve the performance of this miniature propulsion system.

The control mechanism of the μ PPTs has much room for improvement as well. Instead of using a pulse generation system, a μ PPT circuit can be designed to include this aspect into the propulsion system. Controllability and robustness of the propulsion system can be then be further improved.

Initial estimates of propellant utilization also show there is much work that can be done to improve upon the performance of these devices. Increasing the propellant utilization will directly translate to increased total impulse or a reduced propulsion system mass to orbit requirement. Mass reduction studies may include trying smaller capacitors with less energy to improve overall mass since capacitors are the heaviest components in this propulsion system. Different kinds of capacitors with a range of capacity 0.2 μ F to 0.5 μ F might be enough to generate a main discharge by using a pulse initiator.

Summary

μ PPT are simple and highly reliable propulsion systems but contamination effects should not be forgotten when employing these miniature thrusters. There is still further research to be done to investigate μ PPTs and to improve their performance.

Appendix

Test-1 Results

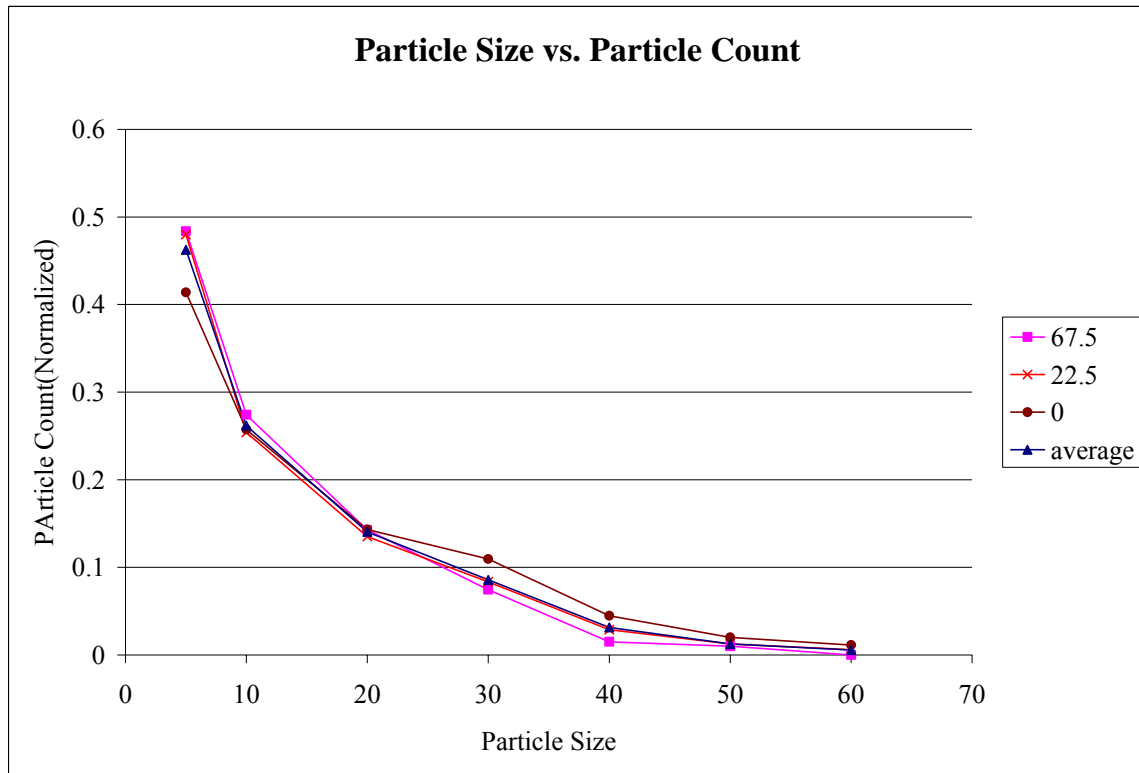


Figure 39. Particle size vs. Particle count TEST-1 (3960 pulses)

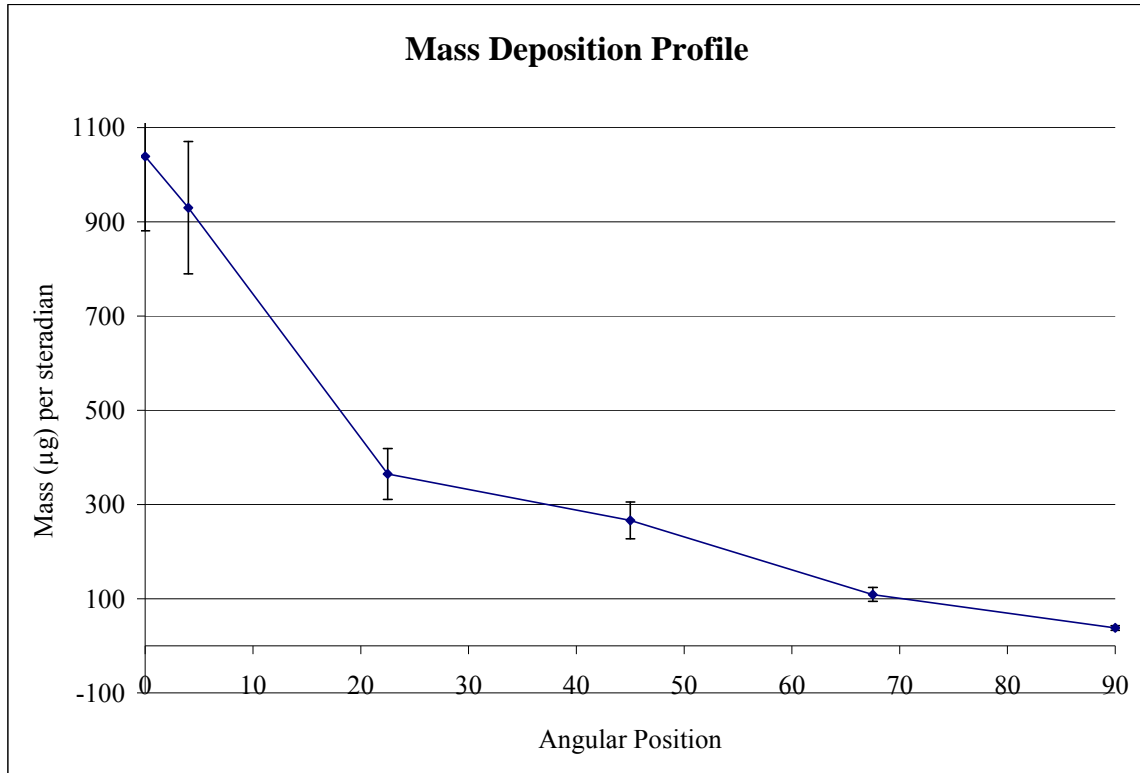


Figure 40. Mass Deposition profile TEST-1 (3960 pulses)

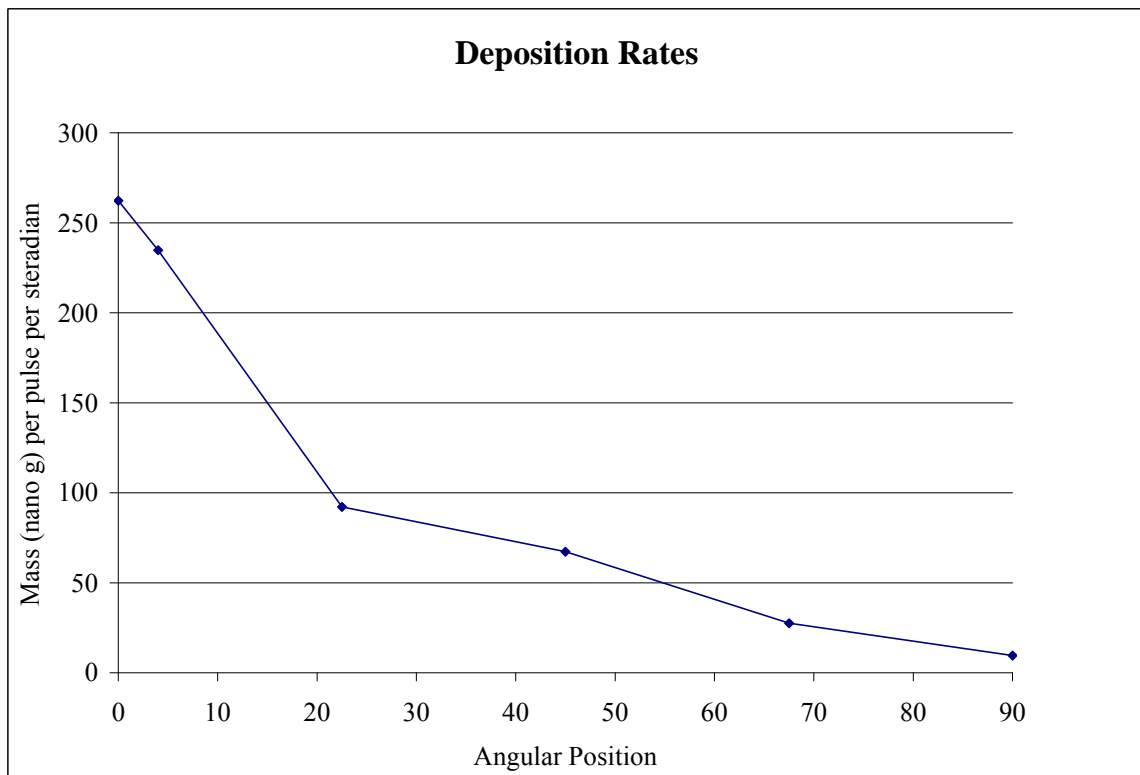


Figure 41. Deposition rates TEST-1 (3960 pulses)

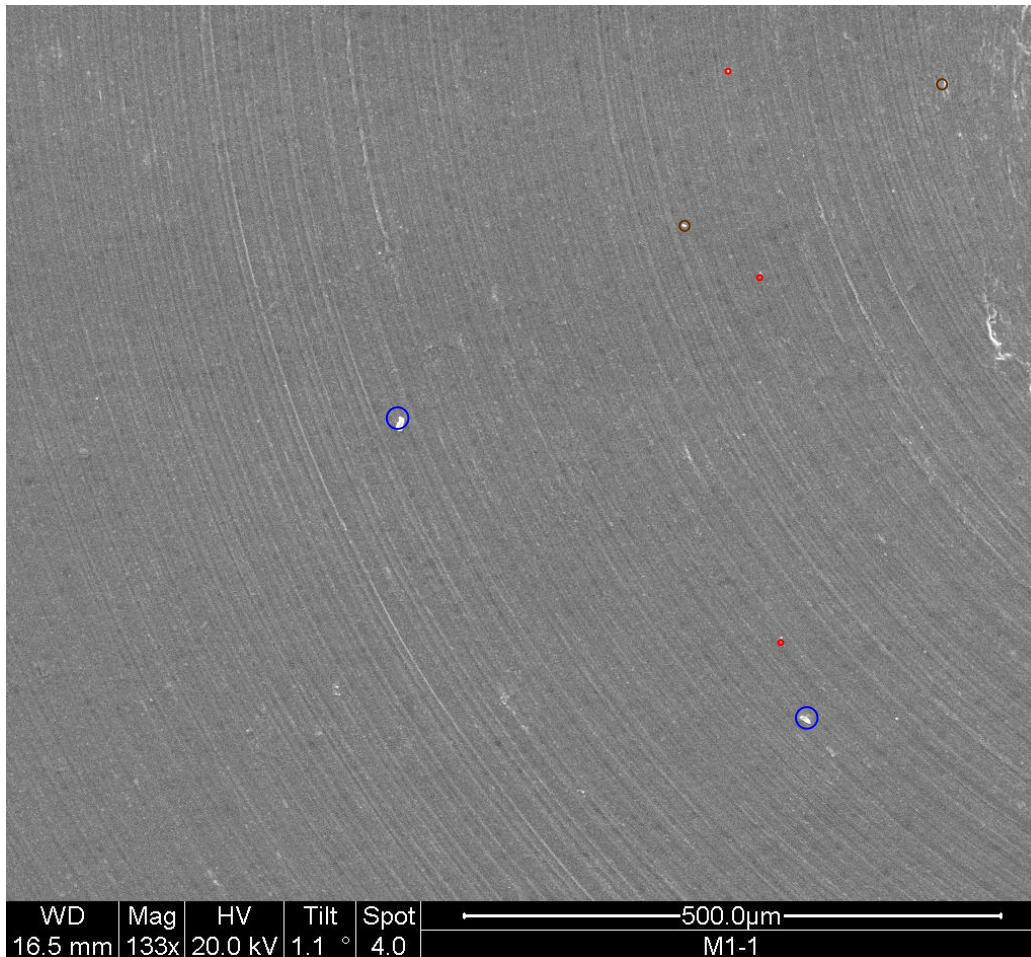
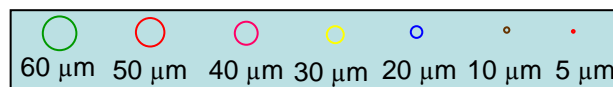


Figure 42. Angular Location 90° Test-1



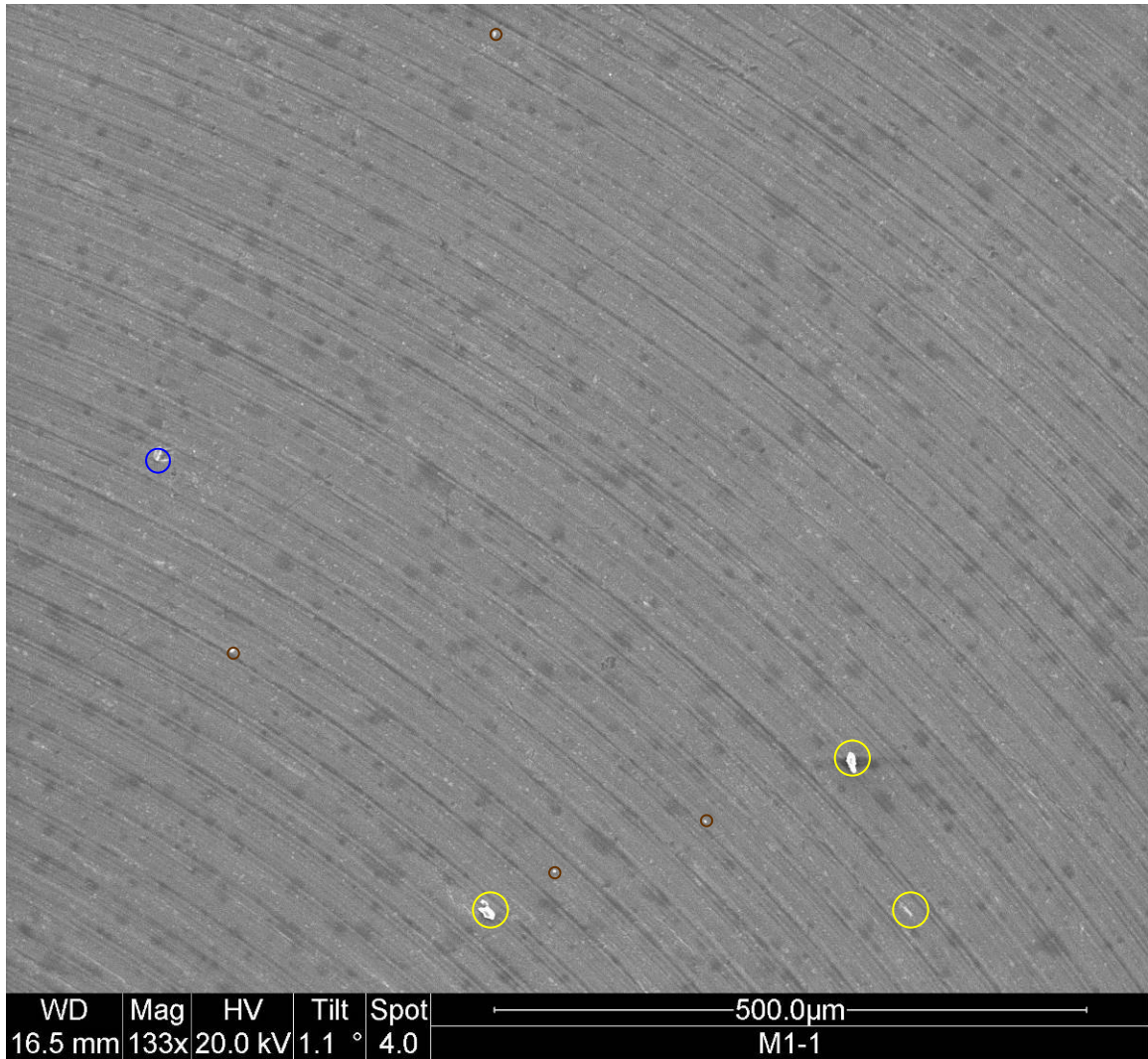
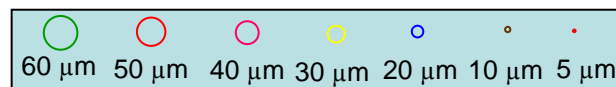


Figure 43. Angular Location 67.5° Test-1



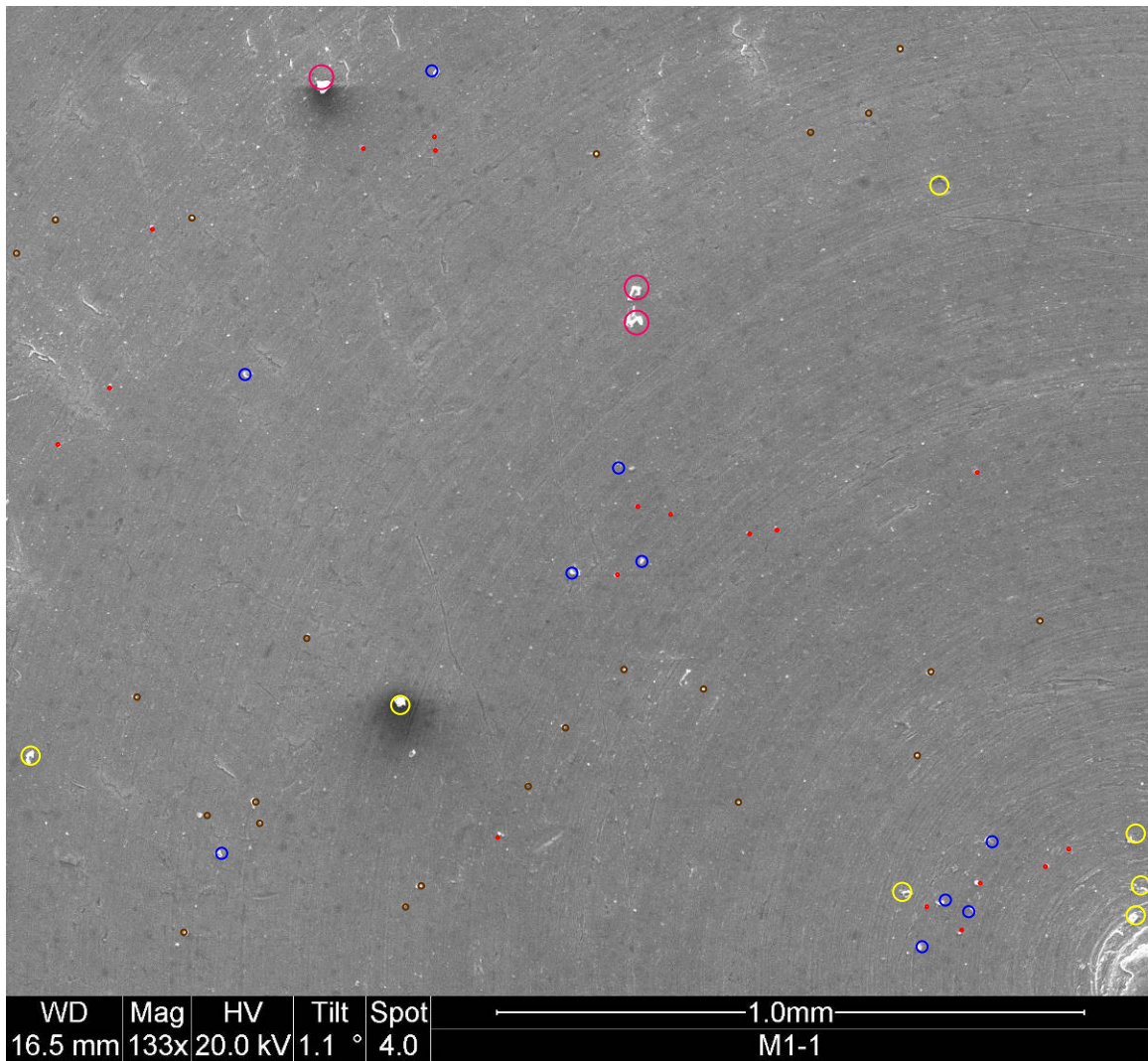
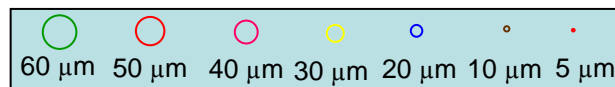


Figure 44. Angular Location 45° Test-1



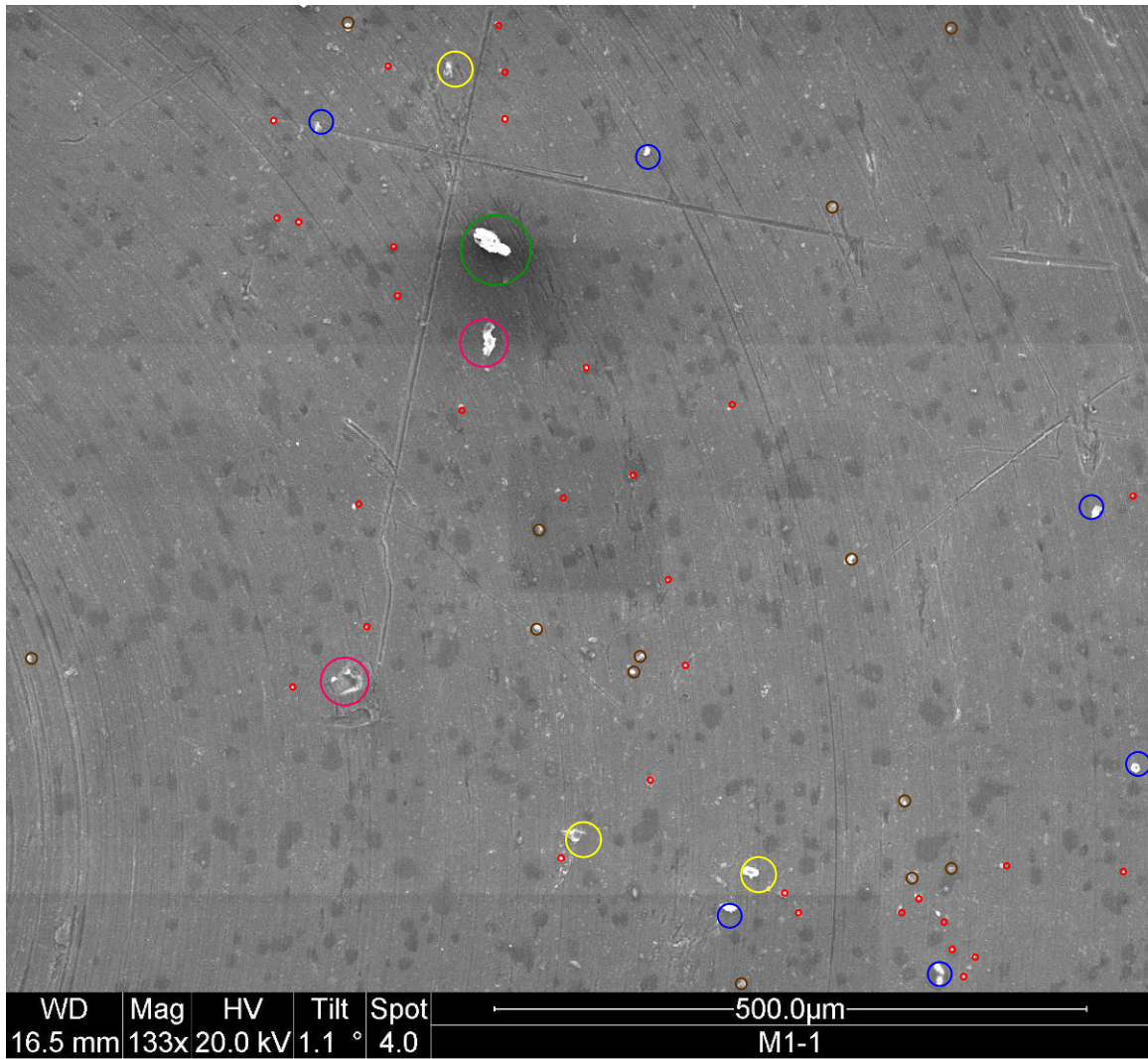
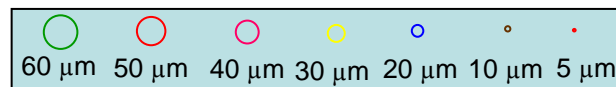


Figure 45. Angular Location 22.5° Test-1



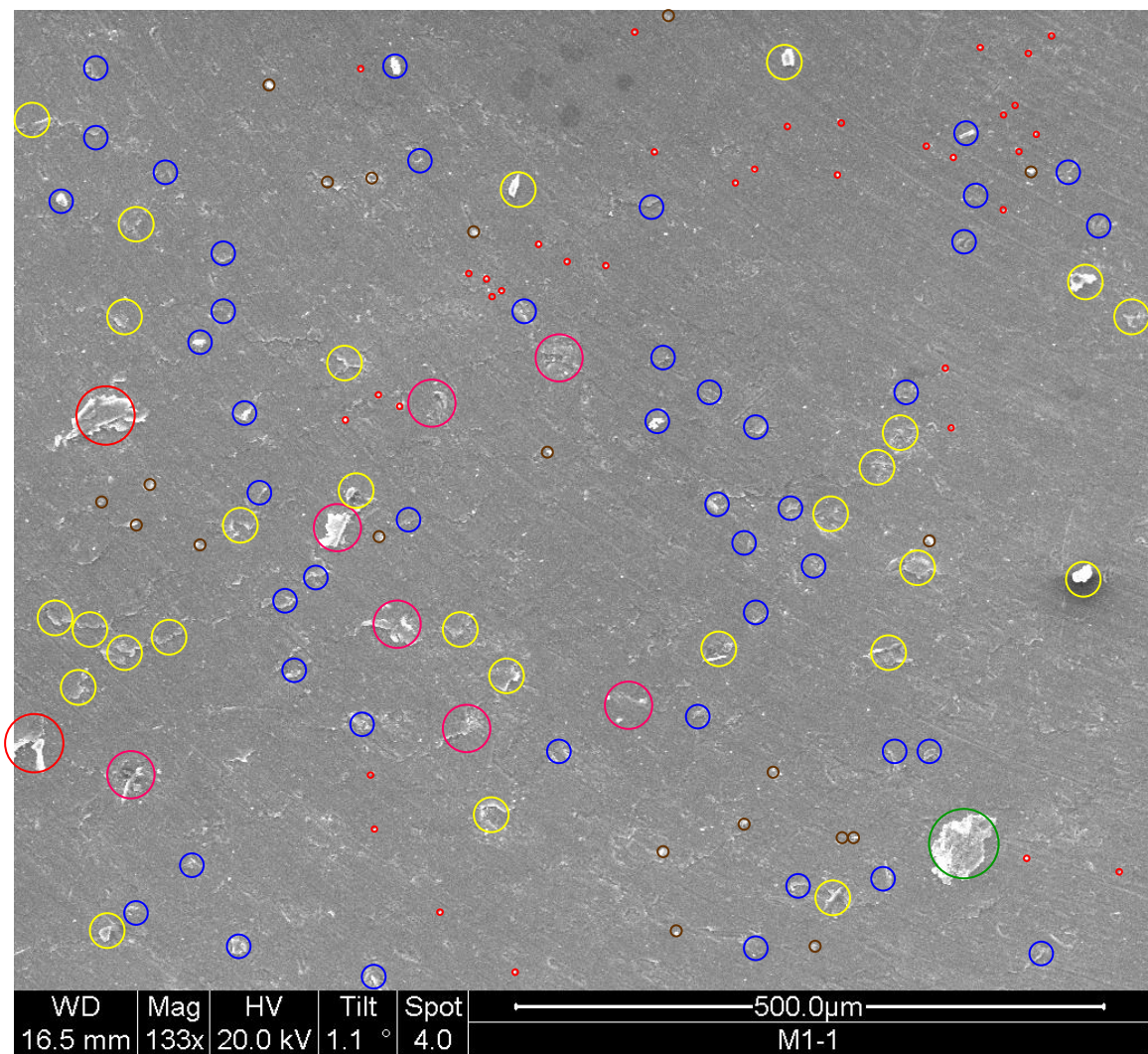
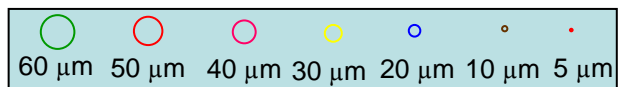


Figure 46. Angular Location 0° Test-1



Test-2 Results:

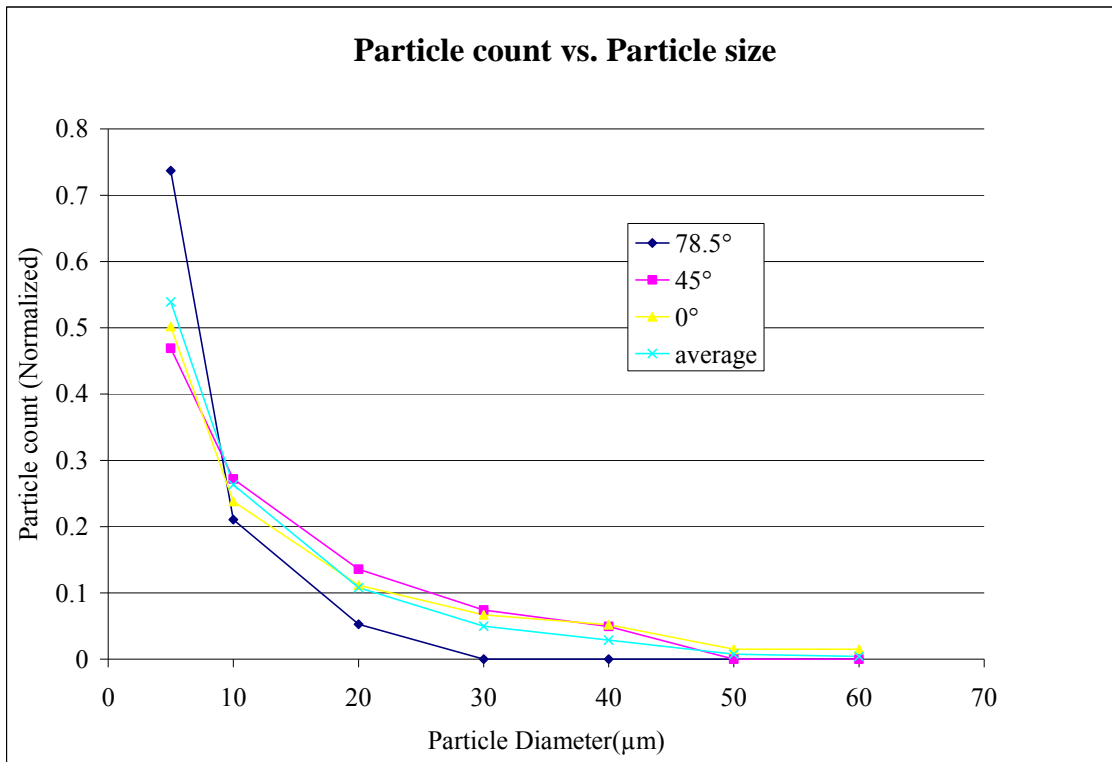


Figure 47. Particle size vs. Particle count TEST-2 (744 pulses)

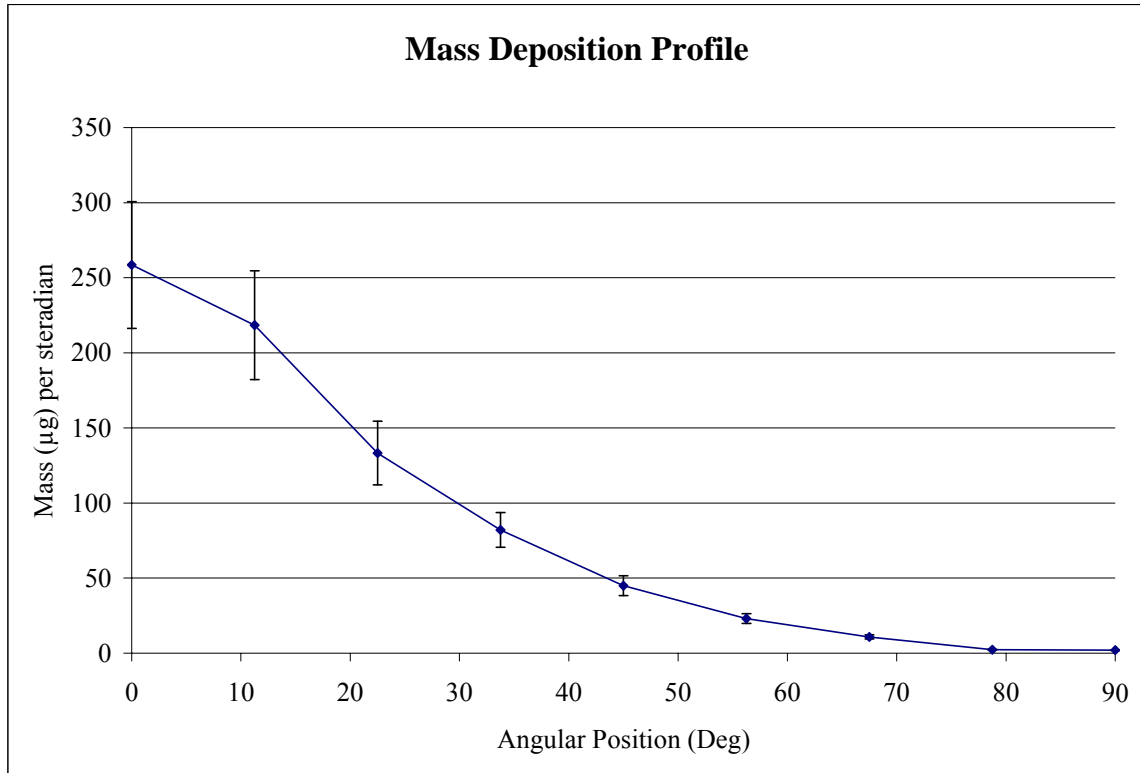


Figure 48. Mass Deposition Profile TEST-2 (744 pulses)

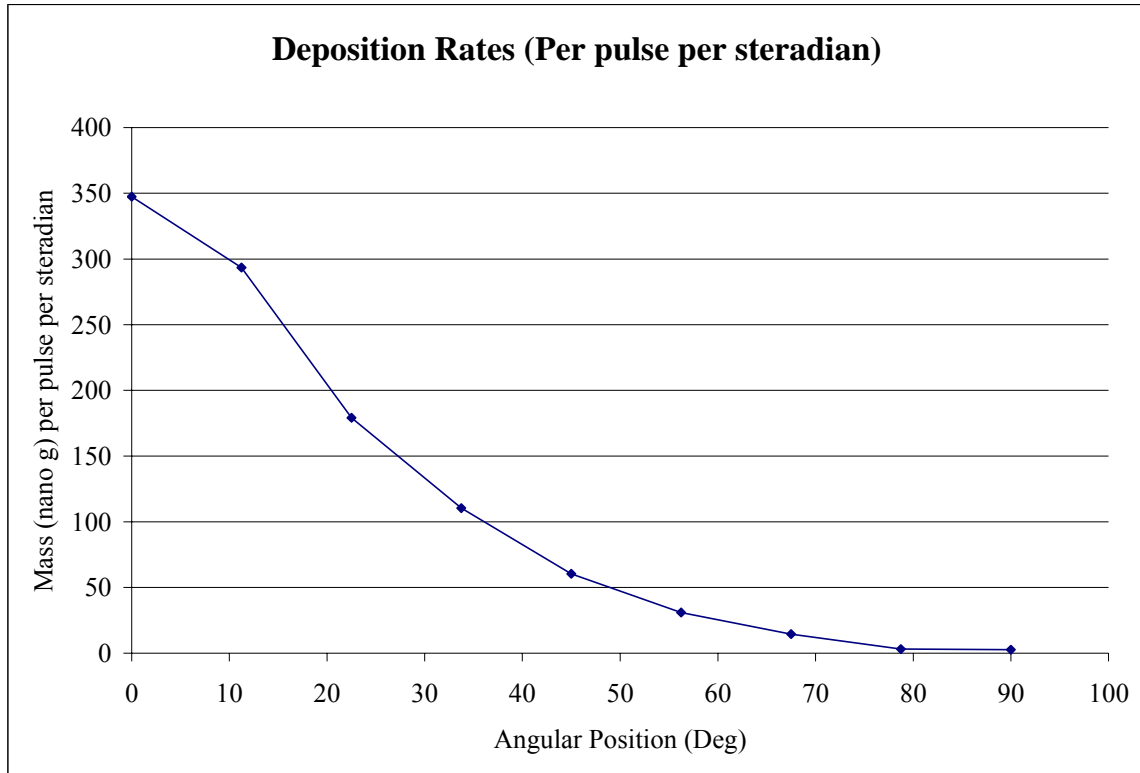


Figure 49. Deposition rates TEST-2 (744 pulses)

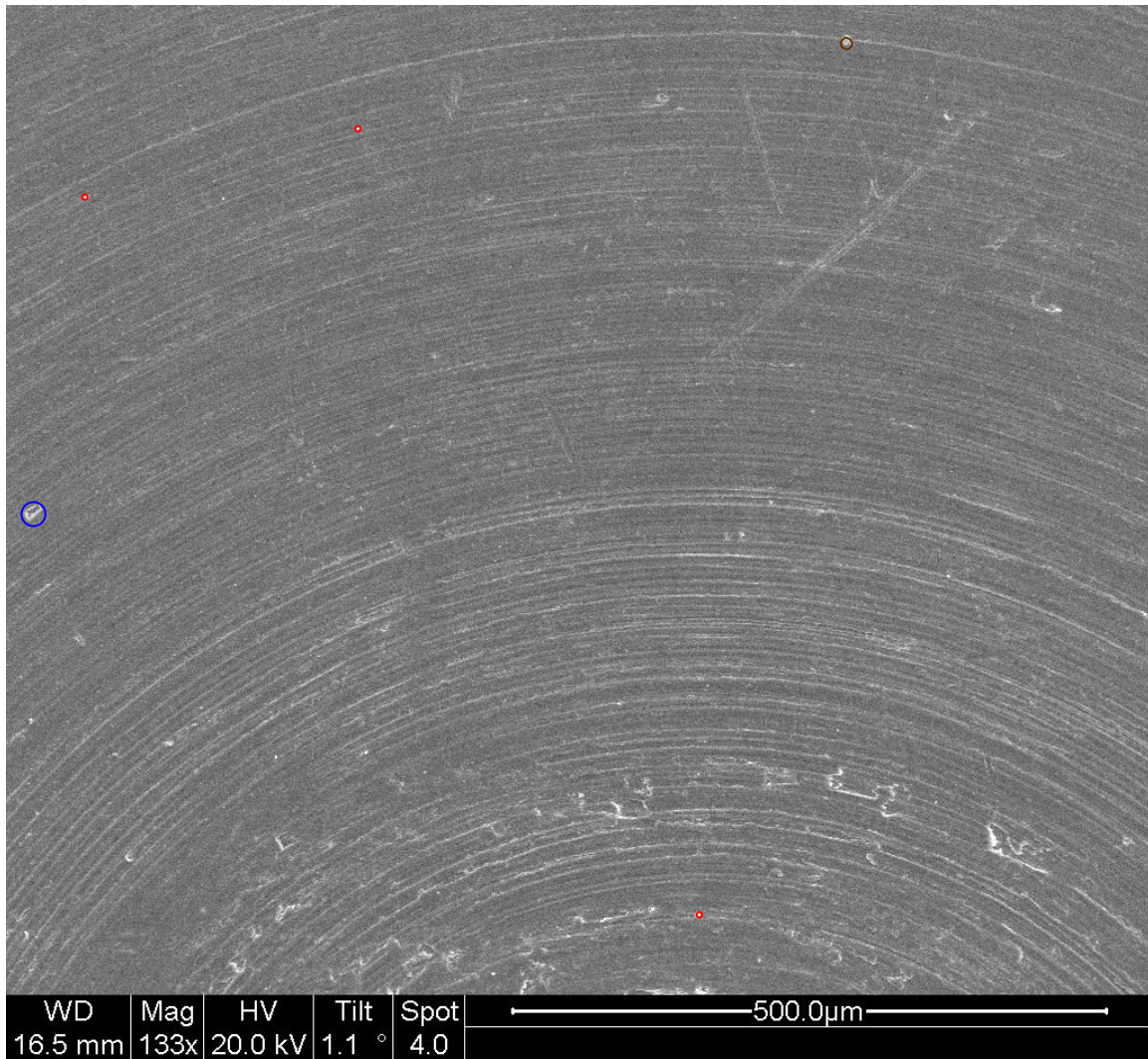
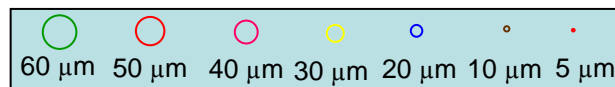


Figure 50. Angular location 90° TEST-2



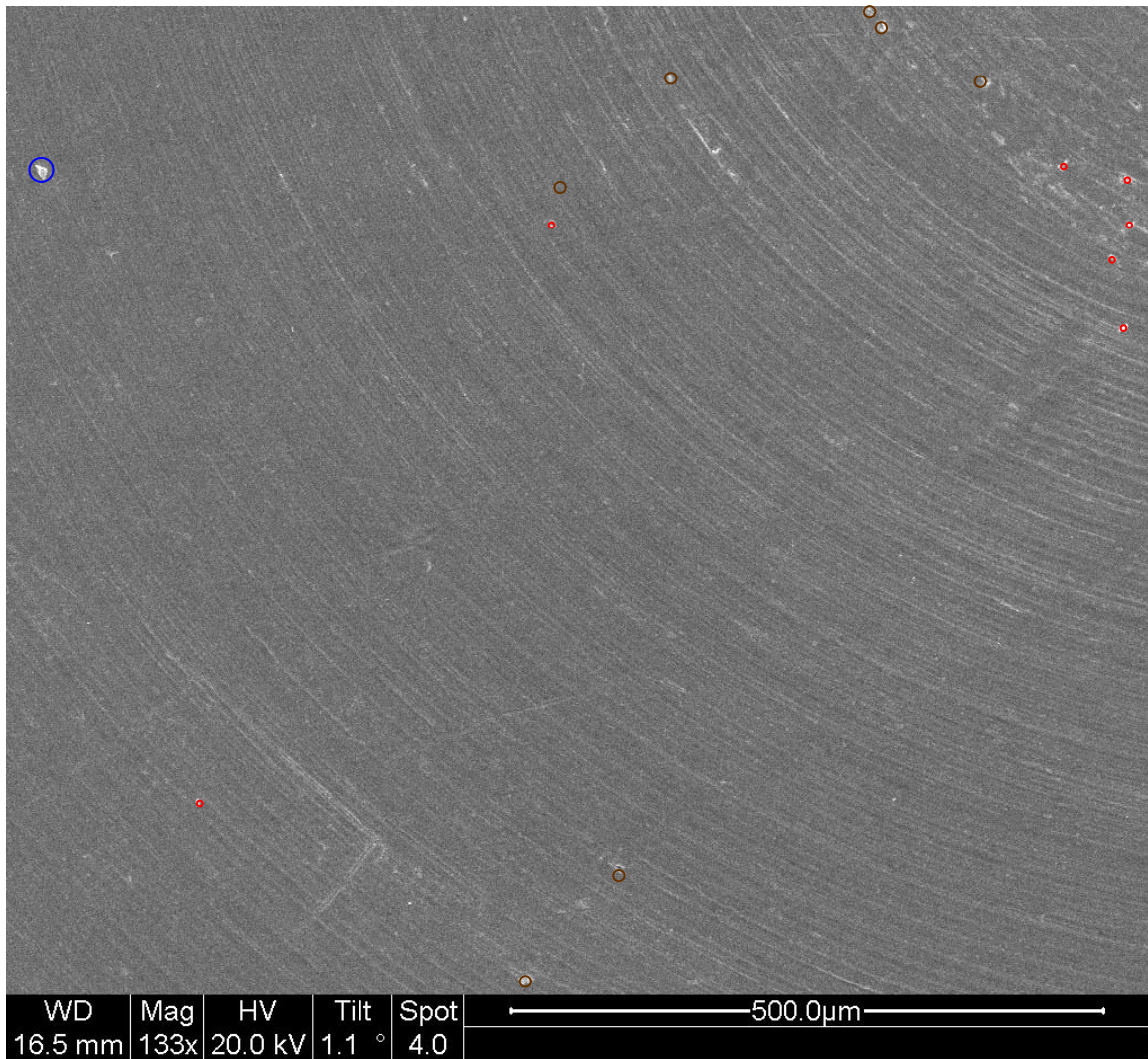
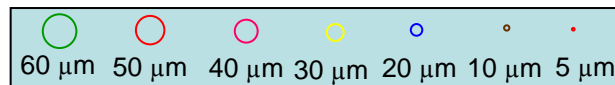


Figure 51. Angular location 78.5° TEST-2



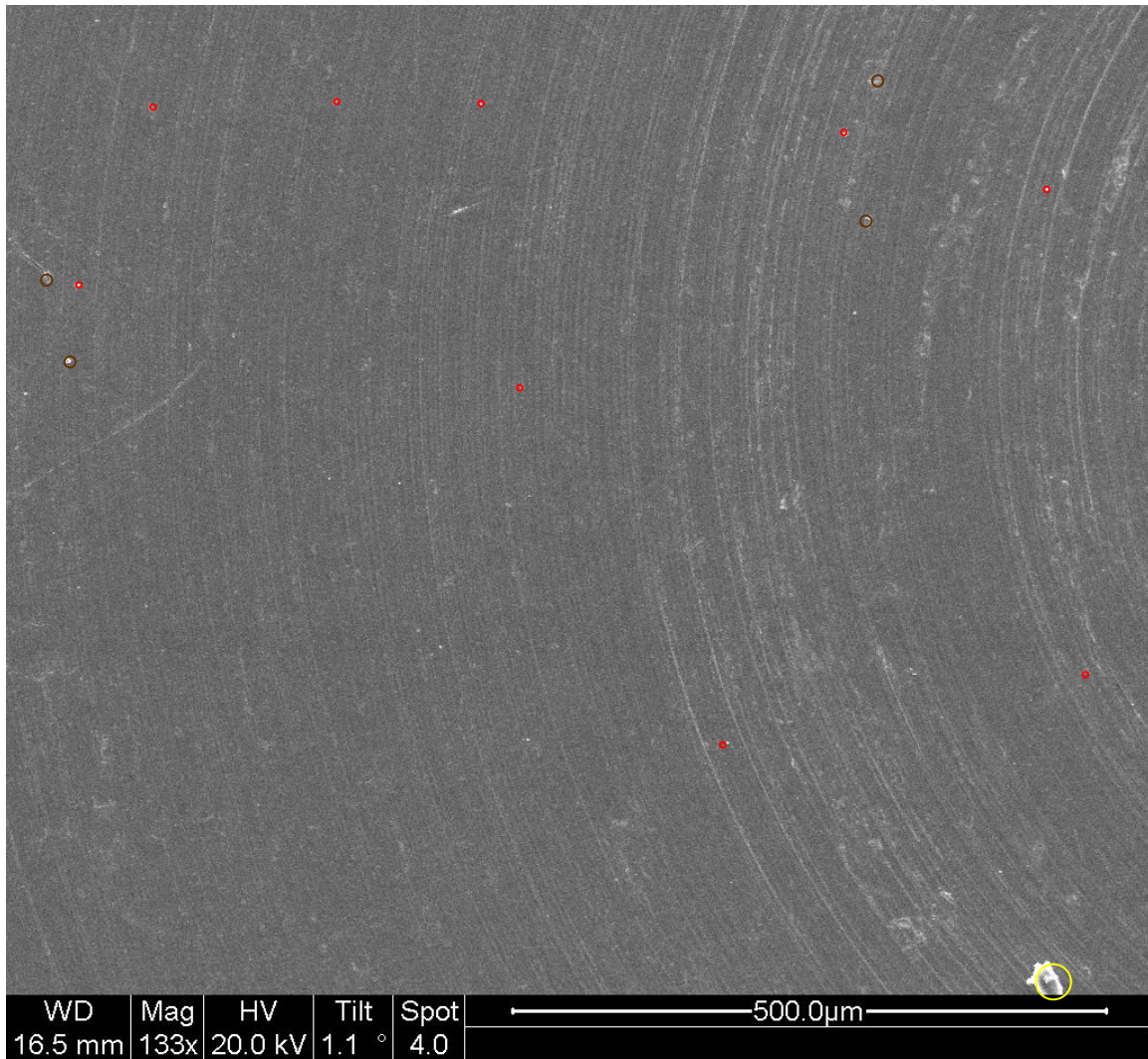
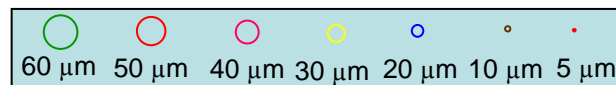


Figure 52. Angular location 67.5° TEST-2



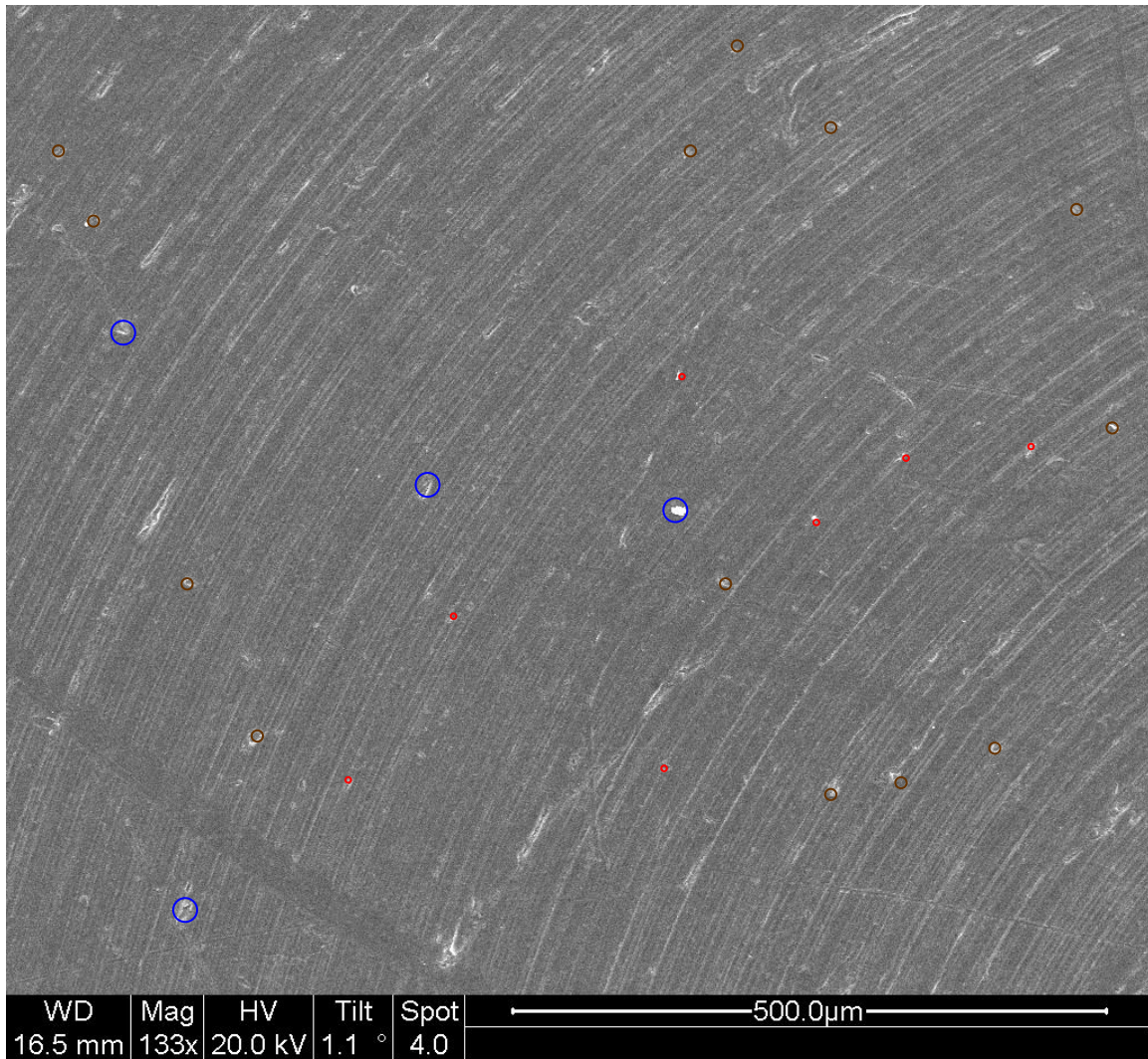
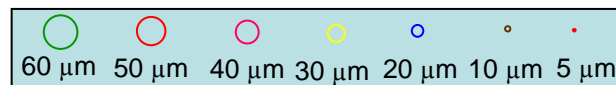


Figure 53. Angular location 56.25° TEST-2



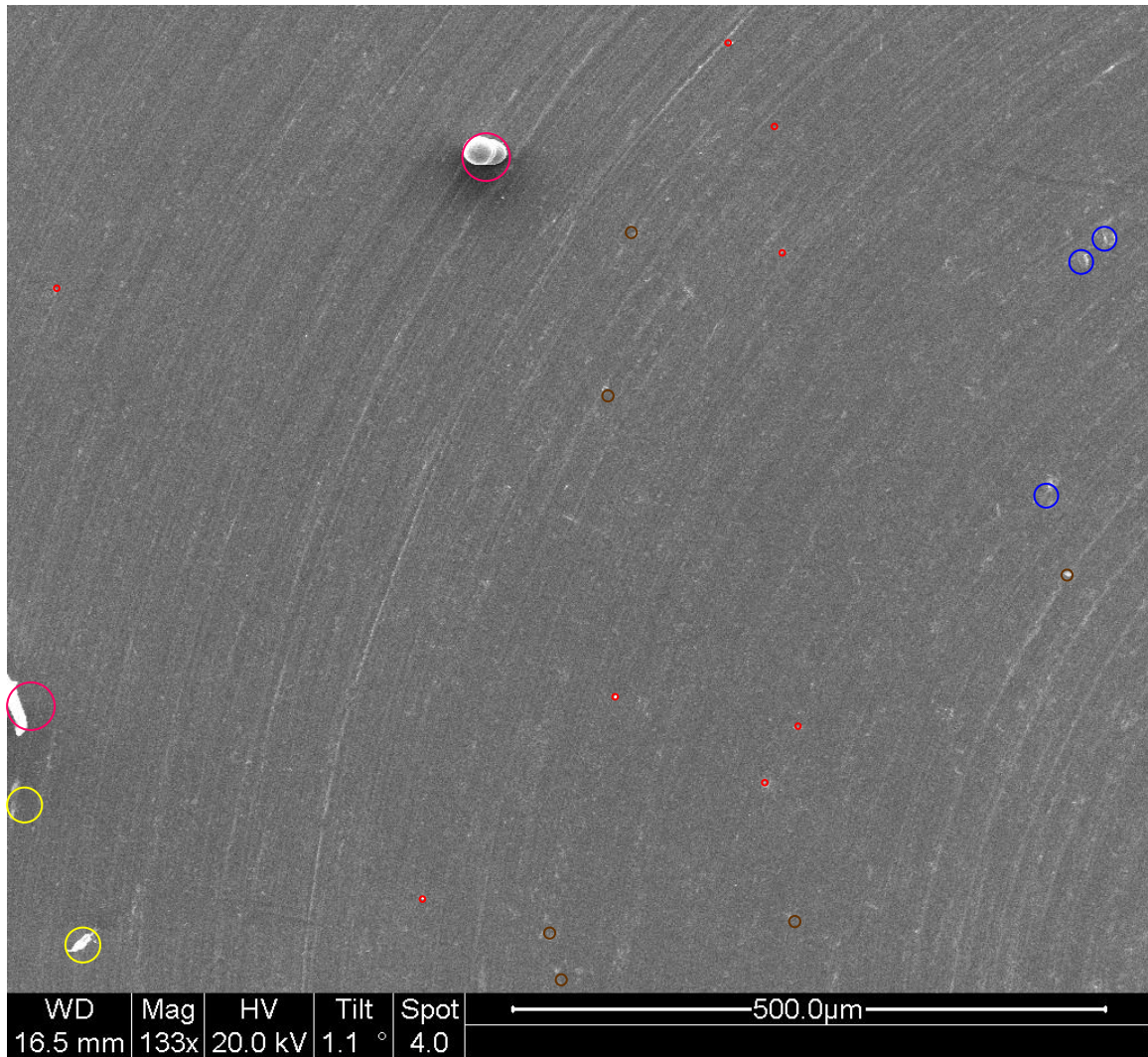
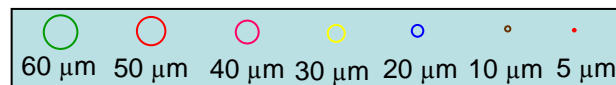


Figure 54. Angular location 45° TEST-2



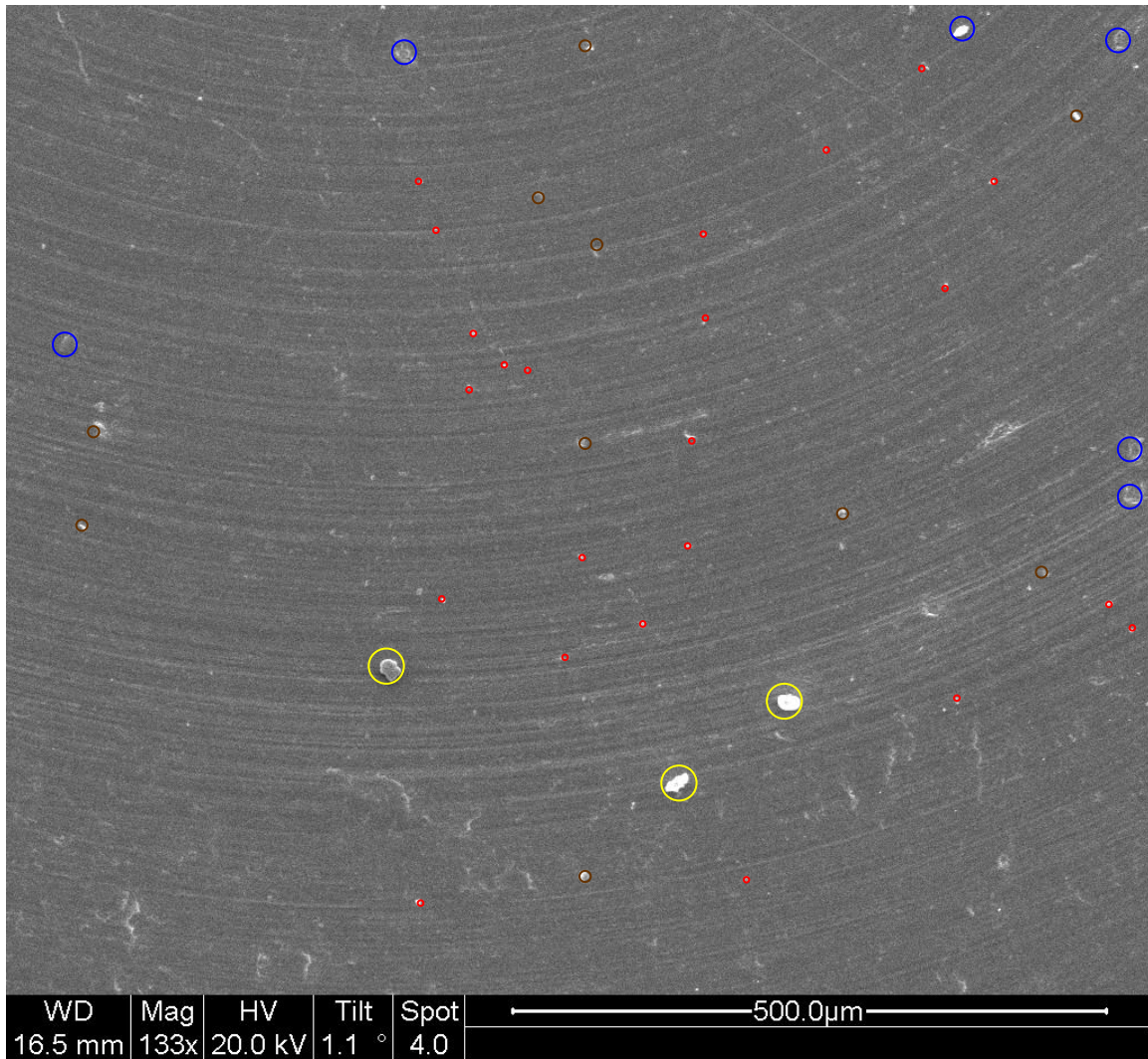
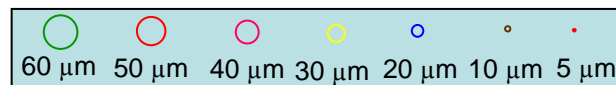


Figure 55. Angular location 33.75° TEST-2



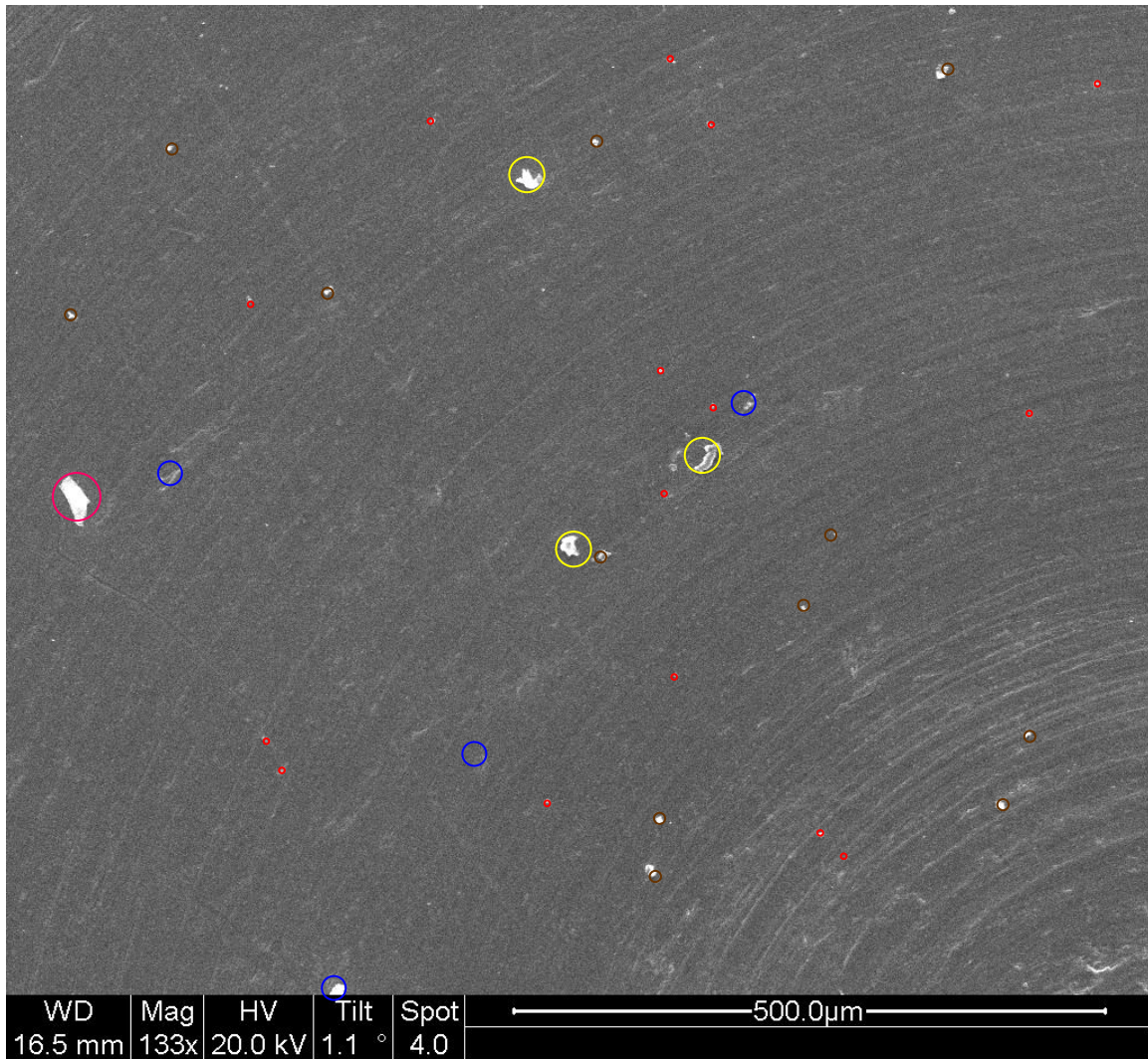
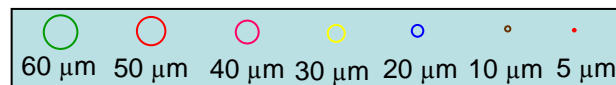


Figure 56. Angular location 22.5° TEST-2



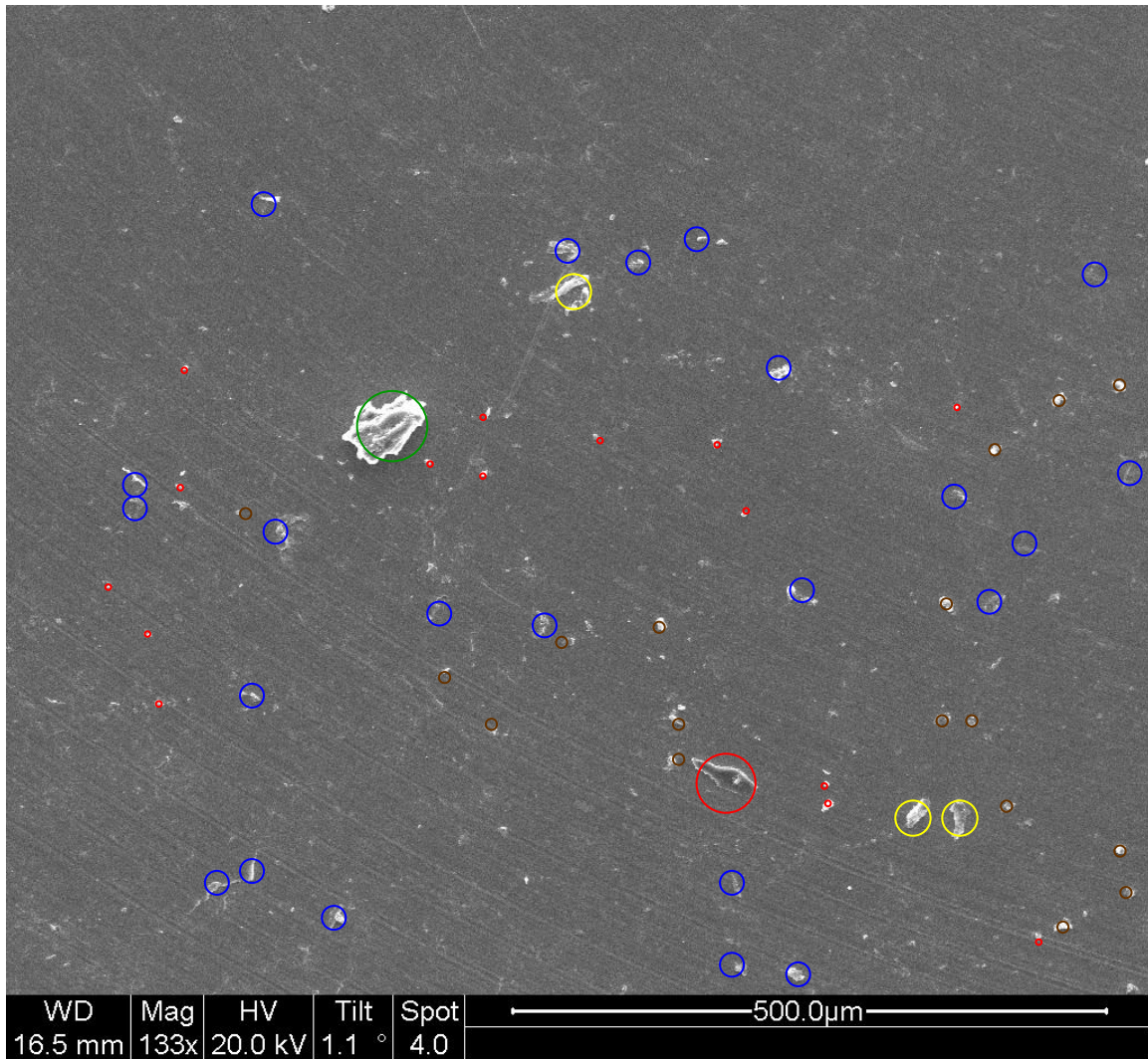
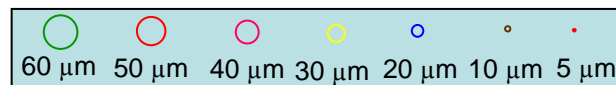


Figure 57. Angular location 11.25° TEST-2



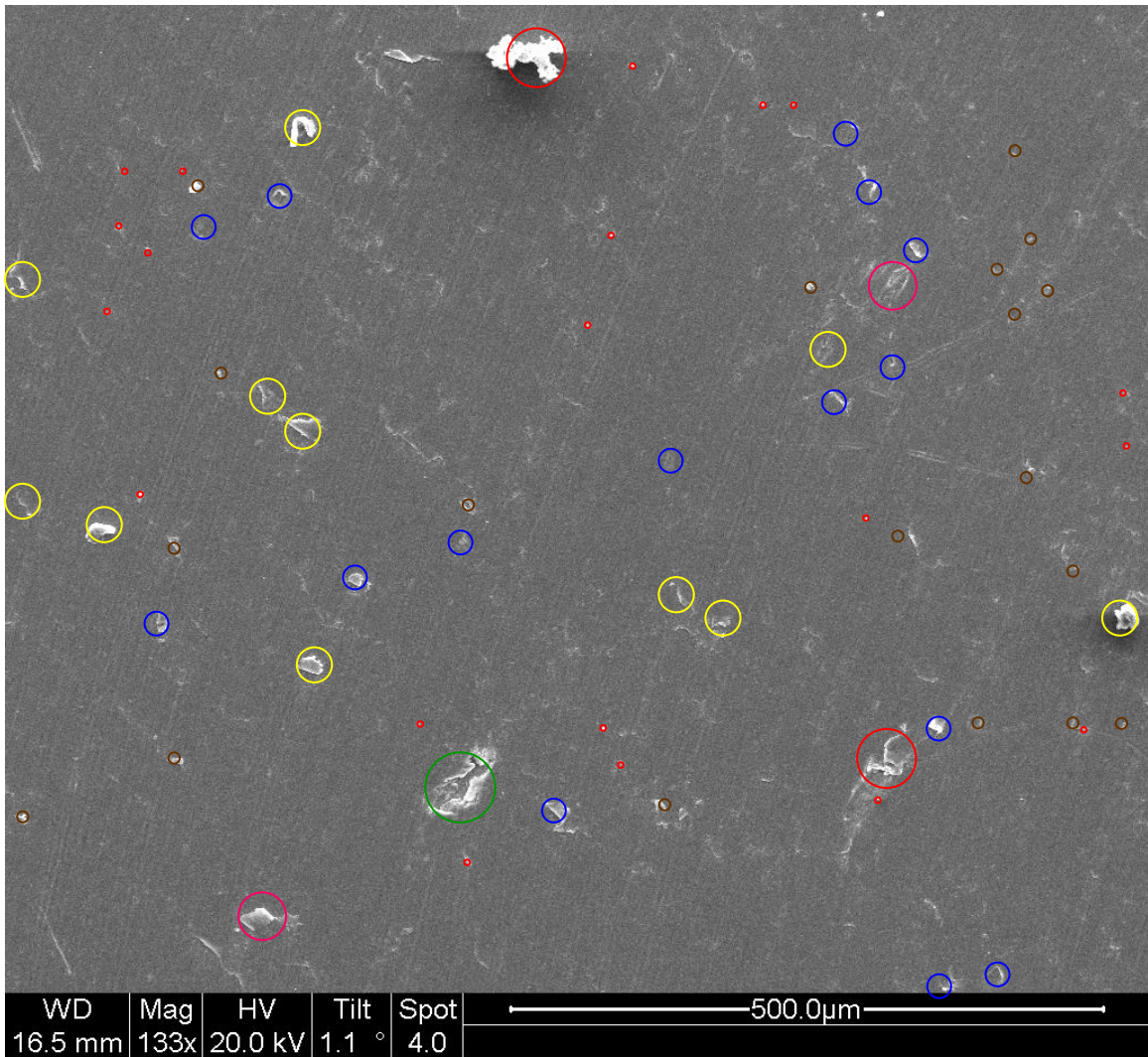
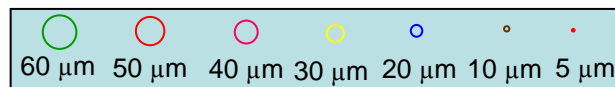


Figure 58. Angular location 0° TEST-2



Test-3 Results:

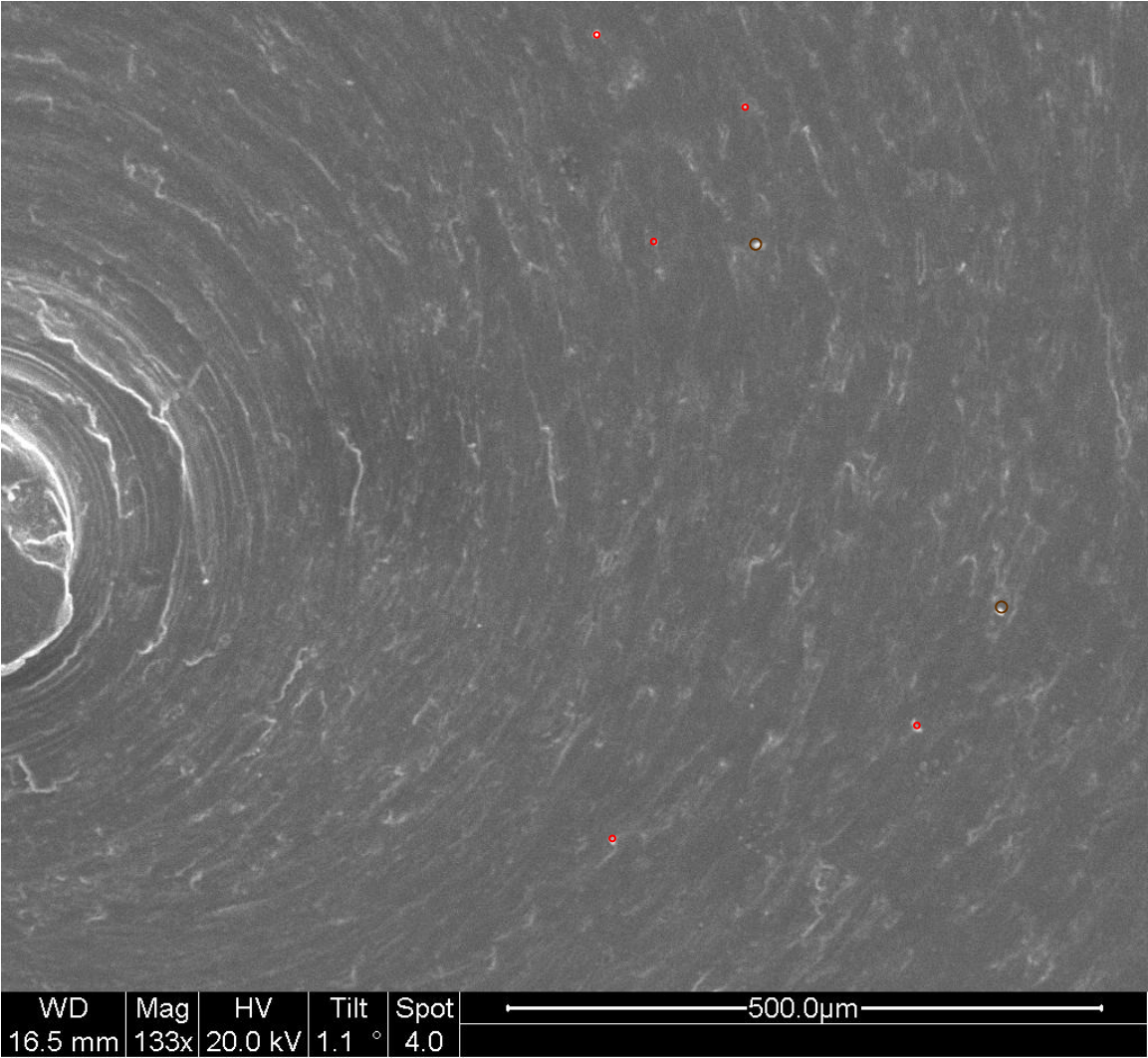
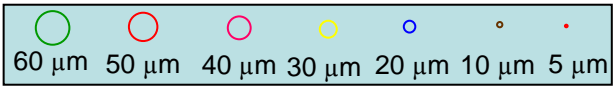


Figure 59. Angular location 90° TEST-3



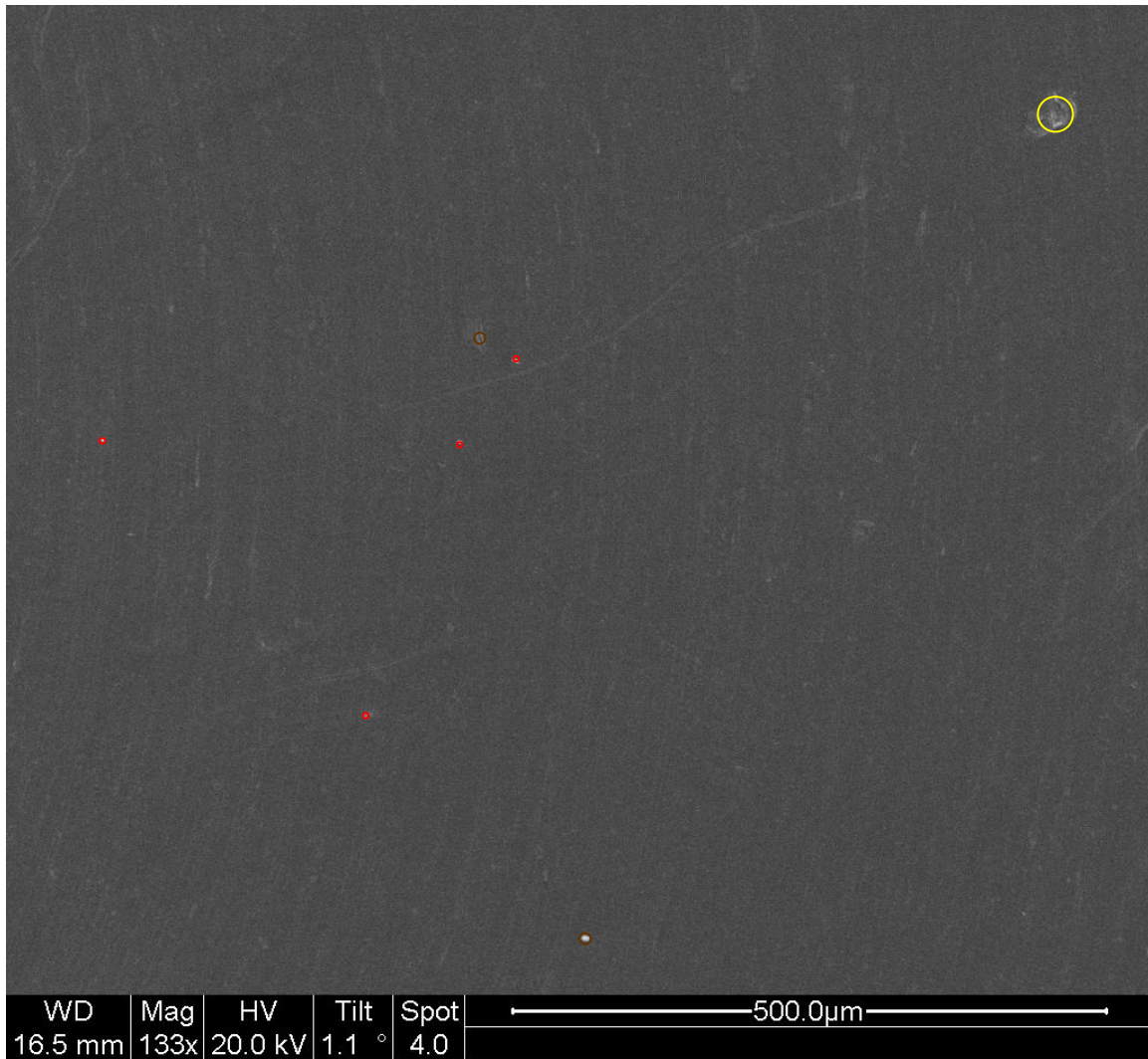
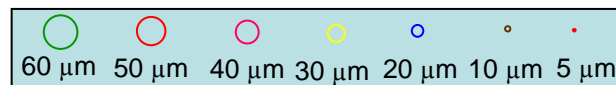


Figure 60. Angular location 78.75° TEST-3



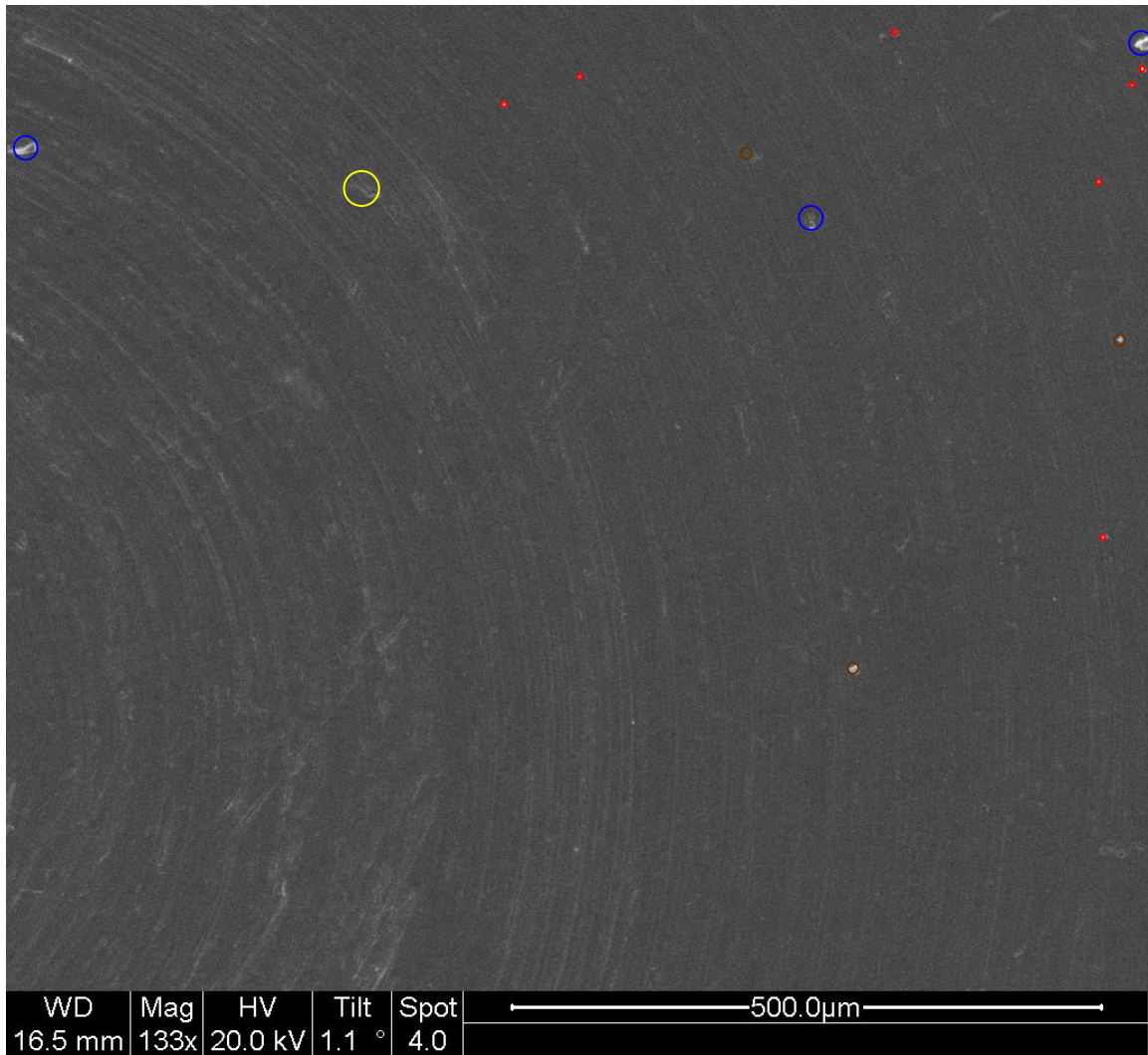
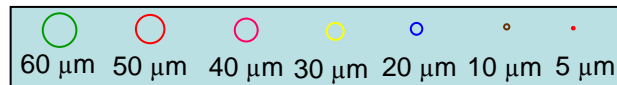


Figure 61. Angular location 67.5° TEST-3



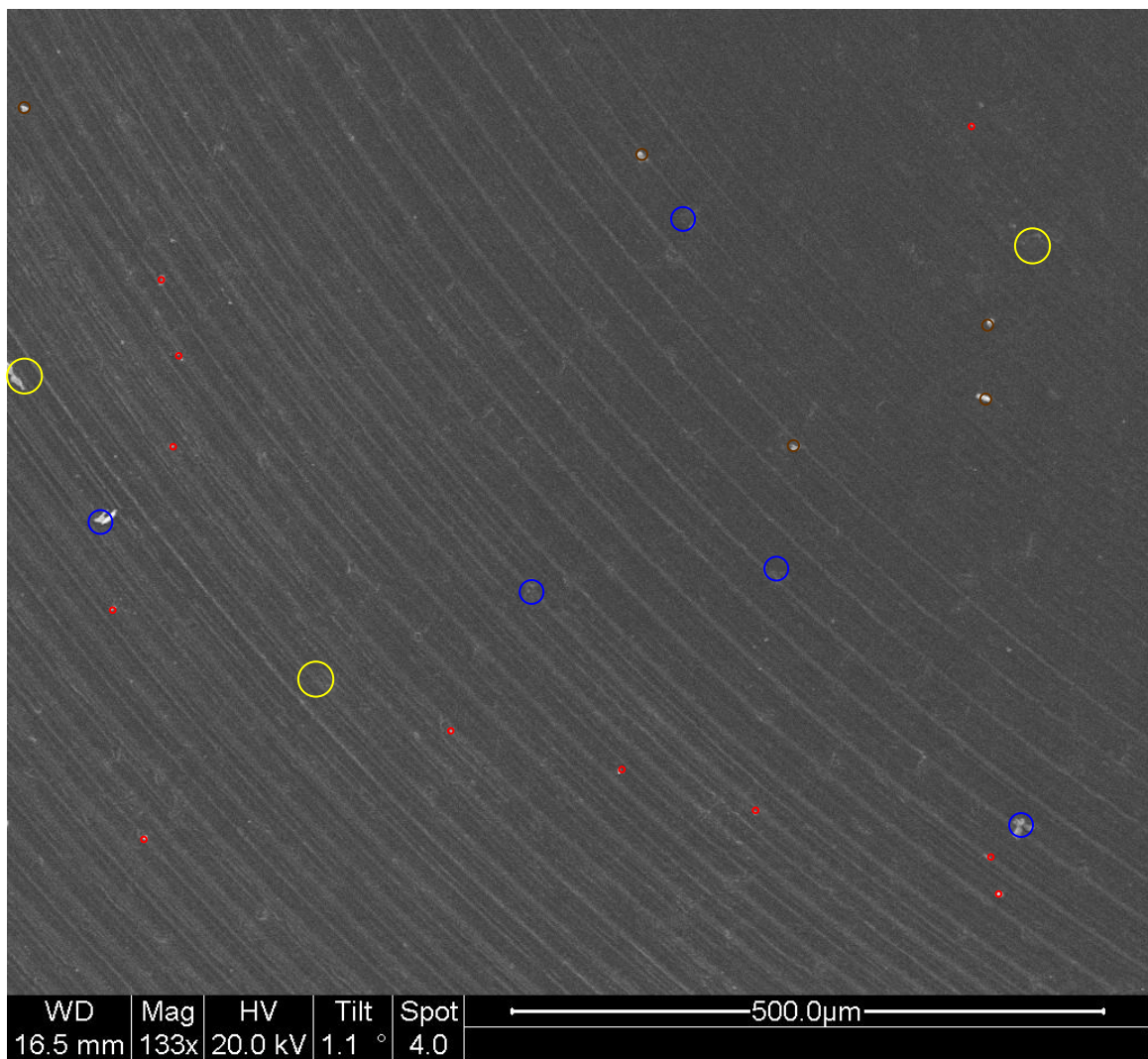
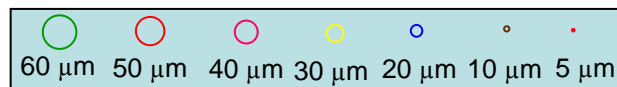


Figure 62. Angular location 56.25° TEST-3



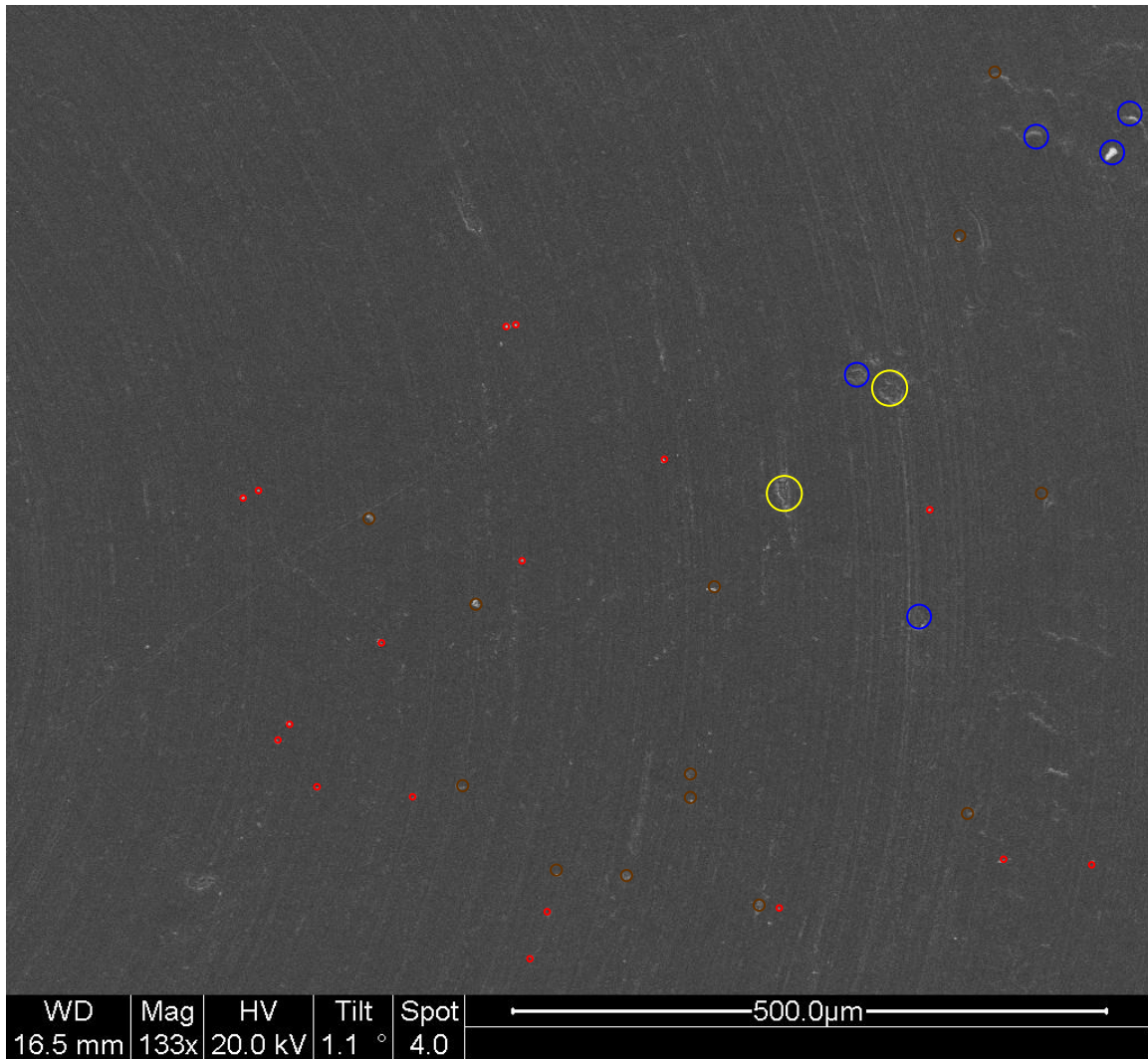
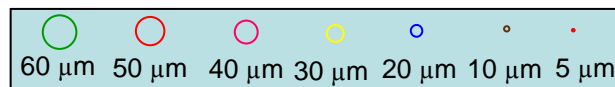


Figure 63. Angular location 45° TEST-3



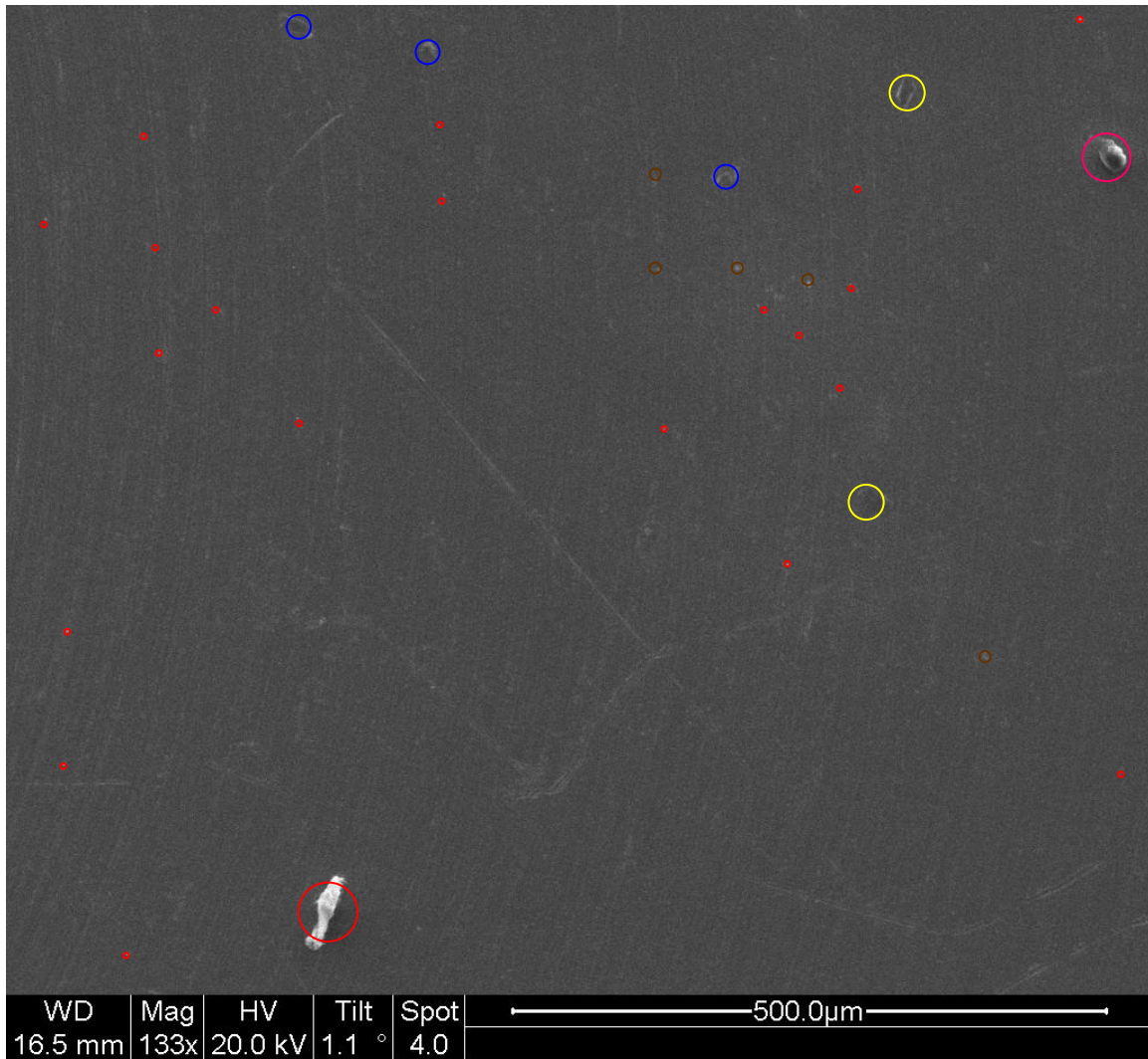
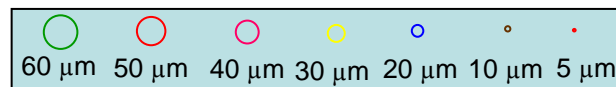


Figure 64. Angular location 33.75° TEST-3



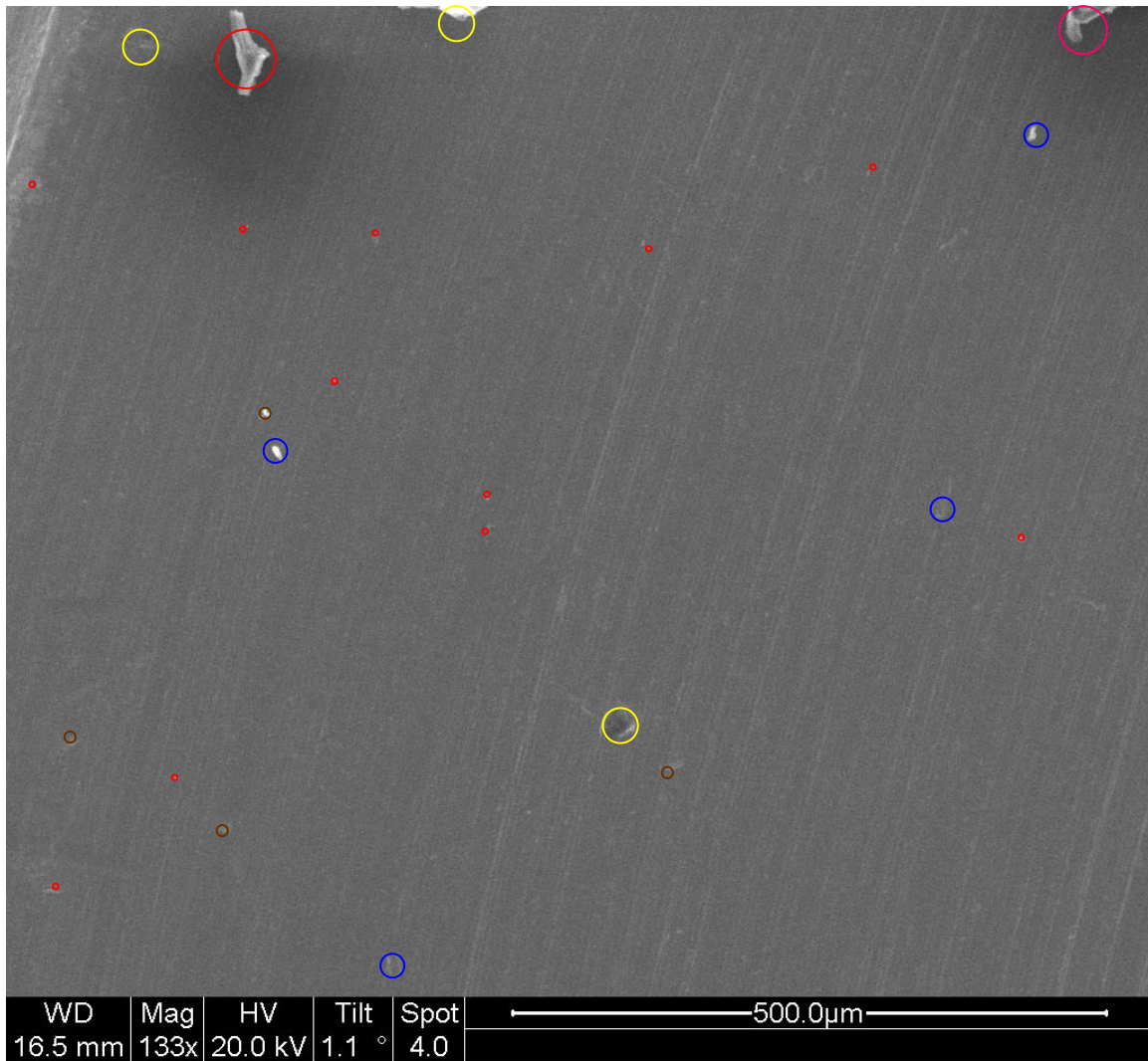
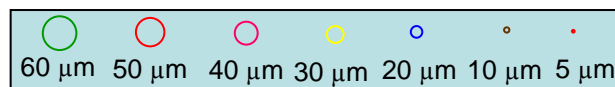


Figure 65. Angular location 28° TEST-3



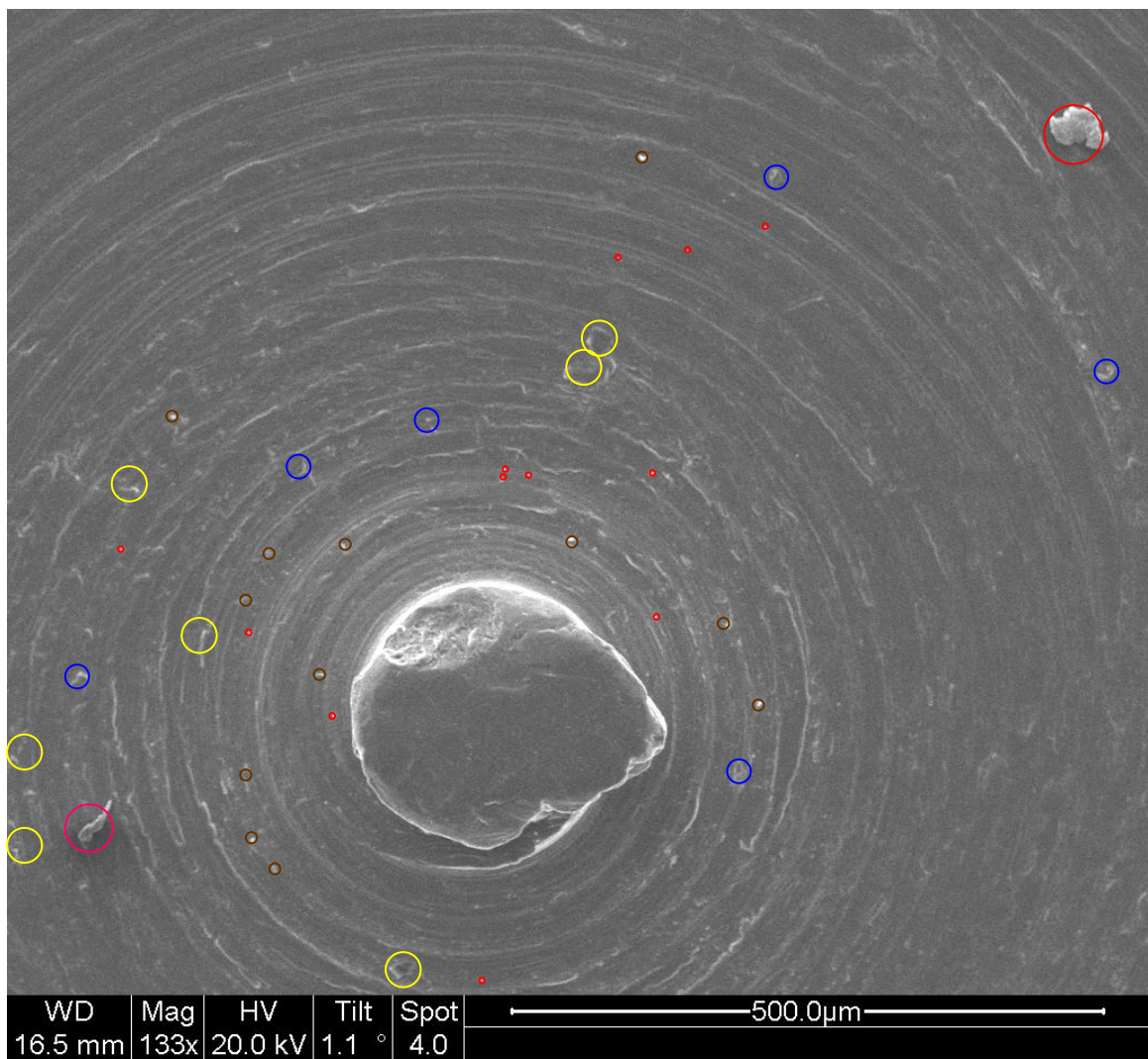
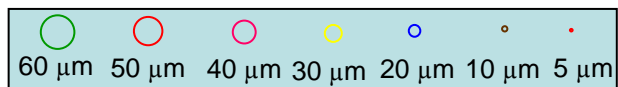


Figure 66. Angular location 22.25° TEST-3



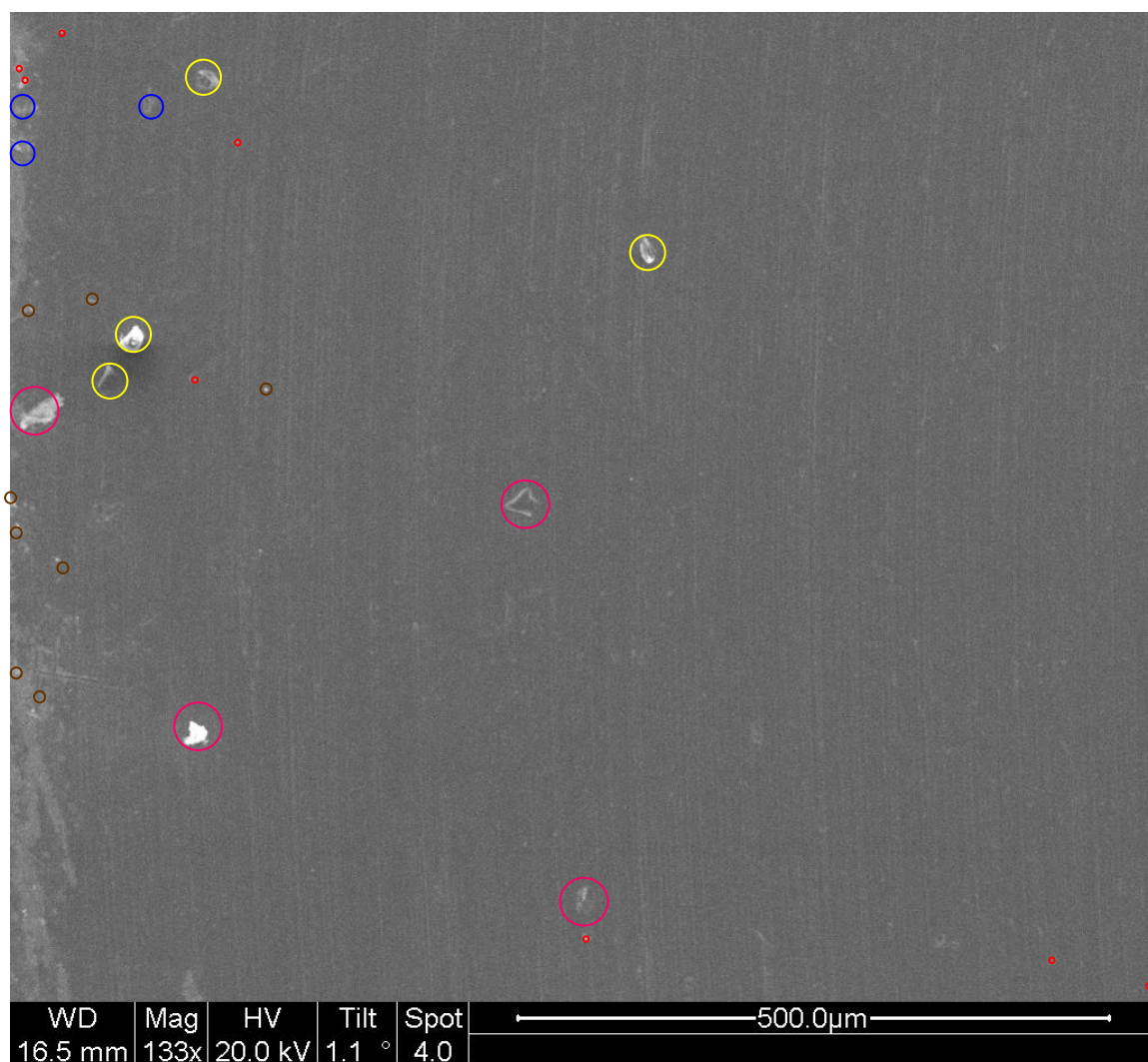
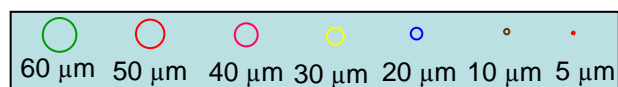


Figure 67. Angular location 20° TEST-3



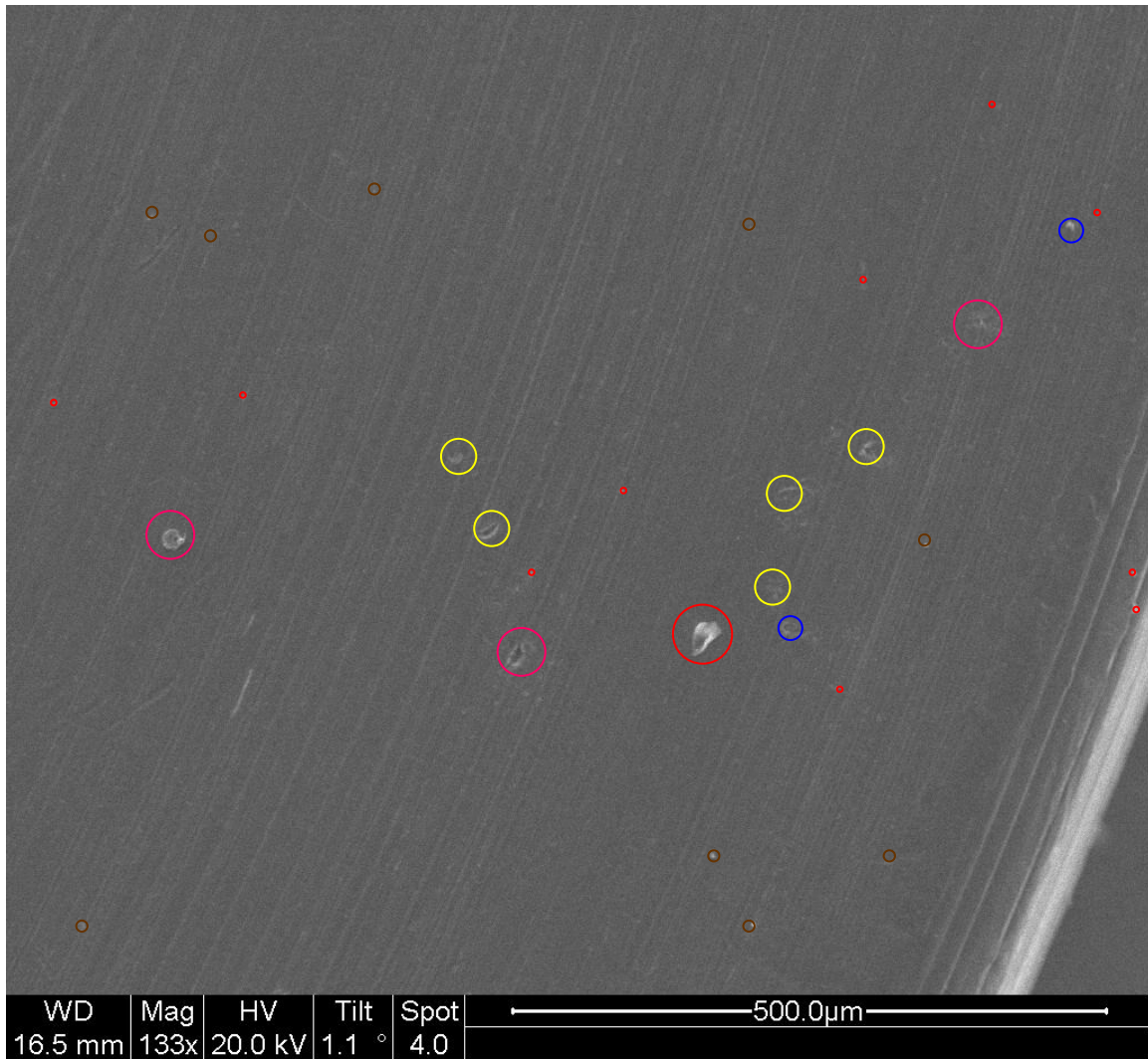
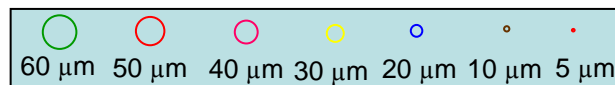


Figure 68. Angular location 17° TEST-3



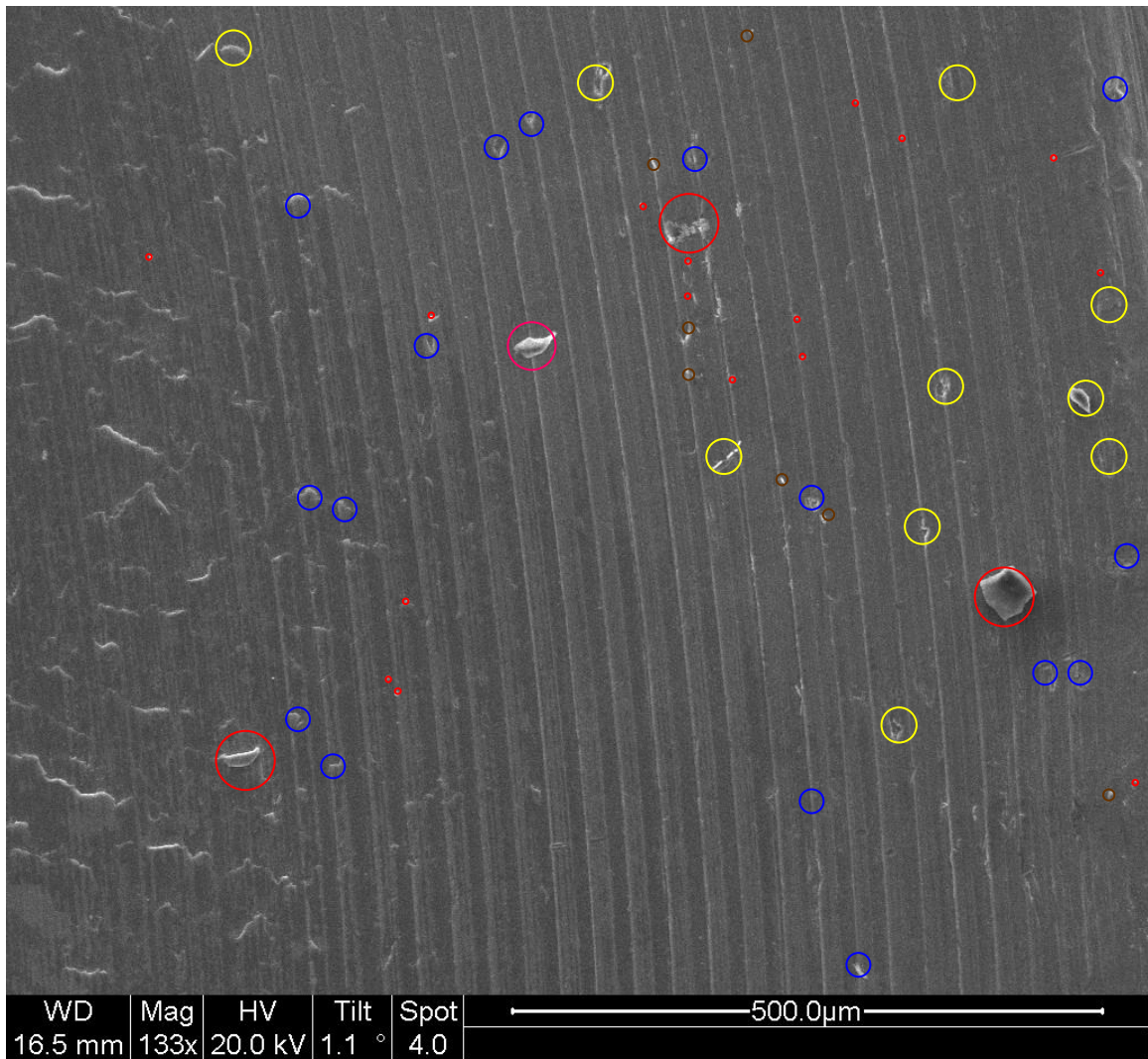
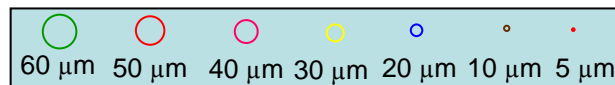


Figure 69. Angular location 14° TEST-3



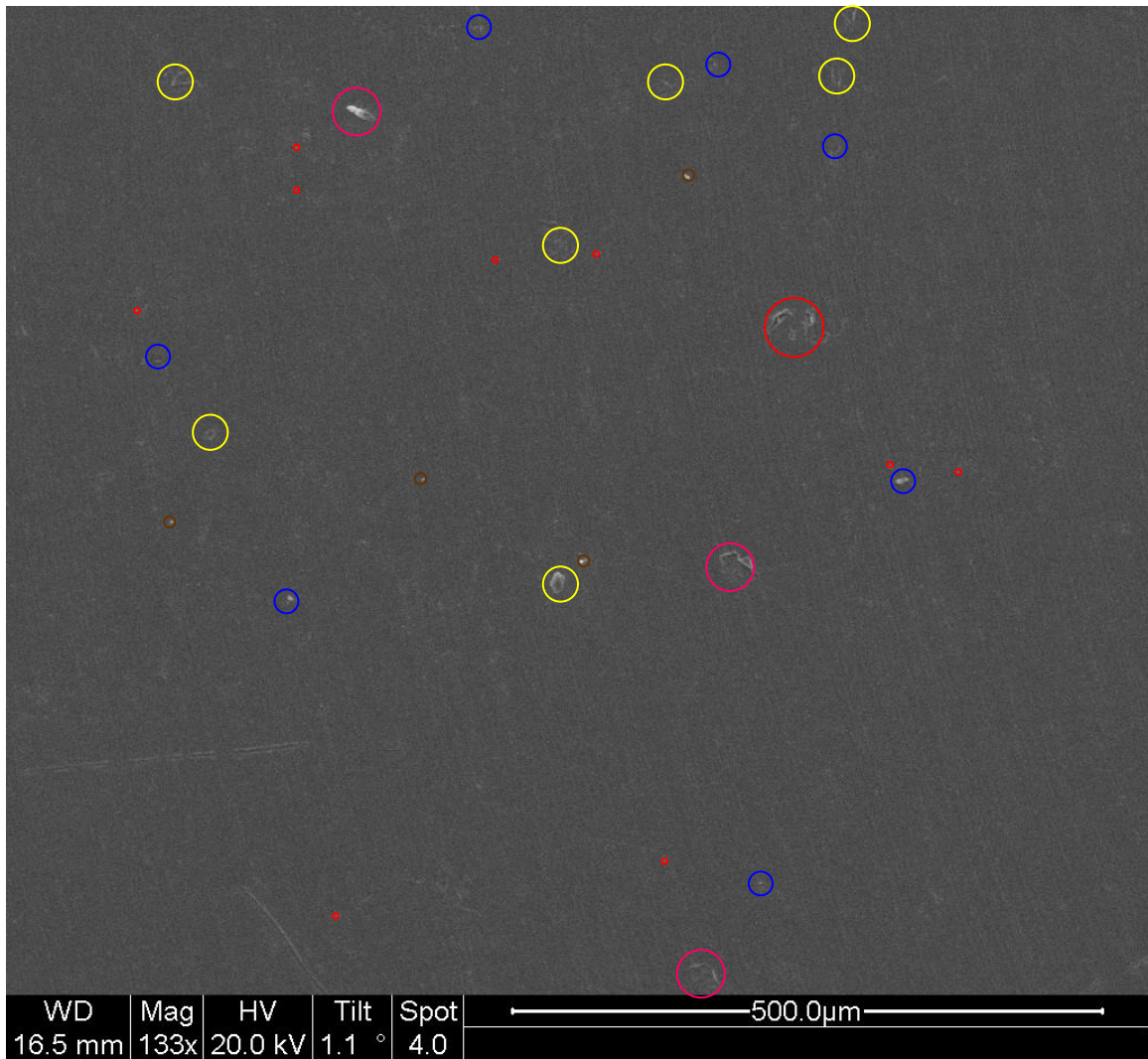
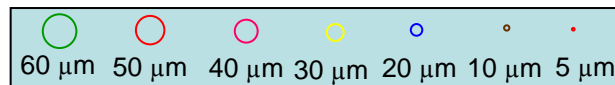


Figure 70. Angular location 8° TEST-3



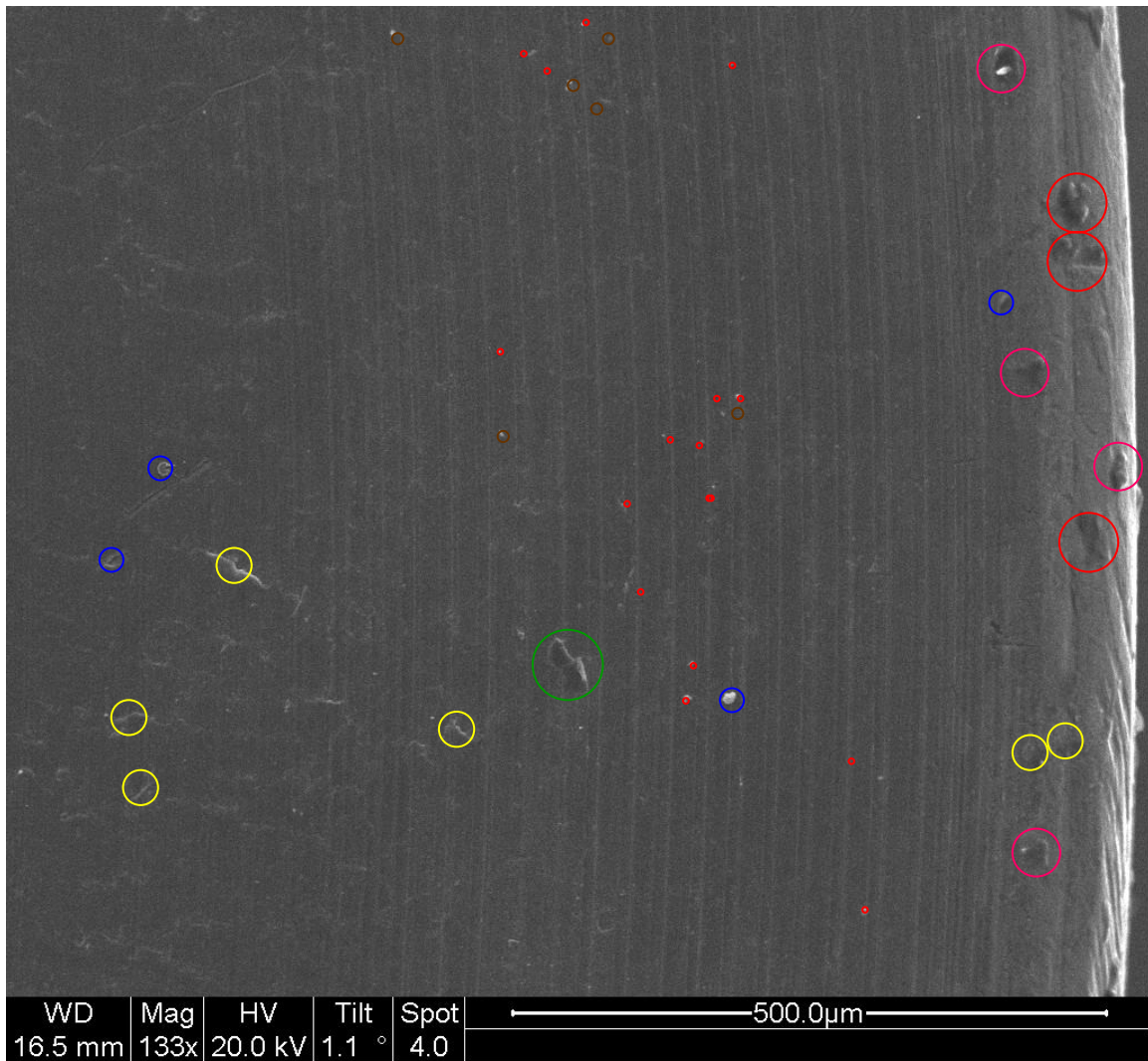
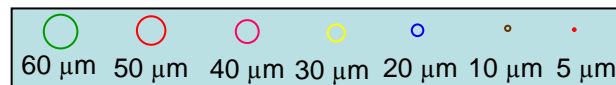


Figure 71. Angular location 5° TEST-3



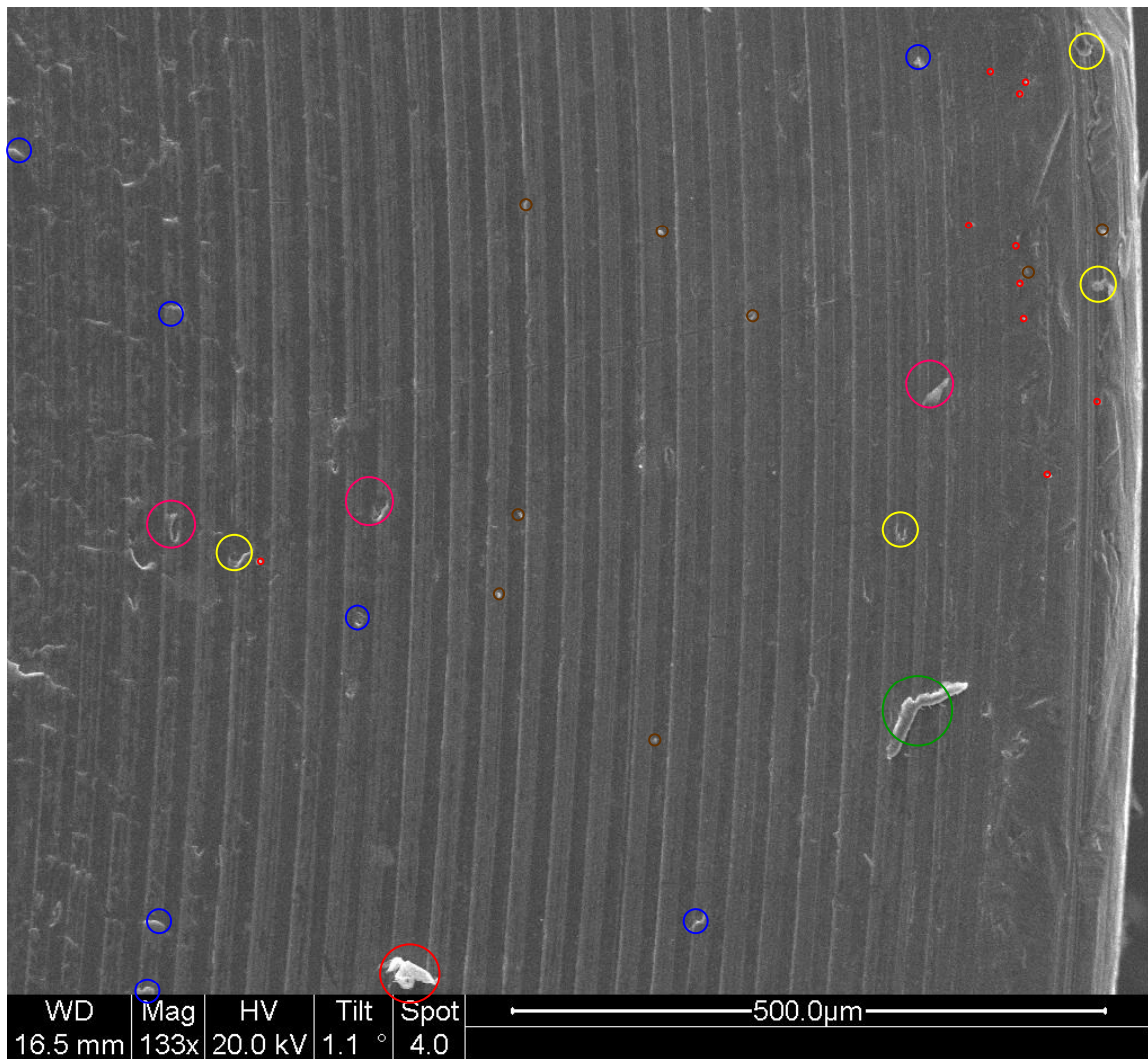
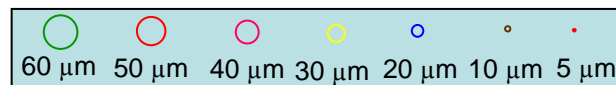


Figure 72. Angular location 4° TEST-3



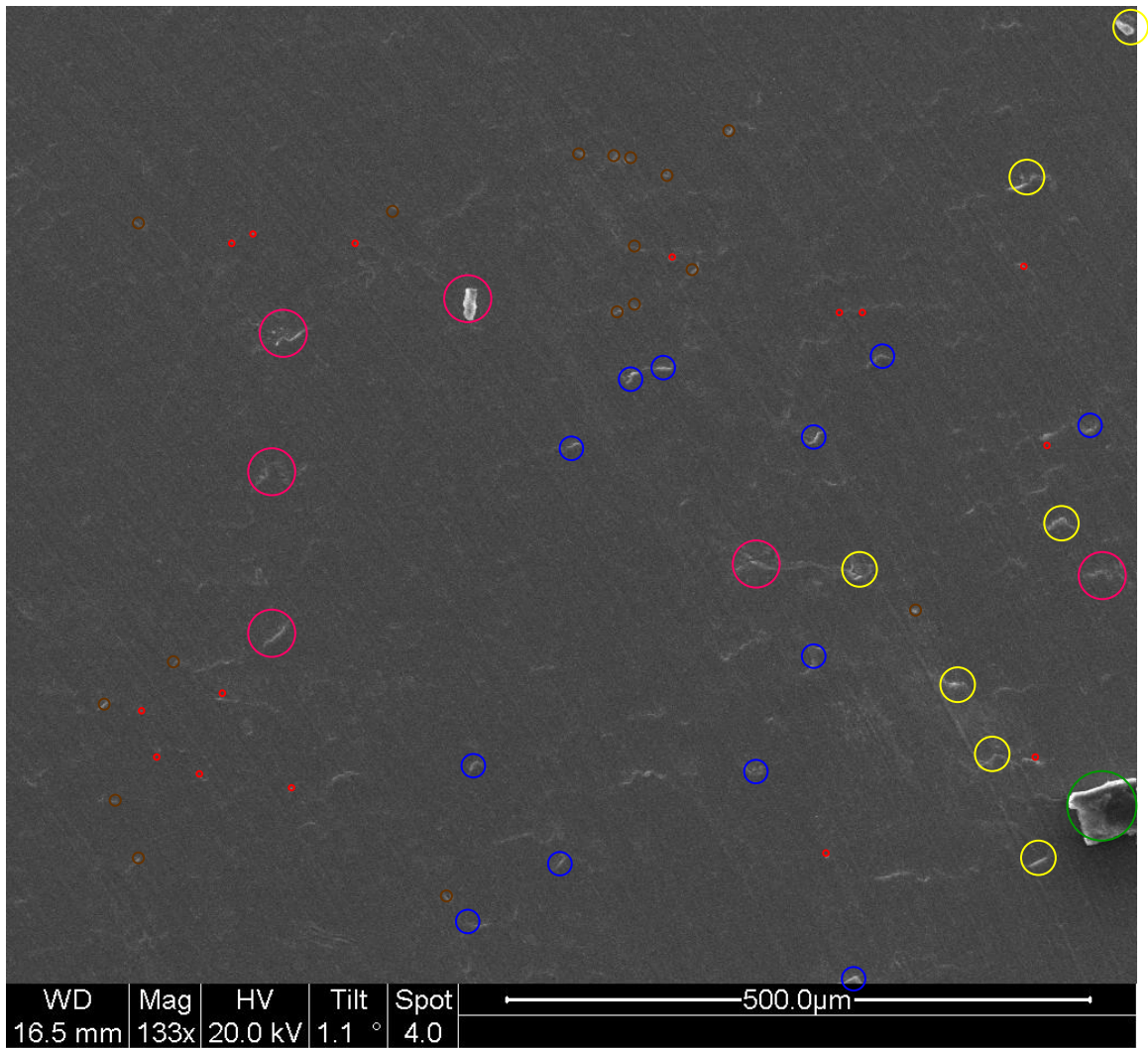
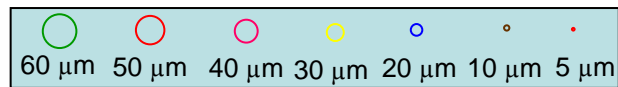


Figure 73. Angular location 2° TEST-3



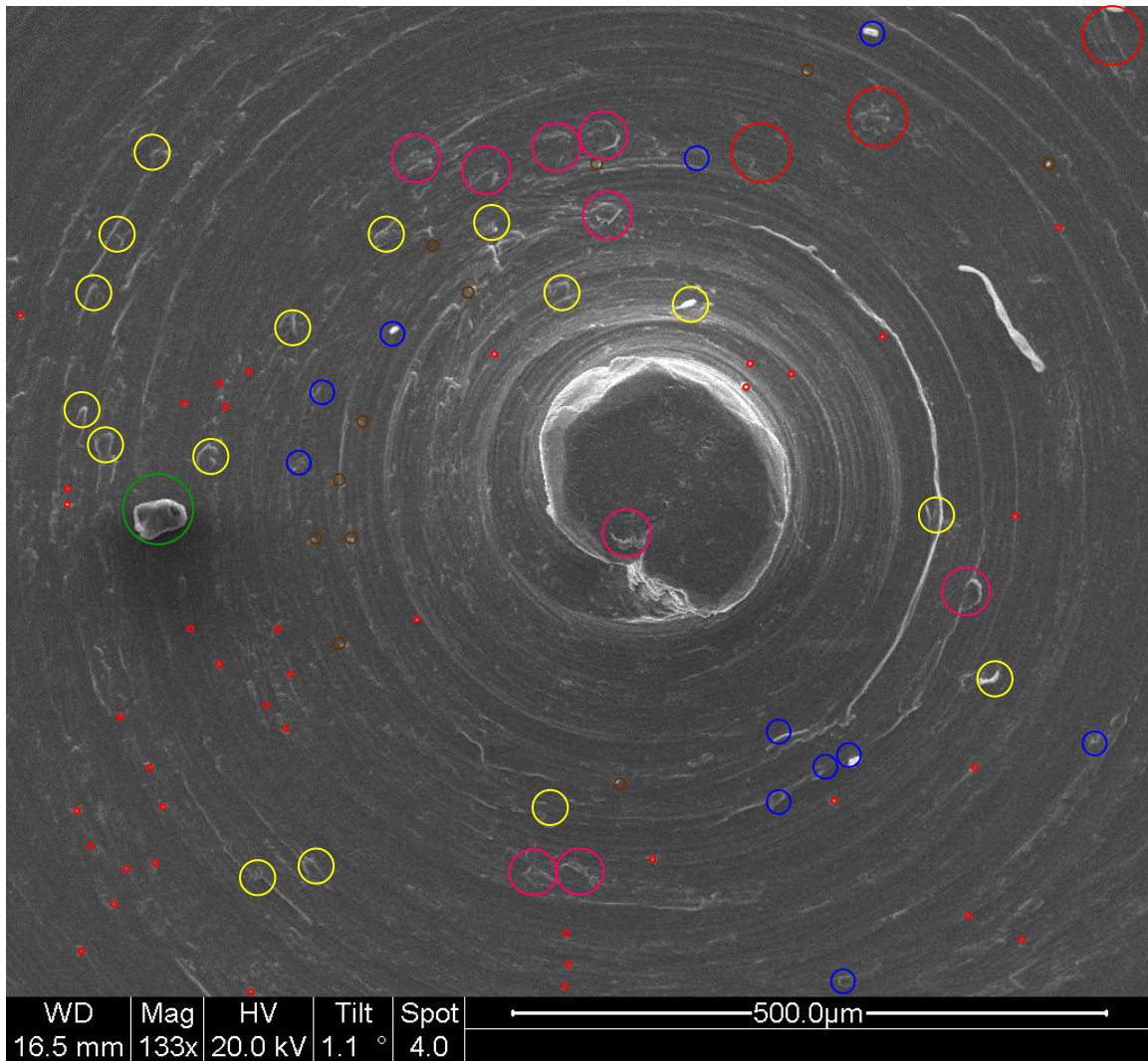
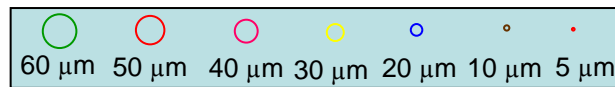


Figure 74. Angular location 0° TEST-3



Vita

1st Lieutenant Ceylan Kesenek graduated from Kuleli Military high school in Istanbul. He finished his undergraduate degree at Turkish Air Force Academy and graduated in August 2002 with a Bachelor of Science degree in Aeronautics Engineering. In August 2006 he entered the Graduate School of Engineering and Management, Air Force Institute of Technology.

Bibliography

- ¹ N. Kumagai, M. Igarashi, K. Sato, K. Tamura, K. Kawahara, H. Takegahara “Plume Diagnostics in Pulsed Plasma Thruster,” AIAA 2002-4124 38th AIAA/ASME/ASEE Joint Propulsion Conference & Exhibit 7-10 July 2002 Indianapolis, Indiana
- ² R. M. Myers and L. A. Arlington “Pulsed Plasma Thruster Contamination,” AIAA Meeting Papers on Disc, July 1996 A9636958, AIAA-96-2729 32nd AIAA/ASME/SAE/ASEE, Joint Propulsion Conference and Exhibit, , Lake Buena Vista, FL, July 1-3, 1996
- ³ R. G. Jahn *Physics of Electric Propulsion* New York: McGraw-Hill Inc, 1968
- ⁴ R. W. Humble, G. N. Henry, W. J. Larson *Space Propulsion Analysis and Design* McGraw-Hill Inc, 1995
- ⁵ R.L.Burton, P. J. Turchi “Pulsed Plasma Thruster”, Journal of Propulsion and Power Vol. 14. No. 5, September-October 1998
- ⁶ W. A. Hoskins and C. Rayburn C. Sarmiento “Pulsed Plasma thruster Electromagnetic Compatibility: History, Theory, and the Flight Validation on EO-1” 39th AIAA/ASME/SAE/ASEE Joint Propulsion Conference and Exhibit 20-23 July 2003, Huntsville, Alabama
- ⁷ C. D. Rayburn, M. E. Campbell, and A. T. Mattick “Pulsed Plasma Thruster System for Microsatellites” Journal Of Spacecraft And Rockets Vol. 42, No. 1, January–February 2005 AIAA-15422-496

⁸ E. Y. Choueiri “Overview of U.S. Academic Programs in Electric Propulsion” AIAA 99-2163 35th AIAA/ASME/SAE/ASEE Joint Propulsion Conference and Exhibit 20-24 June 1999 Los Angeles, California

⁹ D. H. Simon, H. B. Land, “Micro Pulsed Plasma Thruster Technology Development” 40th AIAA/ASME/SAE/ASEE Joint Propulsion Conference and Exhibit 11-14 July 2004, Fort Lauderdale, Florida

¹⁰ G. G. Spanjers, J. B. Malak, R. J. Leiweke, Ronald A. Spores “The Effect of Propellant Temperature on Efficiency in the Pulsed Plasma Thruster” AIAA 1997 2920-705 July 1997

¹¹ R. M. Myers, L. A. Arlington, Eric J. Pencil, Justin Carter, Jason Heminger and Nicolas Gatsonis “Pulsed Plasma Thruster Contamination” AIAA, ASME, SAE, and ASEE, Joint Propulsion Conference and Exhibit, 32nd, Lake Buena Vista, FL, July 1-3, 1996

¹² Frank S. Gulczinski, Michael J. Dulligan, James P. Lake, Gregory G. Spanjers “Micropropulsion Research at AFRL”, AIAA 2000-3255 38th Joint Propulsion Conference & Exhibit 16-19 July 2000 Huntsville, Alabama

¹³ L.A. Arlington, “Pulsed Plasma Thruster Plume Study: Symmetry and Impact on Spacecraft Surfaces” AIAA-2000-3262 36th AIAA/ASME/SAE/ASEE Joint Propulsion Conference July 17-19, 2000 / Huntsville, AL

¹⁴ C. A. Smith “Leveraging COTS Hardware for Rapid Design and Development of Small Satellites at the USAF Academy” 2nd Responsive Space Conference April 19–22, 2004 Los Angeles, CA

¹⁵ K. E. Siegenthaler, T. J. Lawrence, D. A. Miller, II, D. E. Swanson, M. J. Meerman, D. J. Barnhart, M. G. McHarg, and J. White “Nurturing Our Satellite Space Workforce at the United States Air Force Academy” AIAA 2005-6779 Space 2005 30 August - 1 September 2005, Long Beach, California

¹⁶ R.L. Sackheim “Overview of United States Space Propulsion Technology and Associated Space Transportation Systems” AIAA 23257-518 Journal Of Propulsion And Power Vol. 22, No. 6, November–December 2006

¹⁷ J.A. Pobst, G.G. Spanjers, I.J. Wysong, J.B. Malak “Basic Research in Electric Propulsion” Raytheon ITSS Air Force Research Laboratory AFRL/PRS Edwards AFB, CA February 2002 Interim Report

¹⁸ R. M. Myers, L. A. Arrington, E. J. Pencil, J. Carter, J. Heminger, N. Gatsonis “Pulsed Plasma Thruster Contamination” AIAA, ASME, SAE, and ASEE, Joint Propulsion Conference and Exhibit, 32nd, Lake Buena Vista, FL, July 1-3, 1996 AIAA-1996-2729

¹⁹ L. A. Arlington NASA Glenn Research Center, C. M. Marrese, J. J. Blandino California Institute of Technology “Pulsed Plasma Thruster Plume Study: Symmetry and Impact on Spacecraft Surfaces” 36th AIAA/ASME/SAE/ASEE Joint Propulsion Conference July 17-19, 2000 / Huntsville, AL AIAA-2000-3262-967

²⁰ M. Keidar, I. D. Boyd University of Michigan, E. L. Antonsen and R. L. Burton University of Illinois, G. G. Spanjers Air Force Research Laboratory Kirtland Air Force Base “Optimization Issues for a Micropulsed Plasma Thruster” Journal of Propulsion and Power Vol.22 No. 1 January February 2006

-
- ²¹ Michael Keidar, Iain D. Boyd University of Michigan, Erik L. Antonsen University of Illinois, Frank S. Gulczinski, Gregory G. Spanjers Air Force Research Laboratory Kirtland Air Force Base “Optimization Issues for a Micropulsed Plasma Thruster” Journal of Propulsion and Power Vol.20 No. 6 November December 2004
- ²² C. A. Scharlemann, T.M. York, “Mass Flux Measurements in the plume of a Pulsed Plasma Thruster” 42nd AIAA/ASME/SAE/ASEE Joint Propulsion Conference and exhibit 9-12 July 2006 Sacramento CA AIAA-2006-4856
- ²³ Michael Keidar and Iain D. Boyd “Progress in Development of Modeling capabilities of Micro-Pulsed Plasma Thruster” AIAA-2003-5166 39th AIAA/ASME/SAE/ASEE Joint Propulsion Conference & Exhibit 20-23 July 2003 Huntsville, Alabama
- ²⁴ *Basic Vacuum Practice* Third Edition 1992 Varian Associates Inc.
- ²⁵ J.H. Debevec “Vacuum Chamber Construction And Contamination Study Of A Micro Pulsed Plasma Thruster” AFIT M.S. Thesis. December 2006
- ²⁶ G.G. Spanjers, J.S. Lotspeich, K.A. McFall, R.A. Spores “Propellant Losses Because of Particulate Emission in a Pulsed Plasma Thruster ” Journal of Propulsion and Power Vol. 14, No. 4, July–August 1998

REPORT DOCUMENTATION PAGE				Form Approved OMB No. 074-0188	
<p>The public reporting burden for this collection of information is estimated to average 1 hour per response, including the time for reviewing instructions, searching existing data sources, gathering and maintaining the data needed, and completing and reviewing the collection of information. Send comments regarding this burden estimate or any other aspect of the collection of information, including suggestions for reducing this burden to Department of Defense, Washington Headquarters Services, Directorate for Information Operations and Reports (0704-0188), 1215 Jefferson Davis Highway, Suite 1204, Arlington, VA 22202-4302. Respondents should be aware that notwithstanding any other provision of law, no person shall be subject to a penalty for failing to comply with a collection of information if it does not display a currently valid OMB control number.</p> <p>PLEASE DO NOT RETURN YOUR FORM TO THE ABOVE ADDRESS.</p>					
1. REPORT DATE (DD-MM-YYYY) 14 March 2008		2. REPORT TYPE Master's Thesis		3. DATES COVERED (From – To) Sep 2006 – March 2008	
4. TITLE AND SUBTITLE CONTAMINATION STUDY OF MICRO PULSED PLASMA THRUSTERS				5a. CONTRACT NUMBER	
				5b. GRANT NUMBER	
				5c. PROGRAM ELEMENT NUMBER	
6. AUTHOR(S) Kesenek, Ceylan, 1 st Lt, TuAF				5d. PROJECT NUMBER	
				5e. TASK NUMBER	
				5f. WORK UNIT NUMBER	
7. PERFORMING ORGANIZATION NAMES(S) AND ADDRESS(S) Air Force Institute of Technology Graduate School of Engineering and Management (AFIT/EN) 2950 Hobson Way, Building 640 WPAFB OH 45433-8865				8. PERFORMING ORGANIZATION REPORT NUMBER AFIT/GA/ENY/08-M03	
9. SPONSORING/MONITORING AGENCY NAME(S) AND ADDRESS(ES) Dr. William A. Hargus, Jr. AFRL/PRSS 1 Ara Road Edwards AFB, CA 93524 DSN: 525-6799				10. SPONSOR/MONITOR'S ACRONYM(S)	
				11. SPONSOR/MONITOR'S REPORT NUMBER(S)	
12. DISTRIBUTION/AVAILABILITY STATEMENT APPROVED FOR PUBLIC RELEASE; DISTRIBUTION UNLIMITED.					
13. SUPPLEMENTARY NOTES					
14. ABSTRACT Satellite designing trend is progressing towards building smaller satellites. Small satellites require micro propulsion devices for accurate control by the propulsion system. Micro-Pulsed Plasma Thrusters (μPPTs) are highly reliable and simple micro propulsion systems that will offer attitude control, station keeping, constellation flying, and drag compensation for such satellites. As an unfortunate side effect, the plume induces contamination on spacecraft surfaces and may lead to significant problems with sensors and power generation. Solid particulates in the exhaust plume may deposit on spacecraft instrument and the solar array surfaces limiting or reducing the mission capability as well as the lifetime of a satellite. To better understand these contamination issues, a detailed characterization of the exhaust plume is necessary. This research employs μPPTs, first developed at the Air Force Research Lab at Edwards AFB, CA, and is being operated in a simulated space environment, at the Air Force Institute of Technology micro-propulsion vacuum facilities.					
15. SUBJECT TERMS Micro-Pulsed Plasma Thrusters, exhaust plume, contamination, solid particles, space environment					
16. SECURITY CLASSIFICATION OF:			17. LIMITATION OF ABSTRACT	18. NUMBER OF PAGES	19a. NAME OF RESPONSIBLE PERSON Richard Branam, Maj, USAF
a. REPORT U	b. ABSTRACT U	c. THIS PAGE U			19b. TELEPHONE NUMBER (Include area code) (937) 255-6565, ext 7485 (Richard.branam@afit.edu)